SATELLITE REMOTE SENSING AND MODELING OF THE HYDROSPHERE FOR UNDERSTANDING TERRESTRIAL WATER CYCLE DYNAMICS AT DIFFERENT SCALES

by

WONDWOSEN MEKONNEN SEYOUM

(Under the Direction of ADAM MILEWSKI)

ABSTRACT

Water resources are important to both society and ecosystems. However, humans put pressure on water resources with stresses that are likely to be exacerbated by the change in climate. Nonetheless, the lack of continuous data availability and inadequate monitoring networks has been a challenge to the scientific community. Recent advancements in satellite-based hydrology have demonstrated hydrologic variables can be measured from space with sufficient accuracy at limited regional and global scales (GRACE's spatial resolution is 200,000 km^2). Therefore, research on the enhancement of the utility of satellite products in understanding and monitoring the water cycle at local scales (with size of 5,000 km^2) is necessary, especially to complement studies in the absence or malfunctioning of in-situ observations. This dissertation sought to (1) estimate the spatial and temporal variation of hydrologic fluxes and storages at different scales using satellite remote sensing data, (2) assess the efficacy of publically available data (e.g. satellite remote sensing data) on our ability to predict/understand the terrestrial water cycle and the implications for water management, and (3) measure the relative

effect of human-induced (e.g. abstraction) vs. climatic variability on the terrestrial water cycle. Moreover, the potential of multi-source datasets and integrated approaches for predicting the variability were evaluated. The work presented in this research has been conducted using a combined approach of processing and interpretation of satellite data, numerical modeling, analysis of in-situ data, and statistical and geospatial analysis in an effort to overcome data paucity. The results demonstrated the capability of GRACE at measuring water storage variations on a regional scale based on results from a robust integrated hydrologic model. Further, merging GRACE data with other data sources in an ANN (Artificial Neural Network) model reproduced the observed TWS (Terrestrial Water Storage) and groundwater storage anomaly at local scales. This downscaled product also replicated the natural water storage variability due to climatic and human impacts. Finally, the relative impact between humans vs. climate variability was distinguished and measured in Ethiopia using an integrated approach that can be transferable to similar settings. The implications utilizing satellite data for improving local and regional water resources management decisions and applications are clear. This is especially true with areas lacking hydrologic monitoring networks.

INDEX WORDS: SATELLITE REMOTE SENSING, GRACE, TERRESTRIAL WATER STORAGE, INTEGRATED HYDROLOGIC MODEL, NEURAL NETWORK, THE HIGH PLAINS, RIFT VALLEY LAKES

SATELLITE REMOTE SENSING AND MODELING OF THE HYDROSPHERE FOR UNDERSTANDING TERRESTRIAL WATER CYCLE DYNAMICS AT DIFFERENT SCALES

by

WONDWOSEN MEKONNEN SEYOUM

BS, ADDIS ABABA UNIVERSITY, ETHIOPIA, 1999

MS, ADDIS ABABA UNIVERSITY, ETHIOPIA, 2005

MS, KENT STATE UNIVERSITY, 2012

A Dissertation Submitted to the Graduate Faculty of The University of Georgia in Partial Fulfillment of the Requirements for the Degree

DOCTOR OF PHILOSOPHY

ATHENS, GEORGIA

2016

SATELLITE REMOTE SENSING AND MODELING OF THE HYDROSPHERE FOR UNDERSTANDING TERRESTRIAL WATER CYCLE DYNAMICS AT DIFFERENT SCALES

by

WONDWOSEN MEKONNEN SEYOUM

Major Professor: ADAM M. MILEWSKI
Committee: JOHN F. DOWD
TODD C. RASMUSSEN
ASSEFA M. MELESSE

Electronic Version Approved:

Suzanne Barbour
Dean of the Graduate School
The University of Georgia
May 2016

DEDICATION

I dedicate this work to the two most important women in my life, my late mother – Shewaye Tilahun and my wife – Helen Woldeyohannes for being a constant source of love, my pillars of support, and my source of inspiration and strength.

ACKNOWLEDGEMENTS

The accomplishment of this dissertation research is the result of nearly four years of work where I have been supported by a great many people. I owe my gratitude to all those people who have made this dissertation possible. First, I am deeply indebted to my advisor, Dr. Adam Milewski, for guiding my progress as a researcher, honing in my critical thinking skills, and for providing me with ample support, feedbacks to my write-ups and presentations, and consistent encouragement. I sincerely thank you for helping me to succeed, I have learned so much, and I look forward to future collaborations. I gratefully acknowledge my dissertation committee members, Dr. John Dowd, Dr. Todd Rasmussen, and Dr. Assefa Melesse for their valuable time, constructive criticism, and encouragements. I would like to extend my appreciation to the past and current members of WRRS lab, especially Khalil (for consistently making coffee), Mike, and Rachel.

Many friends and family members have helped me stay sane through these difficult years. Their support and care helped me overcome setbacks and stay focused on my graduate study. I greatly value their companionship and being there for me whenever I needed them, and I deeply appreciate for believing in me. Most importantly, none of this would have been possible without the love, support, and patience of my wife, Helen and immediate families (Mekonnen, Tekea, Gedion, Yemati, Sveinaage, Yidne, Yetnayet, Worknesh, Sintish, and Abi). I would like to express my heart-felt gratitude to all my family. I warmly appreciate my extended family (Beyecha and Emuti, Selam and Sam, Tade, and Tewahido) who helped and encouraged me throughout this endeavor.

ABBREVIATIONS

ANN – Artificial Neural Nework

ASTER – Advanced Spaceborne Thermal Emission and Reflection Radiometer

CRV – Central Rift Valley

CSR – Center for Space Research

DEM – Digital Elevation Model

dTWS/dt – Terrestrial Water Storage Anomaly

ET – Evapotranspiration

GFZ – German Research Center

GRACE – Gravity Recovery and Climate Experiment

GRGS – The Space Geodesy Research Group

GWSA – Groundwater Storage Anomaly

HPA – High Plains Aquifer

HPRCC – High Plains Regional Climate Center

HRU – Hydrological Response Units

IHM – Integrated Hydrologic Model

JPL – Jet Propulsion Laboratory

LAI – Leaf Area Index

MCM – Million Cubic Meter

ME – Mean Error

MK – Mann-Kendall

MNDWI – Modified Normalized Difference Water Index

MODIS – Moderate Resolution Imaging Spectroradiometer

NASA – National Aeronautics and Space Administration

NDNR – Nebraska Department of Natural Resources

NDVI – Normalized Difference Vegetation Index

NDWI – Normalized Difference Water Index

NHP – Northern High Plains

NOAA – National Oceanic and Atmospheric Administration

NSE – Nash-Sutcliffe Efficiency

RMSE – Root Mean Square Error

SPI – Standard Precipitation Index

SWAT – Soil Water Assessment Tool

TRMM – Tropical Rainfall Measuring Mission

TWS – Terrestrial Water Sotrage

USDA – US Department of Agriculture

USGS – US Geological Survey

VIC – Variable Infiltration Capacity

TABLE OF CONTENTS

Page

LIST OF TABLES

Page

LIST OF FIGURES

Page

CHAPTER 1

INTRODUCTION AND LITERATURE REVIEW

1.1. Background

Fresh water resources are essential for life. Water also plays a key role in Earth system processes such as weather and climate and biogeochemical cycles (e.g. carbon cycle). Conversely, the effect of climate variability (e.g. changes in precipitation and temperature) and human activities (e.g. water abstraction, and landuse change) on the water cycle is a major concern in water resources management [*St. Jacques et al.*, 2010; *Ferguson and Maxwell*, 2012]. Humans impact the hydrologic cycle at various scales. At a global scale, human-driven climate change is observed through alternating patterns and intensity of precipitation and temperature [*Bates et al.*, 2008] which in turn affects surface and groundwater storages. At local scales, water abstraction and consumption by humans directly alters surface water (e.g. lakes, rivers) and groundwater storages. Equally, natural climate variability, variation in intensity and duration of wet and dry condition, is as significant as human-driven processes that affect the water cycle [*Hulme et al.*, 1999; *Chen et al.*, 2012]. Thus, understanding the hydrologic system not only helps to solve water resources and environmental management problems but also facilitates the understanding of the Earth system processes.

Measurements of the various components of the terrestrial water cycle are necessary to better understand water cycle dynamics, assess the availability of fresh water resources, and evaluate the impacts on the water cycle due to humans and global changes.

However, the lack of continuous data availability and inadequate monitoring networks has been a challenge to the scientific community. It restricts our understanding of the spatial and temporal dynamics of the water cycle. For instance, most basins throughout the world, specifically those in non-industrialized countries, are poorly gauged but have increasing demands for water and a commensurate need to understand the hydrologic cycle. Fortunately, recent advancements in satellite-based hydrology have demonstrated that some water cycle components can be directly or indirectly estimated from space [*Njoku et al.*, 2003; *Famiglietti et al.*, 2004; *Andreadis and Lettenmaier*, 2006; *Alsdorf et al.*, 2007; *Milewski et al.*, 2009; *Vinukollu et al.*, 2011]. Some of the applications which use satellite remote sensing data to measure important terrestrial water balance components area discussed below.

1.2. Literature Review on Satellite Applications in Hydrology

Runoff

Runoff or stream flow estimation techniques from remote sensing satellite data, generally, can be categorized into two methods: (1) discharge - inundation area/width method and (2) discharge - stage/ water level elevation method. Variables such as stream inundation area/width, elevation or stream stage, or stream velocity and river morphology data can be remotely collected from satellites and used to estimate river discharge. The concept of flood inundation area mapping using satellite data is extended to estimate runoff with the assumption that stream inundation area/width has a relationship with stream stage or discharge. Most of the pioneering works of flood inundation area/width mapping and stream discharge estimation from remote sensing, as compiled by *Smith*

[1997], used data from passive and active satellite sensors such as Multi Spectral Scanner (MSS), Landsat TM, SPOT, ASTER, MODIS, SAR and SSM/I to extract width or area flooded by a stream. The optical and NIR sensors (e.g., Landsat TM, SPOT, and ASTER) are advantageous due to better spatial resolution but they have a cloud cover problem and poor temporal resolution. The microwave sensors (e.g., SAR, SSM/I) can provide data from hourly to daily range such as SSM/I, however, they have a poor spatial resolution (e.g. SSM/I = 25km) where their application merely depends on the size of the river.

Discharge - stage/water level elevation method from satellite altimetry data is analogous to discharge calculated from ground-based stream stage measurements. Radar altimetry satellites such as: GEOSAT (Frequency: Ku-band and return period: 17 days); TOPEX/Poseidon (T/P) - (Frequency: Ku & C band and return period: 10 days); ENVISAT (Frequency: Ku & S band and return period: 35 days); and more recently Jason-1/2 (Frequency: Ku & C band and return period: 10 days) which were developed for oceanographic applications, are the most successful in terrestrial applications specifically in estimating river discharge [*Kouraev et al.*, 2004; *Roux et al.*, 2008]. One of the disadvantages of satellite altimetry is their Low temporal resolution (e.g. T/P = 10 days and ENVISAT = 35 days) for measuring rapid discharge variation such as detecting flash floods. Moreover, they have poor spatial resolution (e.g., T/P has 0.5 to ~6km along the track spacing). With such poor spatial resolution, the possibility of getting water elevation measurements for most of the rivers in the globe is minimal. Runoff is the most important component of the water cycle, remote sensing based estimate of runoff is vital in data scarce regions where surface water monitoring network is almost nonexistent. It

has also been demonstrated that Satellite derived-runoff data can be used to calibrate hydrologic models in ungauged basins [*Getirana et al.*, 2009].

Evapotranspiration

Evapotranspiration (ET) is a key component of the water balance. Combined with rainfall and runoff, it determines the availability and distribution of water resources on Earth. ET has wide application in agricultural management, irrigation management (e.g. estimation of crop water requirements), drought assessment, climate change/variability (seasonal and inter-annual), etc. Quantifying ET is the most difficult due to surface heterogeneity and presence of several controlling variables (e.g., temperature, land use). Remote sensing provides a solution by representing the spatial heterogeneity of the Earth's surface. However, accuracy and poor spatial resolution are some of the limitations of ET estimation using remote sensing data. Estimation of ET from satellite data is based on the concept of energy balance approach (Equation 1-1), and variables extracted from satellite remote sensing data includes LAI (leaf area index), vegetation canopy, land surface temperature, and surface albedo. The energy balance equation used in ET estimation:

$$Rn = LE + H + G \qquad \text{Equation 1-1}$$

Where Rn: net radiant energy, LE: Latent Energy, H: sensible heat flux and G: soil heat flux.

There are different techniques of estimation of ET using satellite data: (1) a simple, direct empirical method which involves directly relating remote sensing based

thermal bands (e.g. LANDSAT TM band 6) to evapotranspiration using empirical equation; (2) complex energy balance modeling approach (e.g. SEBEL), various methods are summarized by *Courault et al.* [2005]. Sensors and bands used to estimate ET compiled from *Granger* [2000] and *McCabe and Wood* [2006] are:

- LANDSAT TM/ETM+: radiance from Thermal band (Band 6), Band 3 for surface albedo, and Band 3 & 4 used to calculate NDVI,
- ASTER: thermal bands (Bands 10 to 14),
- MODIS: surface temperature and emissivity from Band 11 L2, and NDVI - from MOD09GA product, land surface albedo from MOD03, and air temperature from MOD07, MOD35 - cloud mask, MOD05 - water vapor,
- AVHRR: surface temperature from channels 4 & 5.

Combinations of bands from different sensors are used to estimate surface albedo, vegetation and land surface parameters other than the thermal bands.

Soil moisture

Soil moisture is another key component of water cycle at the interface between land and atmosphere. It plays a key role in weather and climate processes, flooding, agricultural management, drought, and closely linked with other hydrologic processes such as ET, runoff, infiltration, and recharge. Microwave satellites (MWS) are suitable and being used to estimate soil moisture. Good temporal resolution of the MWS (hourly to daily) makes them convenient to detect soil moisture variability but they have very poor spatial resolution. Microwaves, characterized by large wavelengths, can penetrate vegetation coverage and soil to some extent. Unlike optical sensors, microwaves are less

susceptible to cloud cover and atmospheric effects. Moreover, microwaves, specifically active microwave satellites, are capable of collecting data during night times. Soil moisture retrieval from satellite data is based on the relationship between soil moisture and soil dielectric constant which influences brightness temperatures from passive microwaves sensors.

Some of the sensors and frequencies related to soil moisture measurement using satellite remote sensing are [*Kerr*, 2007; *Wagner et al.*, 2007; *Gruhier et al.*, 2010]:

- SSM/I: frequency 19 GHz (measures brightness temperature)
- AMSR-E (Advanced Microwave Scanning Radiometer): frequency 6.9, 10.7 and 36.5 GHz (all measures brightness temperature),
- TRMM-TMI: frequency 10.7 GHz (radiometer - measures the intensity of radiation)

Rainfall

Rainfall estimation from remote sensing data generally categorized into two: using visible (VIS) and infrared (IR) data and microwave (MW) satellite data. The VIS provides qualitative information about clouds. The thickest the cloud is the more opaque for the wavelength ranges in VIS. While IR sensors-based technique extract information indirectly by correlating rain rate to cloud reflected radiances or cloud temperature. MW based rainfall estimates works based on the interaction between microwaves with clouds and rain surface. This includes absorption - where raindrops absorb or emit MW radiation, and scattering - where the presence of ice particles scatters MW radiations. Microwaves are influenced by the nature of the emitting surface whether it is rough or

smooth, wet or dry and the size of particles through which it passes. The most commonly used VIS/IR and MW sensors are:

- GOES I-Imager: VIS and IR
- SSMI/I: passive MW
- TMI/TRRM: passive MW
- AMSR-E: passive MW
- GPM: Microwave Imager (GMI) and the Dual-frequency Precipitation Radar (DPR)

There are various algorithms that use data collected from a constellation of satellites in VIS/IR and MW products to estimate rainfall/precipitation. Some of the existing algorithm products are PERSIANN, CMORPH, TMPA, and IMERG.

Lake surface area and lake level

Measurement of lake height/inundation area from satellite remote sensing is analogous to the satellite-based stream flow measurement technique. Lake inundation area can be detected using VIS/NIR sensors whereas lake level/height is measured by satellite altimetry method. There are several methods for delineating lake/water inundation areas using VIS/NIR based remote sensing imagery [*Smith*, 1997; *Alsdorf et al.*, 2007; *Prigent et al.*, 2007; *Ward et al.*, 2014]. The Normalized Difference Water Index (NDWI), a commonly used optical remote sensing method, involves spectral index calculation of two or more spectral bands. Several NDWI equations were previously developed and tested for different satellite products [*Gao*, 1996; *McFeeters*, 1996; *Rogers and Kearney*, 2004; *Xu*, 2006]. *Ji et al.* [2009] analyzed different Modified

Normalized Difference Water Index (MNDWI) equations to determine the best performing index and establish appropriate thresholds for identifying water features from imageries such as LANDSAT, ASTER, and MODIS satellites. They suggested the MNDWI equation of (green - SWIR) / (green - SWIR), where the SWIR band in the region of shorter wavelength (1.2 - 1.8 mm), has the most stable threshold to map water bodies. The calculated MNDWI values range from -1 to 1with water pixels identified by MNDWI values within a range of 0 to 1. However, adjustment of a threshold value is necessary based on actual site conditions [*Ji et al.*, 2009].

Similar to stream stage measurement from satellite altimetry data, satellites are used to measure height variation of lakes. Some of the radar altimetry satellites used in measurement of height of water bodies include GEOSAT (Frequency: Ku-band and return period: 17 days); TOPEX/Poseidon (T/P) (Frequency: Ku & C band and return period: 10 days); ENVISAT (Frequency: Ku & S band and return period: 35 days); and more recently Jason-1/2 (Frequency: Ku & C band and return period: 10 days). Most of the existing satellite altimeters have poor temporal and spatial resolution. They have a limitation in capturing the rapidly varying terrestrial waters such as lake levels and river flows. The future advanced altimetry satellite – Surface Water & Ocean Topography (SWOT) mission will produce a water mask able to resolve 100 meter wide rivers and lakes wetlands, and reservoirs of 250 m^2 in size. It also provides water level elevations with an accuracy of 10 cm and a slope accuracy of 1 cm/1 km and has a repeat period of 20 days [*Biancamaria et al.*, 2015].

Terrestrial Water Storage (TWS) from GRACE

The GRACE satellite mission provides a global scale observation of changes in aggregated terrestrial water storage including a change in snow, surface water, soil moisture, and groundwater storages from space [*Rodell and Famiglietti*, 1999; *Wahr*, 2004]. GRACE mission has twin satellites flying in a tandem orbit approximately 220 km apart. The onboard microwave ranging system enables measuring orbital perturbations or (distance variations) between the satellites. This orbital perturbation data is related to variation in gravity caused by mass redistribution, beneath the satellites, on or below the surface of the earth. Water is a major contributor to this mass change on a monthly temporal scale, which allows the gravity anomaly data measured from GRACE to be processed and converted into a terrestrial water storage anomaly product [*Wahr et al.*, 1998]. The original GRACE's sensor data is converted into application, TWS end product by multiple processing centers including Center for Space Research (CSR), NASA Jet Propulsion Laboratory (JPL), German Research Centre for Geosciences (GFZ), and The Space Geodesy Research Group (GRGS). The different level of data and processing steps from sensor to end product (Water storage anomaly) are summarized below (source: processing centers web-site):

Level - 0: is the original sensor telemetry data which contains binary encoded instrument communication packet. It consists of science data (time stamp packet and science application packet) and housekeeping data (sensor calibration data).

Level - 1A: is a product after a non-destructive (reversible to level - 0) processing on level - 0 data. The processing involves conversion of the binary encoded

measurements to engineering units using sensor calibration factors. In addition, editing, quality control, time tagging of the data to the satellite receiver time, and reformatting for next processing is accomplished at the stage.

Level - 1B: a destructive (irreversible) processing applied at this stage. The data correctly time tagged, edited and decimated from the high rate samples of the instrument to low rate samples useable for further science processing. The content of the data at this level is:

- Dual-one-way ranging data (from the K-band),
- Star camera data (altitude)
- Accelerometer data (non-gravitational data)
- GPS tracking data
- Housekeeping data (instrument health and calibration data)
- Timing
- Orbital data

The processes from level - 0 to level - 1B collectively called Level - 1 processing.

Level - 2: gravity spherical harmonics data and the processing involve estimates of spherical harmonic coefficients of the exterior geopotential that represent the time-variable and average Earth gravity field.

To understand the differences between the available GRACE products, it is necessary to understand some of the concepts behind the level - 2 processing. The geopotential, exterior potential of the Earth system which includes the entire solid and

fluid, at a point exterior to the Earth between a unit mass and the Earth system may be represented by infinite spherical harmonic series. The geopotential at a fixed location (v) is variable in time due to mass movement and exchange between the Earth system components and is provided by GRACE.

$$V(r,\varphi,\lambda;t)=\frac{\mu}{r}+\frac{\mu}{r}\sum_{l=2}^{N_{\max}}\left(\frac{a_e}{r}\right)^l\sum_{m=0}^{l}\bar{P}_{lm}(\sin\varphi)\left\{\bar{C}_{lm}(t)\cos m\lambda+\bar{S}_{lm}(t)\sin m\lambda\right\} \quad \text{Equation 1-2}$$

Where r - geocentric radius, ϕ - geographic latitude, λ - longitude, μ - the gravitational constant of the Earth, and a_e - mean equatorial radius, P_{lm} (sinϕ) are the Associated Legendre Polynomials of degree l and order m; and C_{lm} and S_{lm} are the spherical harmonic coefficients of the geopotential.

GRACE mission provides an update to the existing Earth's gravity field models - the Background Models as well as provides information to previously unmodeled gravitational variations. Thus, there is an existing model and new capability from GRACE. The background model (e.g., EGM96, GGM02C) consists of mathematical models and the associated parameter values, which are used along with numerical techniques to predict the best-known value for the observable (in this case GRACE measured) gravitational field. The background model helps (1) to converge the model during processing of GRACE, (2) represent some geophysical variability that can be better determined by techniques other than GRACE. This model changes with the evolution of processing methods. Therefore, using new information from GRACE data, an update to the background gravity model is computed such that error in the estimate is

reduced. The geopotential product is the combination of the background model and GRACE product.

Level - 3: involves post-processing of GRACE-derived spherical harmonics gravity field into equivalent water thickness. The post-processing for land data uses the most recent released spherical harmonic solution (RL05). The processing steps involve:

- Filtering: two filtering steps applied, summarized from *Landerer and Swenson* [2012]: (1) de-striping which involves removal of systematic/correlated errors, which are stripes oriented north-south, from the spherical harmonics. (2) Gaussian filtering with a half width of 300km that reduces random errors not removed by de-striping. The Gaussian filtering is a smoothing operation that removes spherical harmonics of higher degree coefficients which are important for higher spatial resolution. Thus, this filtering reduces GRACE's spatial resolution.
- The filtering results in signal attenuation in GRACE estimate. Thus, to restore the signal attenuated during filtering operations, the GRACE TWS anomaly data is multiplied by a gain factor (Scaling) which was computed by applying the same filtering techniques (1 & 2) applied to GRACE data into a global land-hydrology model (NCAR's CLM4). Basically, this scaling (gain) factor is a multiplicative factor that minimizes the difference between the filtered and unfiltered water storage anomaly data.

- After de-striping, the monthly C20 (degree 2, order 0) coefficients estimated from GRACE, has significant errors, are replaced by those from Satellite Laser Ranging (SLR) analysis (recently they started using improved GRACE data).
- Lastly, correction is applied for atmospheric and Glacial Isostatic Adjustment.

After these processing steps, the equivalent water height over the land is calculated from the monthly gravity spherical harmonics (Cnm (t), Snm(t)):

$$\Delta\eta_{land}(\phi,\lambda,t)=\frac{a_E\rho_E}{3\rho_W}\sum_{n=0}^{40}\sum_{m=0}^{n}\frac{(2n+1)}{(1+k_n)}W_n P_{nm}(\sin\phi)\left\{\Delta\hat{C}_{nm}(t)\cos m\lambda+\Delta\hat{S}_{nm}(t)\sin m\lambda\right\}$$

$$W_n=\exp\left[-\frac{(nr/a_E)^2}{4\ln(2)}\right],$$

Equation 1-3

Where $\Delta\eta_{land}$ is water storage anomalies over the land, ρ_E is the average density of the Earth (5517 kg m-3), ρ_W is the density of fresh water (1000 kg m-3), a_E is the mean equatorial radius of the Earth, φ is the geographic latitude, λ is the longitude, $P_{nm}(\sin\varphi)$ are the fully-normalized Associated Legendre Polynomials of degree n and order m, r is the Gaussian averaging radius, and k_n are load Love numbers of degree n [*Chambers*, -].

The above processing techniques are more related to the processing of JPL, CSR and GFZ centers. They all follow the same approach/steps except in level - 2 processing.

Table 1-1. The differences in the background model and data processing between the GRACE processing centers.

	GRGS/CNES [*Lemoine et al.*, 2007]	**JPL**	**CSR**	**GFZ**
Geopotential field	EIGEN-GRACE-02S to degree and order 150	GIF48 to degree 180	GIF48 to degree & order 360	EIGEN-6C to degree & order 50
3D body perturbation	DE403			
Solid Earth tides	IERS2003	IERS2003	IERS2010	IERS2010
Ocean tides	FES2004 to degree and order 80	GOT4.7 to degree 90	FES2004/GOT4.8	EOT11a max. deg/order to 80
Atmospheric mass	ECMWF	ECMWF	ECMWF	ECMWF
Ocean mass	MOG2D	AOD1B	AOD1B	AOD1B

This means that they may have slightly different spherical harmonics solution, but the same level - 3 processing technique is applied to the spherical harmonic solution to convert it into equivalent water height. They differ in applying a background model (detail specification is found here: http://podaac.jpl.nasa.gov/gravity/grace-documentation). The processing methods are rapidly evolving that now their differences in background model become narrower to the point that the data products are almost identical (See Chapter 2). The GRGS/CNES processing center also follows a similar approach but different algorithm and background model. The major difference between the GRGS solution from the others (JPL, CSR, and GFZ) is that the GRGS use a different ocean barometric model (MOG2D ocean model) in their background model [*Lemoine et al.*, 2007]. To show some differences and characteristics of the background model used

by each processing centers, the information is summarized below (Table 1-1) (the information for JPL, CSR, and GFZ is taken from their documentation website).

GRACE applications

GRACE data have been utilized for various applications in hydrology. For example, it has been used to estimate change in groundwater storage [*Rodell and Famiglietti*, 2002; *Rodell et al.*, 2006; *Yeh et al.*, 2006]. Given information on the other components of change in terrestrial water storage (e.g., change in soil moisture, change in surface storage), one can infer changes in groundwater storage from GRACE data by subtracting the remaining water balance components. Information on the other components of the water cycle are often obtained from global land surface models (e.g. GLDAS). GRACE data have also been applied to estimate rates of groundwater depletion [*Rodell et al.*, 2009; *Feng et al.*, 2013; *Voss et al.*, 2013]. As the GRACE signal is mainly composed of subsurface waters (e.g., soil moisture, groundwater), with exceptions of large reservoirs and inundated areas, integrating GRACE data with land surface models (LSMs) enhances drought monitoring [*Yirdaw et al.*, 2008; *Houborg et al.*, 2012; *Li et al.*, 2012; *Long et al.*, 2013].

In conjunction with satellite altimetry data which provides change in the level of reservoirs, GRACE data was also used to assess wetlands, floodplains, and change in reservoir storage [*Swenson and Wahr*, 2009; *Lee et al.*, 2011]. Most of the global hydrologic simulations (e.g., Noah, VIC, and Mosaic) have limitations in simulating the sub-surface component (e.g. groundwater) of the water cycle. Thus, assimilation of GRACE data into land surface models yield improved simulations of water storage

components in global hydrologic models at a large-scale [*Zaitchik et al.*, 2008; *Werth et al.*, 2009a]. Moreover, *Lo et al.* [2010] and [*Sun et al.*, 2012] employed GRACE data to optimize parameters in land surface and regional groundwater models, respectively. Continental to global scale assessments of water storage characteristics from GRACE has been done in comparison with outputs from global land surface models [*Schmidt et al.*, 2006; *Syed et al.*, 2008; *Boy et al.*, 2011; *Yang et al.*, 2013]. In addition, uncertainty and accuracy analysis of GRACE data and the processing methods has been conducted by *Landerer and Swenson* [2012]; *Riegger et al.* [2012]; and *Werth et al.* [2009b].

Most of the existing applications of GRACE are implemented in regional to global scale. One of the limitations of GRACE satellite data is its poor spatial resolution which applies to some of the existing Earth resources satellite missions. For example, terrestrial water storage (TWS) anomaly from GRACE mission works best for a region with a size of at least 200,000 km^2 [*Yeh et al.*, 2006]. Though the benefit of obtaining the regional or global scale water storage characteristics of a given area from such kind of datasets is not trivial, integrating satellite-based data to solve local (i.e. small-scale) societal and environmental problems is essential. This is true, especially in data scarce regions where water cycle monitoring networks are absent or extremely limited. Therefore, research on the enhancement of the utility of satellite products in monitoring the water cycle at different scales is essential, especially to complement studies in the absence or malfunctioning of in-situ measurements.

Based on the above facts, the following research questions are formulated:

1. What is the spatial and temporal variability of hydrologic fluxes and storages on and below the surface of the Earth at different scales? How can we predict these variations more accurately?
2. How does the lack of data limit our ability to predict the terrestrial water cycle? What are the implications for water management, and understanding earth system processes?
3. How are the water cycle and coupled processes affected by humans, natural climate variability, and global change? Can the individual contributions be separated?

1.3. Research Objectives

The overall objective of this research is to integrate satellite and other (model-based or in-situ) datasets and model the hydrosphere for understanding terrestrial water cycle dynamics in relation to human impacts and climate variability at different scales, local to regional. Specific objectives include:

1. To evaluate terrestrial water storage estimated from two independent approaches: GRACE satellite mission and Integrated Hydrologic Model in the High Plains for understanding regional terrestrial water cycle,
2. To understand local (i.e. small-scale) terrestrial water storage anomaly by integrating GRACE-derived TWS anomaly with other satellite- and mode-based data along with in-situ observations,

3. To assess the relative impact of humans (e.g. abstraction) and climate variability on the terrestrial water cycle components.

References

Alsdorf, D. E., E. Rodríguez, and D. P. Lettenmaier (2007), Measuring surface water from space, *Reviews of Geophysics*, *45*(2).

Andreadis, K. M., and D. P. Lettenmaier (2006), Assimilating remotely sensed snow observations into a macroscale hydrology model, *Advances in Water Resources*, *29*(6), 872-886.

Bates, B., Z. W. Kundzewicz, S. Wu, and J. Palutikof (2008), Climate change and water, *Technical Paper of the Intergovernmental Panel on Climate Change (Geneva: IPCC Secretariat)*, pp 210–214.

Biancamaria, S., D. P. Lettenmaier, and T. M. Pavelsky (2015), The SWOT Mission and Its Capabilities for Land Hydrology, *Surveys in Geophysics*, *37*(2), 307-337.

Boy, J.-P., J. Hinderer, and C. Linage (2011), Retrieval of Large-Scale Hydrological Signals in Africa from GRACE Time-Variable Gravity Fields, *Pure and Applied Geophysics*, *169*(8), 1373-1390.

Chambers, D. P. (-), Converting Release-04 Gravity Coefficients into Maps of Equivalent Water Thickness, *Center for Space Research, University of Texas at Austin*, 9p, doi: http://grace.jpl.nasa.gov/files/GRACE-dpc200711_RL04.pdf.

Chen, Z., Y. Chen, and B. Li (2012), Quantifying the effects of climate variability and human activities on runoff for Kaidu River Basin in arid region of northwest China, *Theoretical and Applied Climatology*, *111*(3-4), 537-545.

Courault, D., B. Seguin, and A. Olioso (2005), Review on estimation of evapotranspiration from remote sensing data: From empirical to numerical modeling approaches, *Irrigation and Drainage Systems*, *19*(3-4), 223-249.

Famiglietti, J. S., R. S. J. Sparks, and C. J. Hawkesworth (2004), Remote sensing of terrestrial water storage, soil moisture and surface waters The State of the Planet: Frontiers and Challenges in Geophysics, *150*, 197-207.

Ferguson, I. M., and R. M. Maxwell (2012), Human impacts on terrestrial hydrology: climate change versus pumping and irrigation, *Environmental Research Letters*, *7*(4), 044022.

Gao, B.-C. (1996), NDWI A Normalized Difference Water Index for Remote Sensing of Vegetation Liquid Water From Space *REMOTE SENS. ENVIRON*, *58*, 257 - 266.

Getirana, A. C. V., M.-P. Bonnet, S. Calmant, E. Roux, O. C. Rotunno Filho, and W. J. Mansur (2009), Hydrological monitoring of poorly gauged basins based on rainfall–runoff modeling and spatial altimetry, *Journal of Hydrology*, *379*(3-4), 205-219.

Granger, R. J. (2000), Satellite-derived estimates of evapotranspiration in the Gediz basin, *Journal of Hydrology*, *229*(1-2), 70-76.

Gruhier, C., et al. (2010), Soil moisture active and passive microwave products: intercomparison and evaluation over a Sahelian site, *Hydrol. Earth Syst. Sci.*, *14*(1), 141-156.

Houborg, R., M. Rodell, B. Li, R. Reichle, and B. F. Zaitchik (2012), Drought indicators based on model-assimilated Gravity Recovery and Climate Experiment (GRACE) terrestrial water storage observations, *Water Resour. Res.*, *48*(7), W07525.

Hulme, M., Elaine M. Barrow, Nigel W. Arnell, Paula A. Harrison, Timothy C. Johns, and T. E. Downing (1999), Relative impacts of human-induced climate change and natural climate variability, *Nature*, *397*, 688-691.

Ji, L., L. Zhang, and B. Wylie (2009), Analysis of Dynamic Thresholds for the Normalized Difference Water Index, *Photogrammetric Engineering & Remote Sensing*, *75*(11), 1307 - 1317.

Kerr, Y. H. (2007), Soil moisture from space: Where are we?, *Hydrogeology Journal*, *15*(1), 117-120.

Kouraev, A. V., E. A. Zakharova, O. Samain, N. M. Mognard, and A. Cazenave (2004), Ob' river discharge from TOPEX/Poseidon satellite altimetry (1992–2002), *Remote Sensing of Environment*, *93*(1-2), 238-245.

Landerer, F. W., and S. C. Swenson (2012), Accuracy of scaled GRACE terrestrial water storage estimates, *Water Resour. Res.*, *48*(4), W04531.

Lee, H., R. E. Beighley, D. Alsdorf, H. C. Jung, C. K. Shum, J. Duan, J. Guo, D. Yamazaki, and K. Andreadis (2011), Characterization of terrestrial water dynamics in the Congo Basin using GRACE and satellite radar altimetry, *Remote Sensing of Environment*, *115*(12), 3530-3538.

Lemoine, J.-M., S. Bruinsma, S. Loyer, R. Biancale, J.-C. Marty, F. Perosanz, and G. Balmino (2007), Temporal gravity field models inferred from GRACE data, *Adv. Space Res.*, *39*(10), 1620-1629.

Li, B., M. Rodell, B. F. Zaitchik, R. H. Reichle, R. D. Koster, and T. M. van Dam (2012), Assimilation of GRACE terrestrial water storage into a land surface model: Evaluation and potential value for drought monitoring in western and central Europe, *Journal of Hydrology*, *446-447*, 103-115.

Lo, M.-H., J. S. Famiglietti, P. J. F. Yeh, and T. H. Syed (2010), Improving parameter estimation and water table depth simulation in a land surface model using GRACE water storage and estimated base flow data, *Water Resour. Res.*, *46*(5), W05517.

Long, D., B. R. Scanlon, L. Longuevergne, A. Y. Sun, D. N. Fernando, and H. Save (2013), GRACE satellite monitoring of large depletion in water storage in response to the 2011 drought in Texas, *Geophysical Research Letters*, *40*(13), 3395-3401.

McCabe, M. F., and E. F. Wood (2006), Scale influences on the remote estimation of evapotranspiration using multiple satellite sensors, *Remote Sensing of Environment*, *105*(4), 271-285.

McFeeters, S. K. (1996), The use of the Normalized Difference Water Index (NDWI) in the delineation of open water features, *International Journal of Remote Sensing*, *17*(7), 1425-1432.

Milewski, A., M. Sultan, E. Yan, R. Becker, A. Abdeldayem, F. Soliman, and K. A. Gelil (2009), A remote sensing solution for estimating runoff and recharge in arid environments, *Journal of Hydrology*, *373*(1–2), 1-14.

Njoku, E. G., T. J. Jackson, V. Lakshmi, T. K. Chan, and S. V. Nghiem (2003), Soil moisture retrieval from AMSR-E, *Geoscience and Remote Sensing, IEEE Transactions on*, *41*(2), 215-229.

Prigent, C., F. Papa, F. Aires, W. B. Rossow, and E. Matthews (2007), Global inundation dynamics inferred from multiple satellite observations, 1993–2000, *Journal of Geophysical Research*, *112*(D12).

Riegger, J., M. J. Tourian, B. Devaraju, and N. Sneeuw (2012), Analysis of grace uncertainties by hydrological and hydro-meteorological observations, *Journal of Geodynamics*, *59-60*, 16-27.

Rodell, M., and J. S. Famiglietti (1999), Detectability of variations in continental water storage from satellite observations of the time dependent gravity field, *Water Resour. Res.*, *35*(9), 2705-2723.

Rogers, A. S., and M. S. Kearney (2004), Reducing signature variability in unmixing coastal marsh Thematic Mapper scenes using spectral indices, *International Journal of Remote Sensing*, *25*(12), 2317-2335.

Roux, E., M. Cauhope, M.-P. Bonnet, S. Calmant, P. Vauchel, and F. Seyler (2008), Daily water stage estimated from satellite altimetric data for large river basin monitoring, *Hydrological Sciences Journal*, *53*(1), 81-99.

Schmidt, R., P. Schwintzer, F. Flechtner, C. Reigber, A. Guntner, P. Doll, G. Ramillien, A. Cazenave, S. Petrovic, and H. Jochmann (2006), GRACE observations of

changes in continental water storage, *Global and Planetary Change*, *50*(1-2), 112-126.

Smith, L. C. (1997), Satellite remote sensing of river inundation area, stage, and discharge: a reveiw, *Hydrological Processes*, *11*, 12.

St. Jacques, J.-M., D. J. Sauchyn, and Y. Zhao (2010), Northern Rocky Mountain streamflow records: Global warming trends, human impacts or natural variability?, *Geophysical Research Letters*, *37*(6), n/a-n/a.

Sun, A. Y., R. Green, S. Swenson, and M. Rodell (2012), Toward calibration of regional groundwater models using GRACE data, *Journal of Hydrology*, *422-423*, 1-9.

Swenson, S., and J. Wahr (2009), Monitoring the water balance of Lake Victoria, East Africa, from space, *Journal of Hydrology*, *370*(1-4), 163-176.

Syed, T. H., J. S. Famiglietti, M. Rodell, J. Chen, and C. R. Wilson (2008), Analysis of terrestrial water storage changes from GRACE and GLDAS, *Water Resour. Res.*, *44*(2), W02433.

Vinukollu, R. K., E. F. Wood, C. R. Ferguson, and J. B. Fisher (2011), Global estimates of evapotranspiration for climate studies using multi-sensor remote sensing data: Evaluation of three process-based approaches, *Remote Sensing of Environment*, *115*(3), 801-823.

Wagner, W., V. Naeimi, K. Scipal, R. Jeu, Mart, iacute, F. nez, aacute, J. ndez, and eacute (2007), Soil moisture from operational meteorological satellites, *Hydrogeology Journal*, *15*(1), 121-131.

Wahr, J., M. Molenaar, and F. Bryan (1998), Time-variability of the Earth's gravity field: Hydrological and oceanic effects and their possible detection using GRACE, *J. Geophys. Res.*, *103*(32), 20530.

Wahr, J., S. Swenson, V. Zlotnicki, and I. Velicogna (2004), Time-variable gravity from GRACE: First results, *Geophysical Research Letters*, *31*(11).

Ward, D. P., A. Petty, S. A. Setterfield, M. M. Douglas, K. Ferdinands, S. K. Hamilton, and S. Phinn (2014), Floodplain inundation and vegetation dynamics in the Alligator Rivers region (Kakadu) of northern Australia assessed using optical and radar remote sensing, *Remote Sensing of Environment*, *147*, 43-55.

Werth, S., A. Güntner, S. Petrovic, and R. Schmidt (2009a), Integration of GRACE mass variations into a global hydrological model, *Earth. Planet. Sci. Lett.*, *277*(1-2), 166-173.

Werth, S., A. Guntner, R. Schmidt, and J. Kusche (2009b), Evaluation of GRACE filter tools from a hydrological perspective, *Geophysical Journal International*, *179*(3), 1499-1515.

Xu, H. (2006), Modification of normalised difference water index (NDWI) to enhance open water features in remotely sensed imagery, *International Journal of Remote Sensing*, *27*(14), 3025-3033.

Yang, T., C. Wang, Z. Yu, and F. Xu (2013), Characterization of spatio-temporal patterns for various GRACE- and GLDAS-born estimates for changes of global terrestrial water storage, *Global and Planetary Change*, *109*, 30-37.

Yeh, P. J. F., S. C. Swenson, J. S. Famiglietti, and M. Rodell (2006), Remote sensing of groundwater storage changes in Illinois using the Gravity Recovery and Climate Experiment (GRACE), *Water Resour. Res.*, *42*(12), W12203 (12201-12207).

Yirdaw, S. Z., K. R. Snelgrove, and C. O. Agboma (2008), GRACE satellite observations of terrestrial moisture changes for drought characterization in the Canadian Prairie, *Journal of Hydrology*, *356*(1-2), 84-92.

Zaitchik, B. F., M. Rodell, and R. H. Reichle (2008), Assimilation of GRACE Terrestrial Water Storage Data into a Land Surface Model: Results for the Mississippi River Basin, *Journal of Hydrometeorology*, *9*(3), 535-548.

CHAPTER 2

MONITORING AND COMPARISON OF TERRESTRIAL WATER STORAGE CHANGES IN THE NORTHERN HIGH PLAINS USING GRACE AND IN-SITU BASED INTEGRATED HYDROLOGIC MODEL ESTIMATES

Seyoum, W. M., and A. M. Milewski, 2016, Monitoring and comparison of terrestrial water storage changes in the Northern High Plains using GRACE and in-situ based integrated hydrologic model estimates, accepted by *Advances in Water Resources*, Reprinted here with permission of publisher.

Abstract

Enhanced measurement of the variation of the terrestrial water cycle are imperative to better understand the dynamics, water availability, and evaluate impacts of global changes on the water cycle. This study quantified storage in the various terrestrial water compartments using an integrated hydrologic model (IHM) – MIKE SHE that simulates the entire terrestrial water cycle and the Gravity Recovery and Climate Experiment (GRACE) satellite data in the intensively irrigated Northern High Plains (area ~ 250,000 km2). The IHM, mainly constructed using in-situ data, was evaluated using field measured groundwater level, stream flow, and soil moisture data. The model was first used to calculate the incremental water storage for each water balance component (e.g. storage in the saturated zone) and then the GRACE equivalent terrestrial water storage anomaly. In the study area, storage in the saturated zone is the major component of the terrestrial water storage (TWS) anomaly. The GRACE-derived TWS anomaly and the anomaly simulated from the model are generally in agreement on a monthly scale with few discrepancies. Generally, both GRACE and the IHM results displayed a statistically significant increasing trend in the total TWS and groundwater storage anomalies from 2002-2013 over the Northern High Plains. This study demonstrates the applicability of an integrated hydrologic model to monitor TWS variations in a large area, and GRACE data and IHMs are capable of reproducing observed trends in TWS.

2.1. Introduction

Integrated measurements of the different components of the terrestrial water cycle are necessary to better understand water cycle dynamics, assess the availability of fresh water resources, and evaluate the impacts on the water cycle due to global changes (e.g. climate change). However, the lack of data availability restricts our understanding of the spatial and temporal dynamics of the water cycle. For instance, most basins throughout the world, specifically those in non-industrialized countries, are poorly gauged but have increasing demands for water and a commensurate need to understand water storage. Fortunately, recent advancements in satellite-based hydrology have demonstrated that some water cycle components can be directly or indirectly estimated from space [*Njoku et al.*, 2003; *Famiglietti et al.*, 2004; *Andreadis and Lettenmaier*, 2006; *Alsdorf et al.*, 2007; *Milewski et al.*, 2009; *Vinukollu et al.*, 2011; *Milewski et al.*, 2015; *Seyoum et al.*, 2015], particularly, the Gravity Recovery and Climate Experiment (GRACE) mission which estimates monthly terrestrial water storage anomaly (dTWS/dt). Therefore, research on the enhancement of the utility of satellite products in monitoring the water cycle is essential, especially to complement studies in the absence, or malfunctioning, of in-situ measurements.

Since its launch in 2002, GRACE has provided continuous measurements of change in TWS, including groundwater, soil moisture, surface water storage, snow and biomass storages, over basins larger than 200,000 km^2 [*Yeh et al.*, 2006], however partitioning the total signal into the aforementioned components has been one of the main challenges of GRACE studies. As such, GRACE data has been utilized for various applications in hydrology. For example, it has been used to estimate rates of groundwater

depletion [*Rodell et al.*, 2009; *Ahmed et al.*, 2011; *Feng et al.*, 2013], drought monitoring [*Houborg et al.*, 2012; *Long et al.*, 2013; *Thomas et al.*, 2014], and assessment of flood and surface reservoir storage changes [*Swenson and Wahr*, 2009; *Lee et al.*, 2011; *X Wang et al.*, 2011; *Zmijewski and Becker*, 2013; *Reager et al.*, 2014]. Integrating GRACE data with global land surface models improved global simulations of the water cycle [*Zaitchik et al.*, 2008; *Werth et al.*, 2009; *Lo et al.*, 2010] and enhanced monitoring of drought [*Yirdaw et al.*, 2008; *Houborg et al.*, 2012; *Li et al.*, 2012; *Long et al.*, 2013]. GRACE, along with in-situ water level measurements, has also been used to enhance the performance of a regional groundwater model [*Sun et al.*, 2012] and global hydrologic models [*Q Zhang et al.*, 2006].

The High Plains (HP) Aquifer is a heavily pumped groundwater system in the US As a result the groundwater levels in parts of this aquifer have declined and have garnered attention from scientists/investigators due to its importance for irrigation. From pre-development (~1950) to 2013, water-level changes in the High Plains range from a rise of 25 m in the north (due to recharge exceeding groundwater abstraction as a result of a combination of decreased withdrawals and increased wet years) to a decline of 78 m in the south [*McGuire*, 2014; *Haacker et al.*, 2015]. Several groundwater monitoring investigations were conducted in the High Plains [*Gutentag et al.*, 1984; *Nativ and Smith*, 1987; *McMahon et al.*, 2007; *Scanlon et al.*, 2012; *Butler et al.*, 2014], with a few using data derived from GRACE [*Jackson et al.*, 2005; *H J Wang et al.*, 2013]. *Strassberg et al.* [2009] included only groundwater and soil moisture as a total TWS component, resulting in a correlation coefficient of 0.72 between seasonal GRACE-based groundwater storage estimates and groundwater storage calculated from observation wells over the HP

Aquifer. In the same region, *Breña-Naranjo et al.* [2014] applied the same approach but accounted for the effect of irrigation on soil moisture and showed the significance of irrigation in estimating groundwater storage changes from GRACE.

Most published studies used a standard and similar approach to evaluate the performance of GRACE and to characterize water storage components from its data. This approach involved disaggregating the total GRACE-derived TWS using parameters (e.g. soil moisture storage) from independent products such as land surface models (e.g. GLDAS), and finally comparing the results with in-situ data (e.g. groundwater level measurements) [*Rodell et al.*, 2006; *Syed et al.*, 2008]. In addition to the bias from GRACE, the land surface model products which are used to disaggregate GRACE usually do not simulate and incorporate all the TWS compartments (e.g. groundwater storage). This potentially induces a large bias on the validation of GRACE products [*Rodell et al.*, 2006]. Therefore, an integrated model which simulates all the components in the terrestrial water cycle is needed to reliably estimate the change in TWS and validate the TWS anomaly from GRACE. Characterizing trends in each component of the TWS are needed as well.

The objective of this research was to compare the change in total water storage estimates and evaluate the GRACE-based dTWS/dt estimates using an integrated hydrologic model (IHM). The Northern High Plains (NHP) was selected to test the objectives on a scale closer to GRACE's resolution (~ 200,000 km^2) [*Yeh et al.*, 2006; *Longuevergne et al.*, 2010]. GRACE-derived change in TWS data were processed, analyzed, and compared with TWS anomaly data estimated using a regional, physically-based IHM (MIKE-SHE), which simulates the entire terrestrial water cycle (overland

flow, channel flow, evapotranspiration, flow in the unsaturated and saturated zone). The model was constructed using in-situ data and calibrated and validated using field measured stream flow, groundwater level, and soil moisture data. Thus, the calibrated model was used to calculate storage in each TWS compartments and estimate total TWS anomaly. Moreover, the trend in the change in TWS and the storage characteristics of each terrestrial water cycle compartments (e.g. unsaturated zone) were analyzed in the NHP.

2.2. Description of the Study Area

The High Plains Aquifer, with an area of 450,000 km^2 in the central part of the US, is an important source of water for drinking, agricultural, and industrial use. From the total groundwater abstraction for irrigation in the US, about 30 % is pumped from the High Plains which constitutes 27 % of the total irrigated land of the country [*Dennehy*, 2000]. The Northern High Plains, the northern section of the High Plains Aquifer, underlies about 250,000 km^2 of South Dakota, Wyoming, Colorado, Nebraska, and Kansas (Figure 2-1). It lies between the Central Lowlands on the east with an elevation of 330 m near the Missouri River and the Rocky Mountains on the west with an elevation of 2400 m. The HP is characterized by windy, less humid and dry climate with moderate precipitation and high evaporation [*Weeks et al.*, 1988]. Generally, the NHP is characterized by high evapotranspiration (average annual AET estimated by National Weather Service ~ 500 mm [*Stanton et al.*, 2011]) with recharge (potential annual recharge estimates in the NHP ranges from 50 – 125 mm [*Stanton et al.*, 2011]) to the aquifer occurring during non-growing seasons when evapotranspiration is low. Precipitation varies from west to east, with annual precipitation ranges from 350 mm in

the western to 750 mm in the eastern sections of the NHP. The average annual minimum and maximum temperatures are ~ 1^0C and 18^0C, respectively. Most of the water pumped from the aquifer is used for irrigation. The landuse is dominated by cropland and rangeland, and the dominant crops growing in the area are corn and soybean (Figure 2-2a).

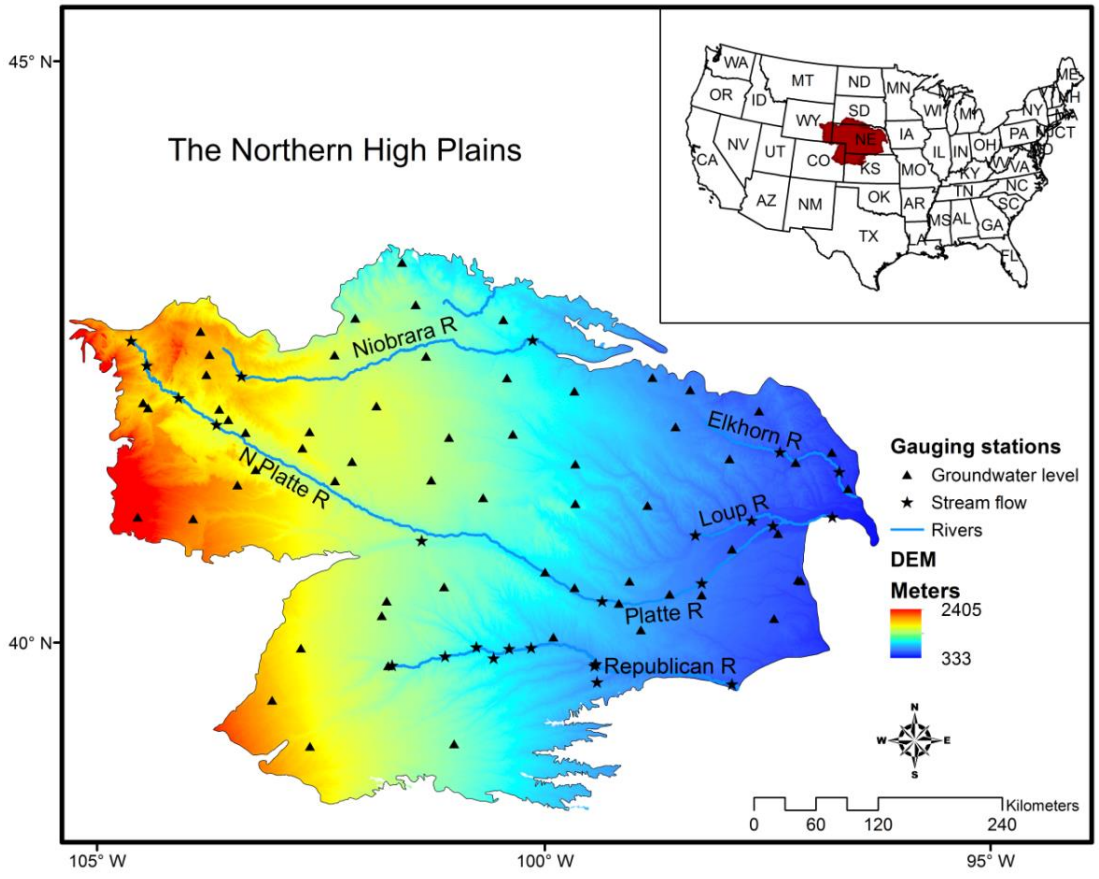

Figure 2-1. Location map of the Northern High Plains Aquifer. Also shown is the topography, rivers (simulated in MIKE11 model), and location of gauging stations used in model construction and evaluation.

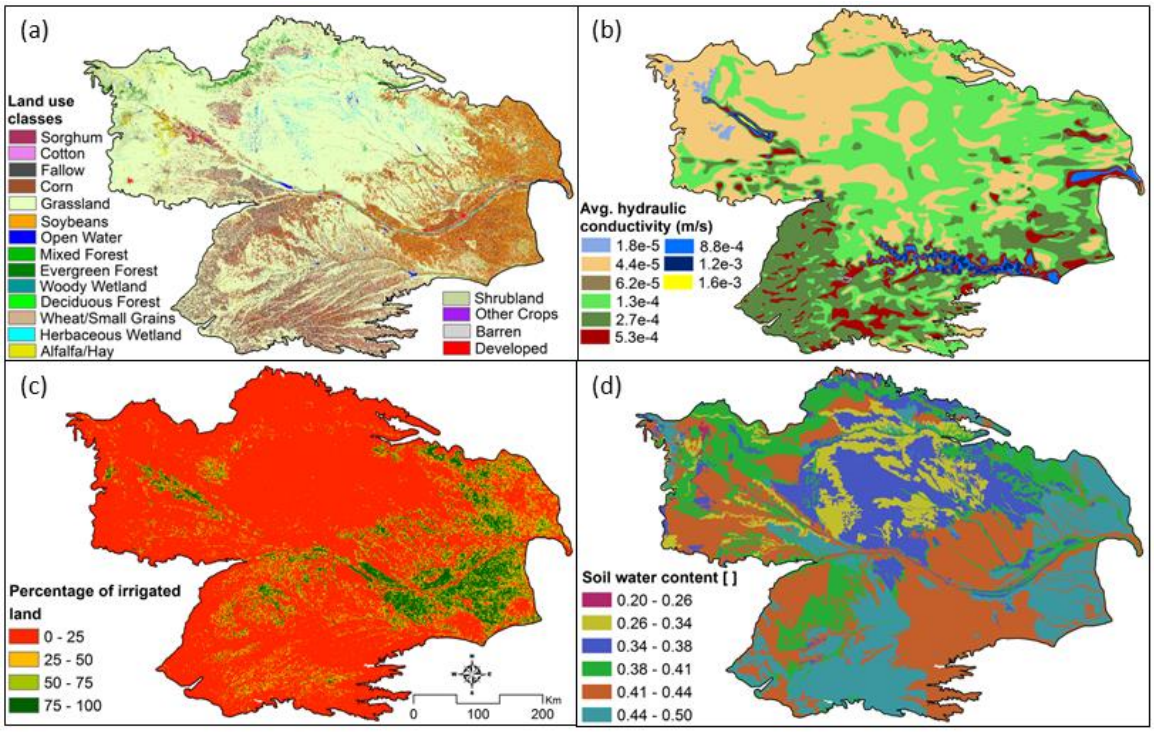

Figure 2-2. Model input data: (a) landuse (modified from [*Houston et al.*, 2011]), (b) hydraulic conductivity (modified from [*Cederstrand and Becker*, 1998]), (c) irrigated land acreage (modified from [*Pervez and Brown*, 2010]), and (d) soil water content at field capacity (modified from [*Miller and White*, 1998]).

The lithological units, groundwater recharge, and pumping vary spatially throughout the NHP, which results in both temporal and spatial variation in total water storage change. For example, from pre-development to 2013, groundwater level declines in the southern section of the NHP in northwest Kansas and rises in the central part of NHP near the sand hills and along the Platte River valley [*McGuire,* 2014]. The High Plains Aquifer consists of six major, interconnected hydrogeologic units of Tertiary and Quaternary age [*Gutentag et al.*, 1984]: the Brule Formation, the Arikaree Formation, the Ogallala Formation, the Sand Hills, the Eastern Nebraska, and the Platte River Valley

units [*Stanton and Qi*, 2007]. The Ogallala Formation, the principal aquifer system, consists of unconsolidated sand, gravel, clay, and silt. The Brule Formation is mainly massive siltstone that contains beds of sandstone, volcanic ash, claystone, and fine sand with little permeability. The Arikaree Formation is predominantly fine-grained sandstone with localized beds of ash, silt, and clay [*Weeks et al.*, 1988].

The Sand Hills is characterized by fine to medium sand, high infiltration rates, and most of the groundwater recharge occurs through this formation found in the northcentral part of the study area. The Northern High Plains aquifer is underlain by bedrock formations of tertiary and cretaceous age and generally has little permeability [*Gutentag et al.*, 1984]. The main soil types in the NHP are silt, loam, and sand; however, clay loam, loam, and sandy loam are also present to a lesser extent.

2.3. Methods and Data

GRACE

The GRACE mission consists of two identical satellites orbiting in tandem at ~500 km altitude with an along-track separation distance of ~220 km and inclination of 89.5^{o} [*Tapley and Bettadpur*, 2004]. The onboard K-band microwave ranging system measures the variation in speed and distance between the twin satellites caused by a variation in the orbital motion of the satellites which is caused by the variations in the gravitational field related to mass change beneath the satellites. Water is a major contributor to this mass change on a monthly temporal scale, which allows the gravity anomaly measurement from GRACE to be processed and converted into a terrestrial water storage anomaly product [*Wahr et al.*, 1998]. The GRACE satellite mission

provides aggregate changes in total terrestrial water storage (i.e. change in snow, surface water, soil moisture, and groundwater) with a global coverage [*Rodell and Famiglietti*, 1999; *Wahr et al.*, 2004]. The GRACE data used in this study is based on the latest version (RL-05 gridded (1^{o}x1^{0})) level-3 data from CSR, JPL, and GFZ processing centers [*Swenson and Wahr*, 2006; *Landerer and Swenson*, 2012]. GRACE land data are available at http://grace.jpl.nasa.gov, supported by the NASA MEaSUREs Program.

The data obtained ranges from April 2002 to November 2014 and was processed for the study site. The GRACE data was multiplied by the supplied scale factors to increase the signal to noise ratio which is reduced during the sampling and post-processing of GRACE observations. The long-term average was removed from each GRACE grid to compare the GRACE data with results from the model simulations [*Landerer and Swenson*, 2012]. According to *Sakumura et al.* [2014], an ensemble GRACE gravity solution from the three processing centers (JPL, GFZ, and CSR) has less noise as compared to the individual GRACE solutions, thus an ensemble mean GRACE solution was processed and used for comparison with dTWS/dt generated from the IHM. To show the variability among these products, area averaged time-series dTWS/dt of the three processing centers and the ensemble was constructed (Figure 2-3). As it is shown in the Figure, there is no large difference between the dTWS/dt products from the different processing centers and all fall within the uncertainty of GRACE data. Moreover, leakage and measurement errors on the scaled GRACE data for the study area were calculated and included in the analysis. Forty- six (1^{0}x1^{0}) GRACE grid cells were considered including cells partly fall on the boundary of the study area.

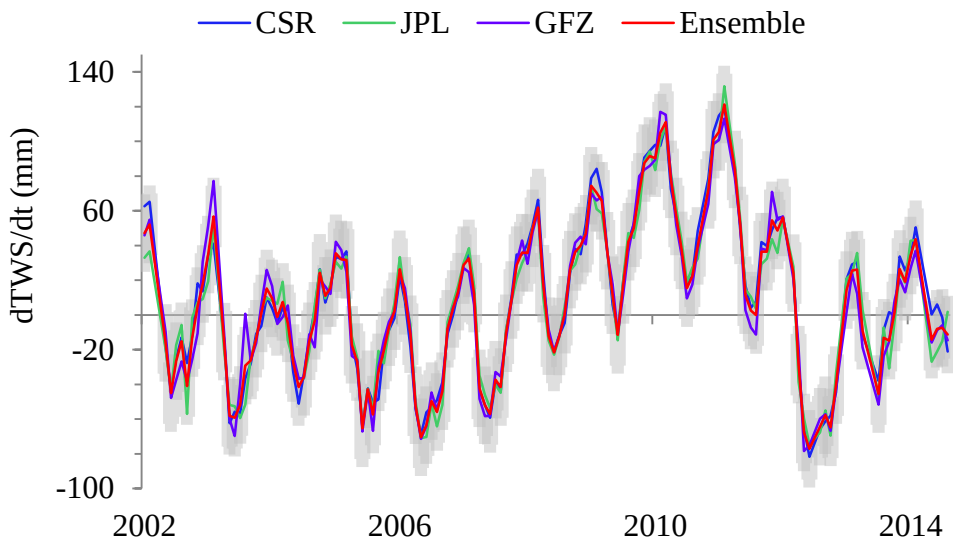

Figure 2-3. Area-averaged time-series of monthly dTWS/dt (mm) for products from different processing centers (CSR, JPL, and GFZ) and their ensemble with error (measurement error and leakage error) (shaded) in the NHP.

Integrated Hydrologic Model (IHM) description

The integrated hydrologic model - MIKE SHE, a fully-distributed physically based model, coupled with MIKE11 simulates the complete terrestrial water cycle including evapotranspiration, overland flow, flow in streams/rivers, flow in the unsaturated zone and saturated zone. The water movement module in MIKE SHE combines different process-based parameters (main model parameters and modules shown in Table 1) each describing the main processes in individual components of the hydrological cycle. MIKE SHE coupled with MIKE11 simulates a 1D channel flow in rivers/streams using diffusive wave version of the Saint Venant equation. As stream flow is an important component of the terrestrial water balance (streams drain water from the aquifer, drain the basin as well), simulating the stream is relevant to estimate the

dTWS/dt. MIKE11 has four components: the river network, the cross-section, boundary condition, and the hydrodynamic components. The coupling (using river link cells) allows MIKE SHE to simulate groundwater surface water interaction using MIKE11. Darcy's equation is used to calculate the balance (inflow and outflow) between the aquifer and rivers on these link cells. Two-dimensional overland flow can be simulated using a finite difference or sub-catchment method.

MIKE SHE simulates flow in the unsaturated zone using Richards' Equation, gravity flow or a two-layer water balance method. A two-layered water balance approach (used in this study), which divides the unsaturated zone into root zone (ET can occur) and below the root zone (where ET doesn't occur), depends on soil parameters such as available water content at saturation, field capacity, and wilting point, ET depth, and the groundwater water table. The saturated zone is simulated by either finite-difference or the linear reservoir method. Evapotranspiration is calculated based on a modification of the *Kristensen and Jensen* [1975] method. Additional information and description of the MIKE SHE model can be referred found in *Abbott et al.* [1986a], *Abbott et al.* [1986b], *Graham and Butts* [2005], and *DHI* [2012]. MIKE SHE has been widely applied in integrated hydrologic studies [*Refsgaard et al.*, 1998; *Andersen et al.*, 2001; *Sonnenborg et al.*, 2003; *McMichael et al.*, 2006; *Zhiqiang et al.*, 2008; *S Wang et al.*, 2012; *Qin et al.*, 2013].

Model characteristics

The NHP model is discretized by a cell size of 1 km by 1 km and consists of nearly 250,000 active cells. The model was simulated on a daily time-scale from 2000 to

2013 and results were calculated on a daily time-scale and aggregated to a monthly time-scale to match the temporal resolution of GRACE. Though the aquifer in the NHP is complex and heterogeneous, the model was constructed as a single-layered aquifer with spatially variable hydraulic conductivity (Figure 2-2b), and vertical hydraulic conductivity was $1/10^{th}$ of the horizontal hydraulic conductivity [*Luckey and Becker*, 1999; *Davis and Putnam*, 2013]. Regionally, the vertical distribution of sediment layers in the High Plains is random [*Gutentag et al.*, 1984], which makes it difficult to build a multi-layered integrated model. In addition, at a regional scale (at the scale of the study), horizontal flow is a significant component of the groundwater flow where the vertical flow is assumed to be much smaller than the horizontal. Thus, a single-layered model is considered in this simulation.

The saturated zone was simulated using a finite-difference method where the unsaturated zone was simulated using a two-layered water balance approach. The aquifer in NHP terminates on the boundary of the study area (except the southern edge) which consists of the erosional extent of the formations of the HPA [*Luckey and Becker*, 1999]). Thus, a no-flow boundary was used. Since only the vertical flow (drainage) was simulated in the unsaturated zone, the same boundary was applied for the unsaturated zone. However, in places where there are surface inflows into the study area (e.g. South Platte River), surface flux boundaries were considered in the MIKE11 model. Large rivers (North Plate, Plate, Republican, Loup, Niobrara, and Elkhorn) were simulated using the coupled MIKE11 model given the significant surface water and groundwater interactions in the area. Tributaries to these rivers were included as inflow boundaries to

the main river channels in the MIKE11 model depending on the availability of in-situ measured discharge data.

Irrigation constitutes the majority (95%) of water consumption which predominantly originates from groundwater in the High Plains, thus is an important component in the water cycle. For instance, in 2005, nearly 95% of groundwater withdrawal in Nebraska (approximately occupies 70% of the study area) was used for irrigation (NDNR water use report: http://www.dnr.ne.gov/swr/nebraska-surface-water-and-groundwater-use---2005, accessed in 11/2/2014). Groundwater contributed approximately 87% of the total water used for irrigation in 2005 with the remaining 13% from surface water. Thus, groundwater withdrawal for irrigation was considered in the model using the irrigation module in MIKE SHE where irrigation from surface water was omitted due the non-practicality in the model and scale of the study area. Omitting irrigation from surface water, however, could lead to an underestimate or overestimate of water balance components (e.g., underestimate of recharge, overestimate of stream flow). Recharge would be underestimated due to the exclusion of the irrigation return flow component from surface water irrigation in the water balance.

Data sources

The main data input requirements for MIKE SHE include climatic data, topography, river channel information, vegetation and landuse, soil properties, and aquifer characteristics. Multi-resolution (3, 10, and 30 m) Digital Elevation Models (DEM) were obtained from GEOSPATIAL DATA GATEWAY of USDA-NRCS (http://datagateway.nrcs.usda.gov/, accessed in 8/21-9/19/2014) and used as topography (30 m resolution) in MIKE SHE and to extract river cross-sections (3 and 10 m

resolutions) for the MIKE11 model. The daily meteorological data, including precipitation data (178 stations) was obtained from the NOAA National Climatic Data Center. The temperature (39 stations) and reference evapotranspiration data (calculated using the Penman method from 53 stations in the study area) were acquired from the High Plains Regional Climate Center (HPRCC) and used as climatic data for the model. The Thiessen polygon spatial interpolation scheme was applied to the meteorological datasets.

The landuse data, obtained from USGS Data Series 777 (available at: http://pubs.usgs.gov/ds/777/), is an annual Model-Backcasted Land-Use/Land-Cover Raster dataset from USGS-EROS [*Houston et al.*, 2011]. Landuse was assumed to be the same for the entire simulation period given the short simulation period; however seasonality of the dominant land cover classes such as corn (Figure 2-2a) were considered in the model. A one km resolution dataset for irrigation acreage data (Figure 2-2c) was obtained from the USGS [*Pervez and Brown*, 2010; *Brown and Pervez*, 2014] and county-based irrigation requirement data was acquired from the Nebraska Department of Natural Resources (http://www.dnr.ne. gov/swr/ net-irrigation-requirement-map-may-2006, accessed 11/2/2014), and used in the irrigation module of MIKE SHE.

Model input data for the unsaturated zone was obtained from CONUS-SOIL, which is a modified version of the STATSGO soil dataset for environmental applications [*Miller and White*, 1998]. From this dataset, soil variables for MIKE SHE such as saturated water content (0.20-0.50), permeability (10^{-3}-10^{-4} m/s), and field capacity (0.1-0.5) (Figure 2-2d) were extracted and used as inputs to the model. The saturated zone

information required in the model, including the aquifer boundary, depth of the bedrock, depth-integrated hydraulic conductivity, and specific yield data were acquired from USGS datasets [*Cederstrand and Becker*, 1998; *Houston et al.*, 2011].

Model calibration and validation

Various approaches were implemented to evaluate the performance of the model. Firstly, the model was calibrated and evaluated using stream flow, water table depth, and in-situ soil moisture data. Model calibration was conducted using data from 2002-2007 while the model was validated with the data from 2008-2013, all the simulations were carried out with a two year warm up period from 2000-2001. Daily continuous stream flow (5 stations) and groundwater level measurements (25 stations) obtained from the USGS were used to calibrate the transient simulation while spatial verification was performed using periodic measurements from an additional 40 spatially distributed groundwater level measurement stations. Furthermore, the water storage estimates from the model were verified using estimates by other studies [*McGuire*, 2009; 2014]. Lastly, output data from the model (e.g., root zone water content, soil infiltration) was compared with in-situ soil moisture data. The model simulated root depths in the NHP ranges from 0 in barren soils to 60 cm; the average root zone depth is about 30 cm. Therefore, the model simulated root zone water content was compared with in-situ average soil moisture content measured at depths of 10, 25, and 50 cm from different locations in Nebraska (obtained from HPRCC).

Model calibration was conducted using both manual and automatic calibration (using the Autocal tool in MIKE SHE) techniques. First, a sensitivity analysis was conducted to identify the sensitive model parameters, followed by calibration of the most

sensitive model parameters. The MIKE SHE model was initialized with baseline input parameter values (Table 2-1), during calibration the model was repeatedly run with alternative parameter values until satisfactory objective functions were achieved. Four objective functions were used to evaluate model performances including the mean error (ME), correlation coefficient (r), root-mean-square-error (RMSE), and Nash-Sutcliffe Efficiency (NSE). Considering the scale and purpose of the model and similar previous regional studies [*Sonnenborg et al.*, 2003; *Van Liew et al.*, 2007; *Zhiqiang et al.*, 2008; *Davis and Putnam*, 2013; *Qin et al.*, 2013], the calibration targets for comparison between observed and simulated data on a daily time scale were ME < 0.5 m, r > 0.5, and RMSE < 1m for groundwater levels and r > 0.5 and NSE > 0.35 values for river discharge data.

TWS anomaly calculation

The following water balance equation was used to represent all compartments of the terrestrial water storage in order to estimate water storage values from the IHM:

$$WS = PWS + CIS + SWE + UZS + SZS \qquad (1)$$

Where WS indicates the total water storage in the basin; PWS represents water stored on the surface (surface water ponding); CIS is canopy interception storage; SWE denotes water stored in the form of snow; UZS is water stored between the ground surface and the water table; and SZS represents water storage below the water table. All of the storage components are instantaneously accumulated water storage values. The GRACE equivalent TWS anomaly from the model was derived by subtracting the long-term average accumulated water storage from each instantaneous water storage value (WS).

Error calculation for water storage estimates from IHM

There are various sources of uncertainties in the estimate of dTWS/dt from the IHM. These include uncertainty from input data to the model, model structure (e.g. conceptual model), and model parameter uncertainties. In addition to model performance evaluation, an uncertainty analysis was implemented to calculate the bias on water storage estimate arising from model structure and model parameter uncertainties. The approach is based on observed and simulated river discharge data of the major rivers. As runoff is a main component of the water balance, estimating error using observed versus simulated runoff may indirectly provide the uncertainty on the estimate of the total water balance calculated from the IHM. Therefore, percent error, which is the difference between the simulated and observed river discharge data as a percentage of the observed, was calculated for the rivers which have an outlet in the model (e.g., Platte, Elkhorn, and Republican rivers). Particularly, the Platte River, which constitutes 90% of the total outflow from the model (the one with relatively significant deviation from the observed), was chosen to represent the percent error calculation.

2.4. Results and Discussion

Model evaluation

The calibration results indicated the model is generally sensitive to the subsurface parameters, hydraulic conductivity, and soil properties (Table 2-1). The water table is most sensitive to hydraulic conductivity, soil water content at field capacity, and water content at saturation. In addition, parameters such as Evapotranspiration (ET) depth and detention storage (overland flow parameter that controls the amount of surface water

ponding) also influence the water table. The surface runoff is highly dependent on surface parameters such as detention storage and the Manning numbers of both overland flow and rivers. Manning numbers control the velocity of surface runoff and flow in the channels, higher manning number results in faster water movement to the outlet of the basin. Hydraulic conductivity, which controls base flow to streams, was a significant subsurface parameter affecting surface runoff.

Root depth distribution (landuse parameter) was also a sensitive parameter for the groundwater table. In such an irrigated region, root depth, which controls the amount of storage in the root zone, plays a significant role in the amount of groundwater recharge. Soil permeability, subsurface drainage characteristics (drainage depth and time constant), and aquifer storage parameters showed little effect on both stream flow and groundwater table depth. Horizontal hydraulic conductivity and detention storage were the two most sensitive parameters for the saturated zone and stream flow, respectively. The scaled sensitivity coefficient values of these parameters were an order of magnitude higher than the rest of the parameters. Horizontal hydraulic conductivity and detention storage would probably have the most contribution to the result regarding uncertainties that comes from model parameters.

Table 2-1. Parameters of the different components of the MIKE SHE/MIKE11 model, model initialization values, and sensitivity ranking (1 is the most sensitive, NS: not sensitive).

Parameters	Initial values	Sensitivity ranking to water table	Sensitivity ranking to stream flow	Aggregate Ranking
Saturated zone				
Horizontal hydraulic conductivity [m/s]	0.0012 - 1.8E-5	1	3	1
Vertical hydraulic conductivity [m/s]	0.1*Kh			
Specific yield [ ]	0.1 - 0.25	NS	NS	NS
Storage coefficient [m^{-1}]	1.00E-05	12	13	12
Unsaturated zone				
Soil permeability[m/s]	1E-4 - 1E-7	12	14	12
Water content at field capacity [ ]	0.1 - 0.5	2	7	2
Water content at saturation [ ]	0.2 - 0.5	3	8	3
Evaporation surface depth [m]	0.2	4	5	4
Overland flow				
Manning number [$m^{1/3}/s$]	10	7	4	8
Detention storage [mm]	40	5	1	5
River				
Manning number [$m^{1/3}/s$]	30	8	2	6
Leakage [s^{-1}]	1.E-05	9	6	9
Evapotranspiration				
LAI [ ]	0 - 6	11	12	11
Root depth [mm]	0 - 600	6	9	7
Snow melt				
Degree day coefficient [mm/C/d]	2	10	10	10
Drainage				
Time of concentration [sec^{-1}]	1.E-07	14	11	14
Drainage depth [m]	1	NS	NS	NS

Model calibration was accomplished through transient simulations using daily continuous groundwater table, stream flow, and soil moisture measurements. Spatial verification was also performed using averaged periodic measurements. The calibration

results are summarized in Table 2-2. The model calibration was considered satisfactory taking into account the scale of the model and complexity of the hydrologic system within the study area, with an average ME, r and RMSE values of -0.11 m, 0.63, and 1.17 m, respectively for the overall simulation period (2002-2013) (groundwater only). Generally, the groundwater simulation was also satisfactorily evaluated using data independent of the calibration period (2008-2013), with the exception that in some of the wells the model validation over-predicted the groundwater table (Figure 2-4b) and did not simulate the seasonal variation due to pumping (Figure 2-4c). Moreover, comparison of average simulated water table depth with average water table depth from periodic groundwater level measurements indicated an R^2 value of 0.99 showing a good simulation spatially.

Some of the groundwater level measurements calibrated by the model performed well with calibration statistics (ME value near 0.30 m, r range between 0.80 – 0.90, and RMSE as low as 0.43 m) (Figure 2-4). However, some groundwater observations have low calibration statistics of -2.95 m, 0.07, and 4.27 m for ME, r, and RMSE, respectively. This is mainly attributed to the necessary simplification in the conceptual model and lack of detailed information about irrigation. As the model is a regional model, local variations may be omitted in the conceptual model (e.g. perched water table). Locally, the aquifer materials in the High Plains are discontinuous and vertically randomly distributed [*Gutentag et al.*, 1984], unlike the model where a continuous single aquifer layer was considered. The other factor could be the lack of irrigation information where the large deviations between the simulated and observed groundwater table depth in few gauging stations occurred during the irrigation season (Figure 2-4c).

Table 2-2. Summary of model performance evaluation statistics (ME: Mean Error, MAE: Mean Absolute Error, RMSE: Root Mean Square Error, STDres: Standard Deviation of Residuals, r: Pearson Correlation, and NSE: Nash-Sutcliffe Efficiency) derived from average daily values from 25 groundwater level and 5 stream flow gauging stations.

		ME	**MAE**	**RMSE**	**STDres**	**r**	**NSE**
Stream flow	Calibration (2002-2007)	-7.70	13.47	18.18	14.86	0.58	0.37
	Validation (2008-2013)	-3.68	14.76	23.66	22.50	0.70	0.48
	Overall (2002-2013)	-5.99	14.02	20.73	18.66	0.70	0.50
Groundwater level	Calibration (2002-2007)	-0.14	0.77	0.94	0.70	0.60	-
	Validation (2008-2013)	-0.02	1.05	1.29	0.83	0.51	-
	Overall (2002-2013)	-0.11	0.92	1.17	0.99	0.63	

The calibrated rivers had average overall statistics (ME, RMSE, r, and NSE) values of -6 m^3/s, 21 m^3/s, 0.70, and 0.50, respectively. The model performs well for the simulation of flow in the upstream rivers (e.g. North Platte River) with calibration statistics as high as r = 0.88 – 0.99 and NSE = 0.76 – 0.97 (Figures 2-5a and 2-5b). However, near the outlets (downstream) of the rivers, the model calibration statistics are relatively low. For example, calibration statistics at the outlets of Republican and Platte rivers show values as low as r = 0.35 – 0.75 and NSE = 0.20 – 0.41 (Figure 2-5c). These rivers are major rivers providing water supply in the area, the major deviation between simulated and observed data is probably due to the exclusion of diversions and reservoirs as well as water consumption from these rivers in the conceptual model. As surface water is one of the major components of the water balance, this may contribute to the total bias in the calculated storage values of the terrestrial water storage components from the model.

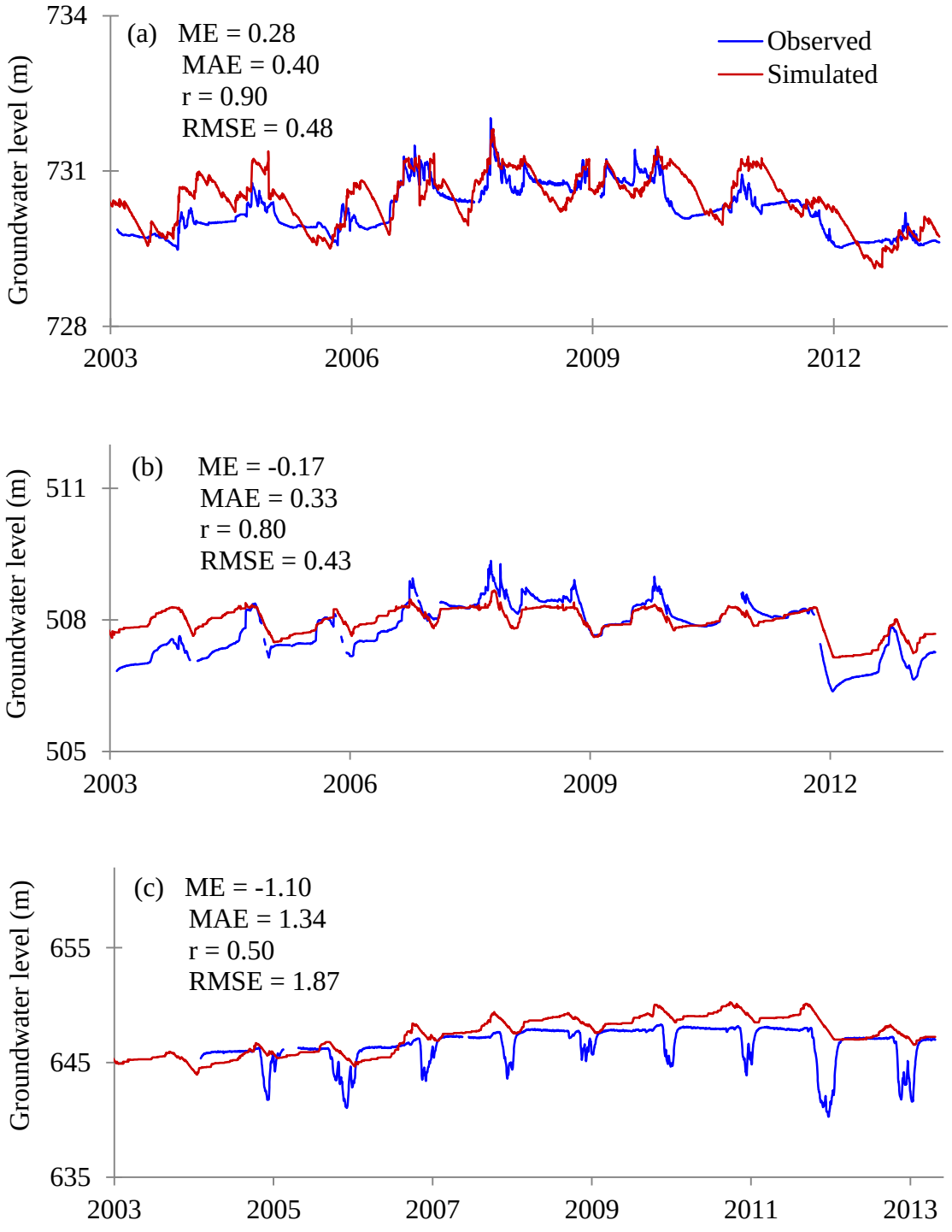

Figure 2-4. Daily observed and model simulated groundwater levels with calibration statistics (a) USGS well no. 404717099460501 (b) USGS well no. 410943097575001 and (c) USGS well no. 413156098591201.

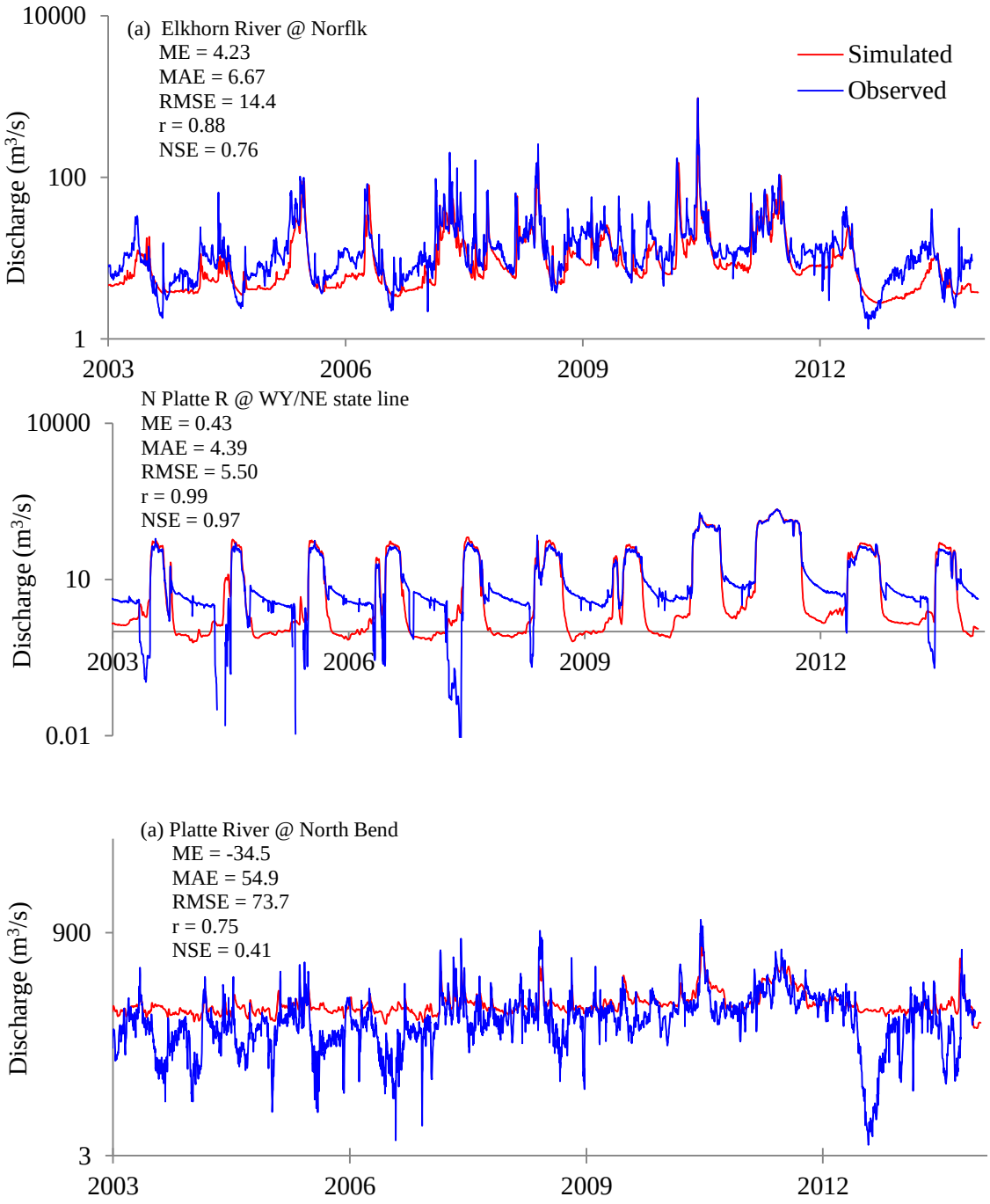

Figure 2-5. Comparison of daily observed and model simulated river discharge with calibration statistics (a) Elkhorn River (b) North Platte River and (c) Platte River.

In-situ soil moisture data was compared with model simulated soil moisture variables (root zone water content) on a daily time scale. The time-series comparison result between model simulated soil water content and in-situ measured soil moisture displayed that the model satisfactorily simulated the moisture content on a daily time scale with correlation coefficients (r) in the range of 0.42 to 0.70 with an average value of 0.56. Figure 2-6 shows the comparison of daily model simulated root zone water content vs. averaged daily in-situ measured soil moisture (measured at 10, 25, and 50 cm) for selected stations within the study area. The model simulated the amplitude/peak moisture contents as well as the timing of the wet and dry periods. Generally, the model simulated the water content satisfactorily except in some instances where the model slightly overestimated (Figure 2-6b) and underestimated water content in the unsaturated zone (Figure 2-6d). Considering the spatial resolution of the model (1 km) and temporal variability of soil moisture content, such correlation with point measurements provides confidence of water storage estimates from the integrated hydrologic model.

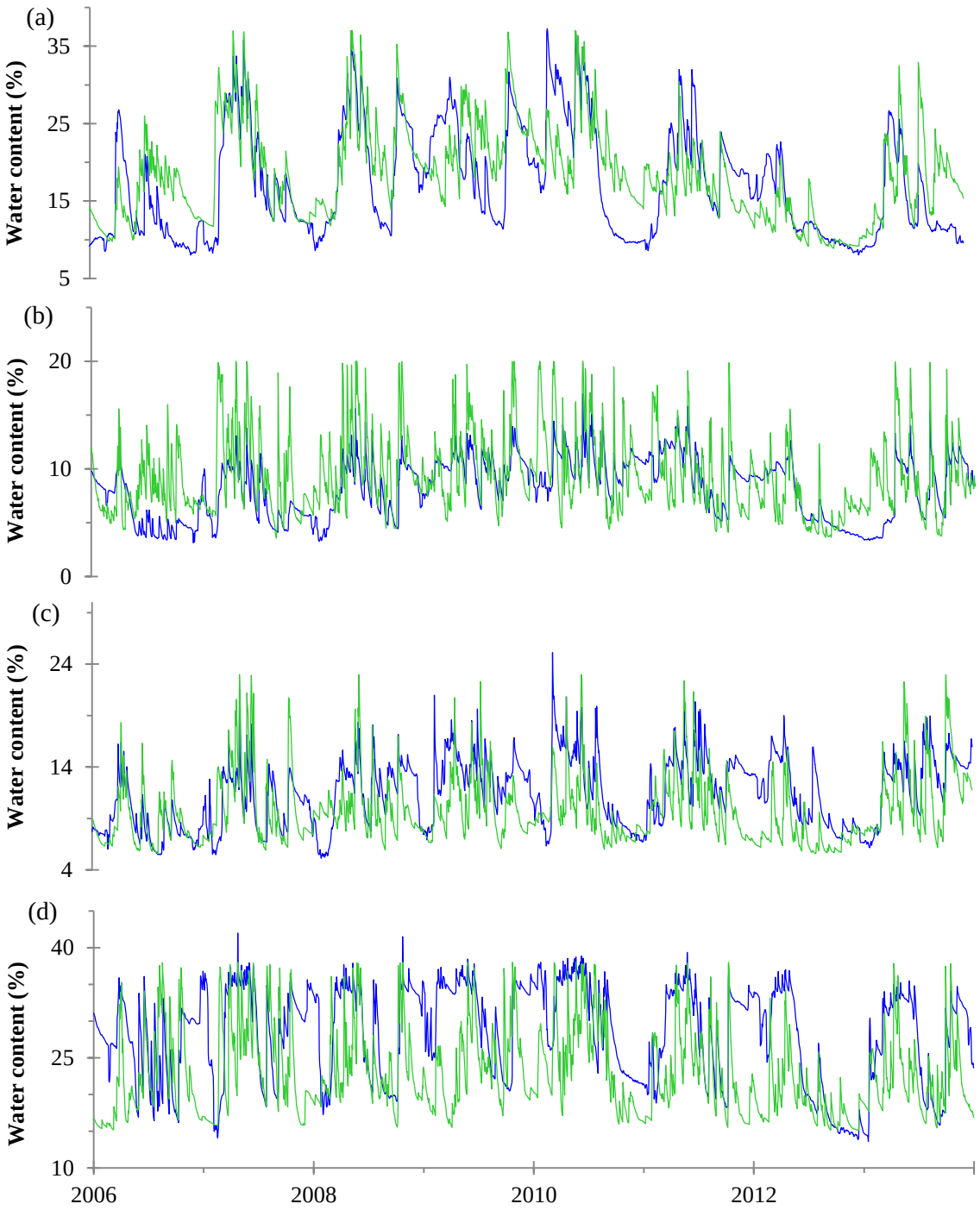

Figure 2-6. Average daily in-situ soil moisture content (blue line) (obtained from HPRCC) and model simulated daily water content in the root zone (green line) at (a) Cozad (b) Gothenburg (c) Merritt and (d) Holdrege stations.

Water storage analysis

Model simulated water storages

Water storage estimated from the integrated hydrologic model, which was mainly constructed based on in-situ data and evaluated by field measured observations such as stream flow, groundwater level, and soil moisture, provide a standard for comparison of terrestrial water storage anomaly estimated from GRACE. First, the annual incremental water balance of each terrestrial water storage compartment (snow, unsaturated zone, surface storage, canopy storage, and saturated zone) generated from the model was analyzed to understand the characteristics of TWS in the Northern High Plains. The monthly average total water balance error was 0.6%. The total terrestrial water storage in the Northern High Plains is dominated by storage in the saturated zone followed by storage in the unsaturated zone and snow storage (Figure 2-7). Surface storage variation and change in canopy storage were insignificant at the annual time scale, as the residence time of these compartments is short and seasonally dependent.

Generally, the total annual TWS anomaly is dictated by storage anomalies in the saturated zone except in 2004 and 2010 where it has the anomalies are in the unsaturated zone. For instance, a decrease in the total anomaly in 2010 simulated by the model (Figure 2-7) is a result of the decrease in storage in the unsaturated zone during this period. This decline in 2010, nearly equal in magnitude to the 2012 drought but for a shorter period, was clearly observed in the in-situ measured soil moisture data (Figure 2-6a, 2-6c, and 2-6d). There is no statistically significant (p-value = 0.92) trend in incremental TWS from 2002 to 2013. However, the inter-annual variability in the major storage compartments (e.g. saturated zone) was observed while other TWS compartments

(e.g. canopy storage) are consistent throughout this period (Figure 2-7). A similar pattern in precipitation is observed during this period (Figure 2-8).

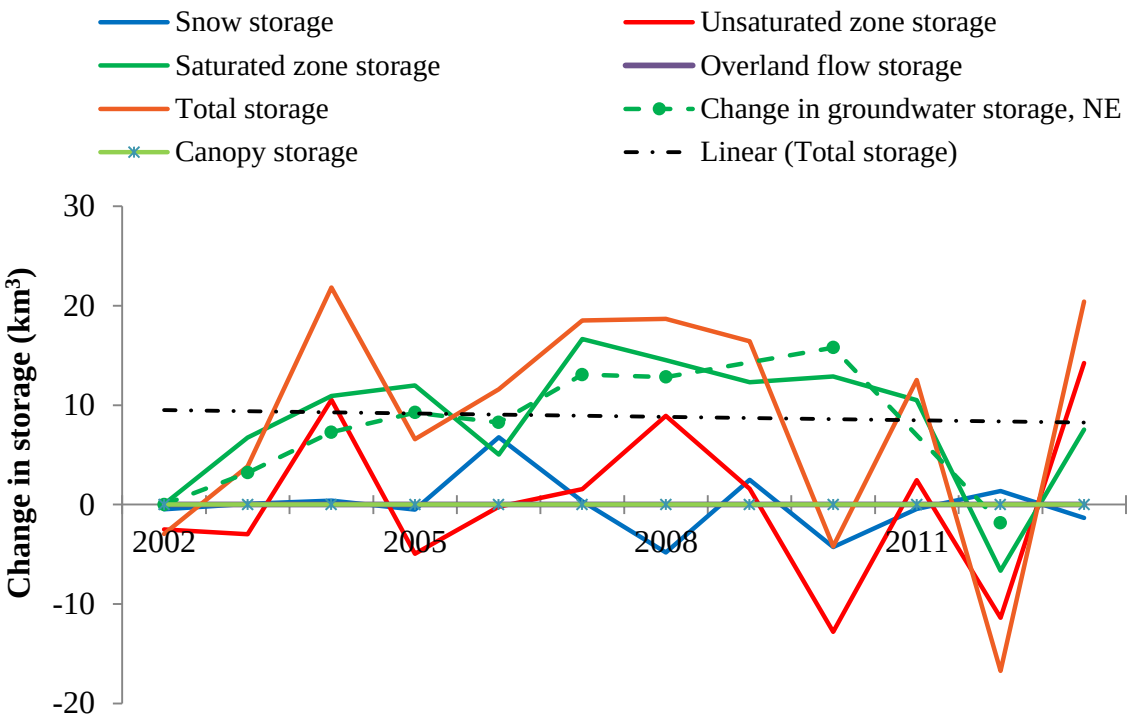

Figure 2-7. Model simulated annual average incremental water balance of the different terrestrial water compartments for the entire Northern High Plains (black dashed line: linear trend on the total water storage increment) and change in groundwater storage measured by USGS in Nebraska (purple dashed line, arithmetic mean was used to calculate the missing years).

In the NHP, specifically in the central and eastern parts of the study area, groundwater level monitoring reports by [*McGuire*, 2014] indicated that groundwater levels have risen by 10 to 25 ft. while the groundwater level is declining in some parts of the southern section (Northwest Kansas). The change in groundwater storage estimated by *McGuire* [2014], using the area-weighted average method of groundwater level

measurements for each state overlying the High Plains, showed that groundwater storage in Nebraska (nearly 70% of the study area (Figure 2-1)) changed by -7.4, -1.73, 3.08, 2.84, 5.92, and -11.84 km^3 in 2005-06, 2006-07, 2007-08, 2008-09, 2009-11, and 2011-13, respectively [*McGuire*, 2009; 2011; 2013; 2014]. The pattern of these changes in groundwater storage variation correlates well (r = 0.90) with the incremental water storage in the saturated zone simulated by the IHM (Figure 2-7). For instance, the large gains in groundwater storage from 2003 – 2007 (~ 15 km^3) as well as the equivalent loss after 2010 (~ 18 km^3) simulated by the model were in equal proportion as calculated by USGS (approximately 13 and 18 km^3 respectively). There is a slight overestimation of incremental water storage in the saturated zone by the model which could be due to an under-estimation of storage in the unsaturated zone (Figure 2-6d) (which results in more drainage or recharge to the saturated zone) and/or underestimation of groundwater abstraction from the aquifer. Groundwater storage changes in the Wyoming, Colorado, and South Dakota portion of the NHP were generally consistent throughout this period with changes in the range of -0.5 to 0.5, -1.85 to 0.9, and -0.5 to 0.15 km^3, respectively [28, 71, 73, 74].

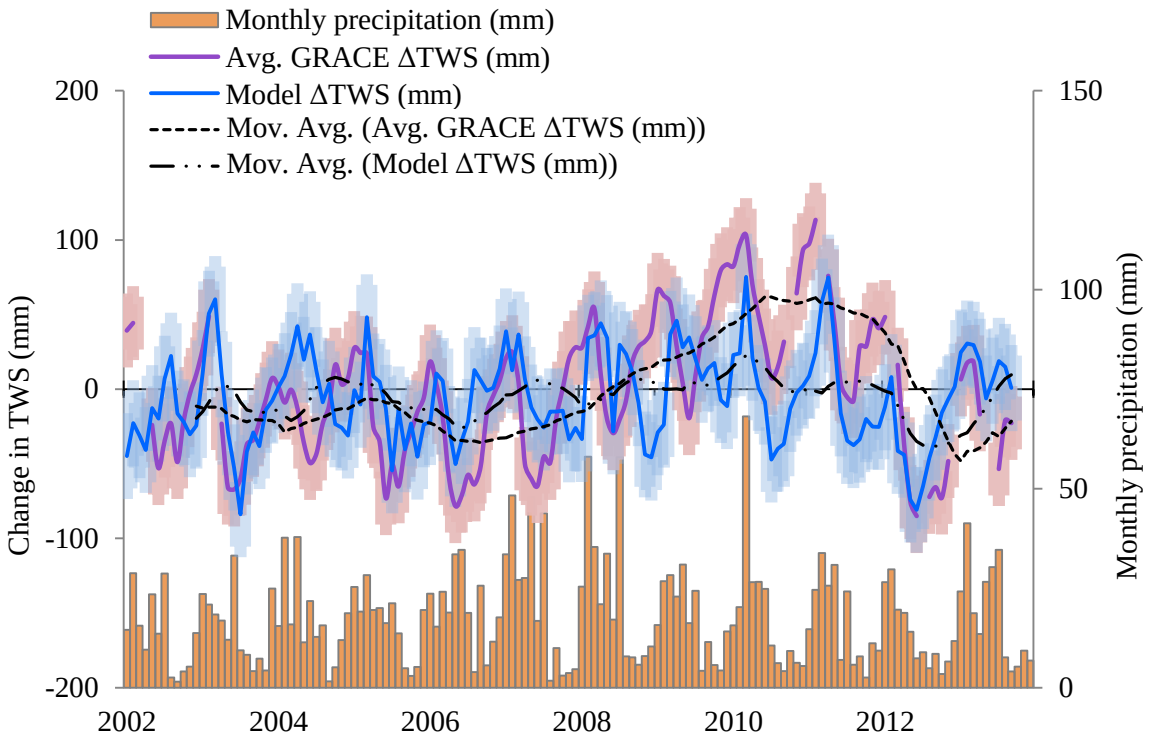

Figure 2-8. Comparison of monthly change in TWS from GRACE (purple line) with average GRACE total error (measurement error and leakage error) (red bars) and model simulated change in TWS (blue line) with uncertainty (green bars) from April-2002 to Dec-2013. Also shows 12-month moving averages over the TWS estimates (dashed lines) and average monthly precipitation for the NHP (red column) (obtained from PRISM Climate Group, Oregon State University, http://prism.oregonstate.edu).

Model vs. GRACE TWS anomaly

Monthly time-series data of changes in TWS from GRACE were compared with model simulated change in TWS (Figure 2-8). As shown in Figure 2-8, both data displayed similar long-term TWS patterns with the exception of an overestimation of TWS anomaly between 2009 and 2012 by GRACE. Generally, both GRACE and Model-derived TWS anomaly data showed a good match within their uncertainties with minor

discrepancies between 2009 and 2012. Before 2009, both data generally have similar amplitude and timing.

The GRACE change in TWS data has smooth and high amplitude characteristics, whereas the model simulated TWS anomaly exhibited lower amplitude and a higher frequency signal. This is due to the characteristics of the source of the datasets. For instance, the model was set up with high temporal (daily) and spatial resolution (1 km) data, while the GRACE data has a very coarse spatial pixel size (1^0 ~ 110 km near the equator) and coarser temporal resolution (monthly). Moreover, the GRACE TWS data is subjected to various processing steps including filtering and smoothing [*Landerer and Swenson*, 2012] that reduces the high-frequency signals.

Generally, considering the total error from GRACE data (measurement error and leakage error indicated by red error bars in Figure 2-8) and model error (32% error calculated based on flow data and indicated by green error bars in Figure 8), the change in TWS data simulated by the model generally fall within GRACE error and both the error bands exhibit overlap in the simulated time period with the exceptions in 2004, 2009, and between 2010 and 2012. While both GRACE and model-derived TWS anomalies are more or less consistent before 2009, between 2010 and 2012 both show a similar pattern but a difference in amplitude where the model underestimates the TWS anomaly. This could be due to the limitation of the irrigation data used in the IHM, overestimation of groundwater abstraction for irrigation during the wet period or exclusion of irrigation from surface water could impact the return flow and thus recharge to the subsurface storages. Less pumping during the wet period permits more recharge to the aquifer and results in positive increases in the TWS anomaly.

On the other hand, a significant decrease in TWS anomaly was simulated by the model at the end of 2010 compared to the GRACE data which is consistent with the drought observed in the unsaturated zone during this period. For instance, a decrease in annual incremental storage in the unsaturated zone (Figure 2-7) and an extended dryness in the root zone (almost comparable in magnitude to the 2012 drought) (Figures 2-6a, 2-6c, and 2-6d) in both model and in-situ data were observed during this period. The drought in 2012 and the recovery thereafter were consistently depicted by both the IHM and GRACE. There is a timing issue between the GRACE and model TWS anomaly data; however the model simulated TWS anomaly exhibits the pattern of precipitation with a relatively smaller delay compared to the GRACE data (Figure 2-8).

Table 2-3. Statistical test results of monthly and seasonal change in TWS values from GRACE and IHM (df: degree of freedom, $\overline{TWS}_{GRACE}$: average monthly TWS anomaly from GRACE, $\overline{TWS}_{MODEL}$: average monthly TWS anomaly from the IHM, and r: Pearson correlation coefficient).

Tests	df	t-score	Statistics		p-value
t-test	238.4	0.43	$\overline{TWS}_{GRACE}$ $\overline{TWS}_{MODEL}$	-0.1 -7.6	0.12
Pearson correlation (monthly)	129	6.18	r	0.38	0.001
Pearson correlation (seasonal)	38	4.54	r	0.40	5.6e-5

Statistical tests were conducted to assess the relationship between change in TWS estimated from GRACE and simulated by the IHM. The t-test result (Table 2-3) conducted on a monthly time-scale from 2002-2013 revealed that there is no statistically significant difference in means between the two datasets. There is a statically significant

correlation between GRACE-derived and model simulated change in TWS (Pearson correlation coefficients are 0.38 and 0.4 in monthly and seasonal time-scale, respectively) (Table 2-3).

The rate of change in TWS was calculated on two discernable significant trends (from 2002-2010 and 2010-2013) (Figure 2-8) using data from both IHM and GRACE. The result is summarized in Table 2-4. The results indicated that the trend from 2002 to 2010 is statistically significant where both model-simulated and GRACE-derived change in TWS data displayed similar trend but different magnitudes in the rate of TWS. For example, between 2002 and 2010, GRACE indicated an annual increase in TWS anomaly of ~ 5 mm while the model predicted an increase half of GRACE's prediction. This equates to 0.55 – 1.55 km^3 volume of water gained during this period in the NHP. Between 2011 and 2013, the model predicted no statistically significant trend while GRACE indicates the NHP is losing water at a rate of 7 km^3 per year. The variation in trend specifically after 2010 is due to the overestimation of the TWS anomaly from GRACE between 2009-2011 periods. Generally, consistency in trend analysis result indicates both GRACE and IHM are capable of reproducing trends in TWS.

Table 2-4. Statistical test result of the rate of change in TWS of both model simulated and GRACE-derived data.

	Monthly Rate (mm)			
	GRACE	p-value	Model	p-value
2002-2009	0.42	0.004	0.24	0.04
2010-2013	-3.3	6.56E-08	0.17	0.72

2.5. Conclusions

This study presents a comparison of TWS change derived from GRACE and an in-situ based integrated hydrologic model that simulates all of the terrestrial waters in the Northern High Plains (~ 250,000 km^2). An integrated hydrologic model – MIKE SHE was applied to simulate the different components of the hydrologic cycle: evapo-transpiration, overland flow, channel flow, and flow in the unsaturated zone and saturated zone. The model results were generally in agreement with in-situ measured groundwater level, stream flow, and soil moisture data.

Of the different TWS compartments simulated by the model, storage anomaly in the saturated zone is the major component of the total TWS. Generally, there is a no statistically significant trend in the annual incremental total TWS and groundwater storage over the Northern High Plains. A similar trend in the groundwater storage change was depicted by USGS groundwater monitoring studies in the study area. The GRACE-derived TWS anomaly and model-simulated TWS anomaly are mostly in agreement within the uncertainties of the data on a monthly scale with some discrepancies between 2009 and 2012. The monthly TWS anomaly predicted by the IHM has characteristics of high frequency and low amplitude whereas GRACE's TWS has characteristics of low frequency and high amplitude which is associated with the processing of GRACE data. Generally, the pattern of the TWS anomaly from both GRACE and the model depicted the climatic variability in the NHP (e.g., 2012 drought).

Agreement between GRACE-derived TWS and IHM-derived TWS anomalies on monthly and seasonal time scales confirms the potential for using GRACE gravity

measurements to infer trends in TWS changes in an area of 250,000 km^2 and in a region with intense irrigation. Moreover, in the irrigation season where in-situ TWS monitoring is difficult, GRACE provides suitable firsthand information to monitor terrestrial water anomalies. For further validation studies of GRACE using integrated hydrologic models in intensively irrigated regions, accurate measurements of irrigation water use/pumping are important to close the terrestrial water balance with the aim to improve dTWS/dt estimates using such models. This study also demonstrates the applicability of using an integrated hydrologic model – MIKE SHE to monitor variations of TWS over a large area (NHP).

References

Abbott, M. B., J. C. Bathurst, J. A. Cunge, P. E. O'Connell, and J. Rasmussen (1986a), An introduction to the European Hydrological System — Systeme Hydrologique Europeen, "SHE", 2: Structure of a physically-based, distributed modelling system, Journal of Hydrology, 87(1–2), 61-77.

Abbott, M. B., J. C. Bathurst, J. A. Cunge, P. E. O'Connell, and J. Rasmussen (1986b), An introduction to the European Hydrological System — Systeme Hydrologique Europeen, "SHE", 1: History and philosophy of a physically-based, distributed modelling system, Journal of Hydrology, 87(1–2), 45-59.

Ahmed, M., M. Sultan, J. Wahr, E. Yan, A. Milewski, W. Sauck, R. Becker, and B. Welton (2011), Integration of GRACE (Gravity Recovery and Climate Experiment) data with traditional data sets for a better understanding of the time-dependent water partitioning in African watersheds, Geology, 39(5), 479-482.

Alsdorf, D. E., E. Rodríguez, and D. P. Lettenmaier (2007), Measuring surface water from space, Reviews of Geophysics, 45(2).

Andersen, J., J. C. Refsgaard, and K. H. Jensen (2001), Distributed hydrological modelling of the Senegal River Basin — model construction and validation, Journal of Hydrology, 247(3–4), 200-214.

Andreadis, K. M., and D. P. Lettenmaier (2006), Assimilating remotely sensed snow observations into a macroscale hydrology model, Advances in Water Resources, 29(6), 872-886.

Breña-Naranjo, J. A., A. D. Kendall, and D. W. Hyndman (2014), Improved methods for satellite-based groundwater storage estimates: A decade of monitoring the high plains aquifer from space and ground observations, Geophysical Research Letters, 41(17), 2014GL061213.

Brown, J. F., and M. S. Pervez (2014), Merging remote sensing data and national agricultural statistics to model change in irrigated agriculture, Agricultural Systems, 127(0), 28-40.

Butler, J. J., G. C. Bohling, A. E. Brookfield, G. Liu, D. O. Whittemore, and B. B. Wilson (2014), Importance of a sound hydrologic foundation for assessing the future of the High Plains Aquifer in Kansas, Proceedings of the National Academy of Sciences, 111(5), E531.

Cederstrand, J. R., and M. F. Becker (1998), Digital map of hydraulic conductivity for the High Plains Aquifer in parts of Colorado, Kansas, Nebraska, New Mexico, Oklahoma, South Dakota, Texas, and Wyoming Rep.

Davis, K. W., and L. D. Putnam (2013), Conceptual and numerical models of groundwater flow in the Ogallala aquifer in Gregory and Tripp Counties, South Dakota, water years 1985–2009. U.S. Geological Survey Scientific Investigations Report 2013–5069, 82.

Dennehy, K. F. (2000), High Plains regional ground-water study Rep. U.S. Geological Survey Fact Sheet FS–091–00, 6 pp.

DHI (2012), MIKE SHE user manual, Volume 2: reference guide. DHI Water and Environment, Danish Hydraulic Institute Rep., 458 pp, Denamark.

Famiglietti, J. S., R. S. J. Sparks, and C. J. Hawkesworth (2004), Remote sensing of terrestrial water storage, soil moisture and surface waters The State of the Planet: Frontiers and Challenges in Geophysics, 150, 197-207.

Feng, W., M. Zhong, J.-M. Lemoine, R. Biancale, H.-T. Hsu, and J. Xia (2013), Evaluation of groundwater depletion in North China using the Gravity Recovery and Climate Experiment (GRACE) data and ground-based measurements, Water Resour. Res., 49(4), 2110-2118.

Graham, D. N., and M. B. Butts (2005), Flexible, integrated watershed modelling with MIKE SHE. In Watershed Models, Eds. V.P. Singh & D.K. Frevert, CRC Press.

Gutentag, E. D., F. J. Heimes, N. C. Krothe, R. R. Luckey, and J. B. Weeks (1984), Geohydrology of the High Plains aquifer in parts of Colorado, Kansas, Nebraska, New Mexico, Oklahoma, South Dakota, Texas, and Wyoming Rep., 63 pp, U.S. Geological Survey Professional Paper 1400–B.

Haacker, E. M. K., A. D. Kendall, and D. W. Hyndman (2015), Water Level Declines in the High Plains Aquifer: Predevelopment to Resource Senescence, Groundwater, n/a-n/a.

Houborg, R., M. Rodell, B. Li, R. Reichle, and B. F. Zaitchik (2012), Drought indicators based on model-assimilated Gravity Recovery and Climate Experiment (GRACE) terrestrial water storage observations, Water Resour. Res., 48(7), W07525.

Houston, N. A., Sophia L. Gonzales-Bradford, A. T. Flynn, S. L. Qi, S. M. Peterson, J. S. Stanton, D. W. Ryter, T. L. Sohl, and G. B. Senay (2011), Geodatabase Compilation of Hydrogeologic, Remote Sensing, and Water-Budget-Component Data for the High Plains Aquifer Rep., 12 pp, USGS.

Jackson, R. B., E. G. Jobbagy, R. Avissar, S. B. Roy, D. J. Barrett, C. W. Cook, K. A. Farley, D. C. le Maitre, B. A. McCarl, and B. C. Murray (2005), Trading water for carbon with biological sequestration, Science, 310(5756), 1944-1947.

Kristensen, K. J., and S. E. Jensen (1975), A model for estimating actual evapotranspiration from potential evapotranspiration, Nordic Hydrology, 6, 170-188.

Landerer, F. W., and S. C. Swenson (2012), Accuracy of scaled GRACE terrestrial water storage estimates, Water Resour. Res., 48(4), W04531.

Lee, H., R. E. Beighley, D. Alsdorf, H. C. Jung, C. K. Shum, J. Duan, J. Guo, D. Yamazaki, and K. Andreadis (2011), Characterization of terrestrial water dynamics in the Congo Basin using GRACE and satellite radar altimetry, Remote Sensing of Environment, 115(12), 3530-3538.

Li, B., M. Rodell, B. F. Zaitchik, R. H. Reichle, R. D. Koster, and T. M. van Dam (2012), Assimilation of GRACE terrestrial water storage into a land surface model: Evaluation and potential value for drought monitoring in western and central Europe, Journal of Hydrology, 446-447, 103-115.

Lo, M.-H., J. S. Famiglietti, P. J. F. Yeh, and T. H. Syed (2010), Improving parameter estimation and water table depth simulation in a land surface model using GRACE water storage and estimated base flow data, Water Resour. Res., 46(5), W05517.

Long, D., B. R. Scanlon, L. Longuevergne, A. Y. Sun, D. N. Fernando, and H. Save (2013), GRACE satellite monitoring of large depletion in water storage in response to the 2011 drought in Texas, Geophysical Research Letters, 40(13), 3395-3401.

Longuevergne, L., B. R. Scanlon, and C. R. Wilson (2010), GRACE Hydrological estimates for small basins: Evaluating processing approaches on the High Plains Aquifer, USA, Water Resour. Res., 46(11), n/a-n/a.

Luckey, R. R., and M. F. Becker (1999), Hydrogeology, water use, and simulation of flow in the High Plains aquifer in northwestern Oklahoma, southeastern Colorado, southwestern Kansas, northeastern New Mexico, and northwestern Texas. Water-Resources Investigations Report 99-4104, pp. 66.

McGuire, V. L. (2009), Water-level changes in the High Plains aquifer, predevelopment to 2007, 2005–06, and 2006–07. U.S. Geological Survey Scientific Investigations Report 2009–5019 Rep., 9 pp.

McGuire, V. L. (2011), Water-level changes in the High Plains aquifer, predevelopment to 2009, 2007–08, and 2008–09, and change in water in storage, predevelopment to 2009. U.S. Geological Survey Scientific Investigations Report 2011–5089 Rep., 13 pp.

McGuire, V. L. (2013), Water-level and storage changes in the High Plains aquifer, predevelopment to 2011 and 2009–11: U.S. Geological Survey Scientific Investigations Report 2012–5291 Rep., 15 pp.

McGuire, V. L. (2014), Water-Level Changes and Change in Water in Storage in the High Plains Aquifer, Predevelopment to 2013 and 2011–13. U.S. Geological Survey Scientific Investigations Report 2014–5218 Rep., 14 pp.

McMahon, P. B., K. F. Dennehy, B. W. Bruce, J. J. Gurdak, and S. L. Qi (2007), Water-quality assessment of the High Plains Aquifer, 1999–2004 Rep., 136 pp, U.S. Geological Survey Professional Paper 1749.

McMichael, C. E., A. S. Hope, and H. A. Loaiciga (2006), Distributed hydrological modelling in California semi-arid shrublands: MIKE SHE model calibration and uncertainty estimation, Journal of Hydrology, 317(3–4), 307-324.

Milewski, A., R. Elkadiri, and M. Durham (2015), Assessment and Intercomparison of TMPA Satellite Precipitation Products in Varying Climatic and Topographic Regimes, Remote Sensing

Milewski, A., M. Sultan, E. Yan, R. Becker, A. Abdeldayem, F. Soliman, and K. A. Gelil (2009), A remote sensing solution for estimating runoff and recharge in arid environments, Journal of Hydrology, 373(1–2), 1-14.

Miller, D. A., and R. A. White (1998), A Conterminous United States Multilayer Soil Characteristics Dataset for Regional Climate and Hydrology Modeling, Earth Interactions, 2(2), 1-26.

Nativ, R., and D. A. Smith (1987), Hydrogeology and geochemistry of the Ogallala aquifer, Southern High Plains, Journal of Hydrology, 91(3–4), 217-253.

Njoku, E. G., T. J. Jackson, V. Lakshmi, T. K. Chan, and S. V. Nghiem (2003), Soil moisture retrieval from AMSR-E, Geoscience and Remote Sensing, IEEE Transactions on, 41(2), 215-229.

Pervez, M. S., and J. F. Brown (2010), Mapping Irrigated Lands at 250-m Scale by Merging MODIS Data and National Agricultural Statistics, Remote Sensing, 2(10), 2388-2412.

Qin, H., G. Cao, M. Kristensen, J. C. Refsgaard, M. O. Rasmussen, X. He, J. Liu, Y. Shu, and C. Zheng (2013), Integrated hydrological modeling of the North China Plain

and implications for sustainable water management, Hydrology & Earth System Sciences, 17(10), 3759-3778.

Reager, J. T., B. F. Thomas, and J. S. Famiglietti (2014), River basin flood potential inferred using GRACE gravity observations at several months lead time, Nature Geosci, 7(8), 588-592.

Refsgaard, J. C., et al. (1998), An Integrated Model for the Danubian Lowland – Methodology and Applications, Water Resour. Manag., 12(6), 433-465.

Rodell, M., and J. S. Famiglietti (1999), Detectability of variations in continental water storage from satellite observations of the time dependent gravity field, Water Resour. Res., 35(9), 2705-2723.

Rodell, M., I. Velicogna, and J. S. Famiglietti (2009), Satellite-based estimates of groundwater depletion in India, Nature, 460(7258), 999-1002.

Rodell, M., J. Chen, H. Kato, J. S. Famiglietti, J. Nigro, and C. R. Wilson (2006), Estimating groundwater storage changes in the Mississippi River basin (USA) using GRACE, Hydrogeology Journal, 15(1), 159-166.

Sakumura, C., S. Bettadpur, and S. Bruinsma (2014), Ensemble prediction and intercomparison analysis of GRACE time-variable gravity field models, Geophysical Research Letters, 41(5), 1389-1397.

Scanlon, B. R., C. C. Faunt, L. Longuevergne, R. C. Reedy, W. M. Alley, V. L. McGuire, and P. B. McMahon (2012), Groundwater depletion and sustainability of irrigation in the US High Plains and Central Valley, Proceedings of the National Academy of Sciences, 109(24), 9320-9325.

Seyoum, W. M., A. M. Milewski, and M. C. Durham (2015), Understanding the relative impacts of natural processes and human activities on the hydrology of the Central Rift Valley Lakes, East Africa, Hydrological Processes.

Sonnenborg, T. O., B. S. B. Christensen, P. Nyegaard, H. J. Henriksen, and J. C. Refsgaard (2003), Transient modeling of regional groundwater flow using parameter estimates from steady-state automatic calibration, Journal of Hydrology, 273(1–4), 188-204.

Stanton, J. S., and S. L. Qi (2007), Ground-water quality of the northern High Plains aquifer, 1997, 2002–04. U.S. Geological Survey Scientific Investigations Report 2006–5138 Rep. U.S. Geological Survey Scientific Investigations Report 2006–5138, 60 pp.

Stanton, J. S., S. L. Qi, D. W. Ryter, S. E. Falk, N. A. Houston, S. M. Peterson, S. M. Westenbroek, and S. C. Christenson (2011), Selected approaches to estimate water-budget components of the High Plains, 1940 through 1949 and 2000 through 2009: U.S. Geological Survey Scientific Investigations Report 2011–5183, pp. 79.

Strassberg, G., B. R. Scanlon, and D. Chambers (2009), Evaluation of groundwater storage monitoring with the GRACE satellite: Case study of the High Plains aquifer, central United States, Water Resour. Res., 45(5), n/a-n/a.

Sun, A. Y., R. Green, S. Swenson, and M. Rodell (2012), Toward calibration of regional groundwater models using GRACE data, Journal of Hydrology, 422-423, 1-9.

Swenson, S., and J. Wahr (2006), Post-processing removal of correlated errors in GRACE data, GEOPHYSICAL RESEARCH LETTERS, 33(L08402:), 1-4.

Swenson, S., and J. Wahr (2009), Monitoring the water balance of Lake Victoria, East Africa, from space, Journal of Hydrology, 370(1-4), 163-176.

Syed, T. H., J. S. Famiglietti, M. Rodell, J. Chen, and C. R. Wilson (2008), Analysis of terrestrial water storage changes from GRACE and GLDAS, Water Resour. Res., 44(2), W02433.

Tapley, B. D., and S. Bettadpur (2004), The gravity recovery and climate experiment: Mission overview and early results, Geophysical Research Letters, 31(9), L09607.

Thomas, A. C., J. T. Reager, J. S. Famiglietti, and M. Rodell (2014), A GRACE-based water storage deficit approach for hydrological drought characterization, Geophysical Research Letters, 41(5), 1537-1545.

Van Liew, M. W., T. L. Veith, D. D. Bosch, and J. G. Arnold (2007), Suitability of SWAT for the Conservation Effects Assessment Project: Comparison on USDA Agricultural Research Service Watersheds, Journal of Hydrologic Engineering, 12(2), 173-189.

Vinukollu, R. K., E. F. Wood, C. R. Ferguson, and J. B. Fisher (2011), Global estimates of evapotranspiration for climate studies using multi-sensor remote sensing data: Evaluation of three process-based approaches, Remote Sensing of Environment, 115(3), 801-823.

Wahr, J., M. Molenaar, and F. Bryan (1998), Time-variability of the Earth's gravity field: Hydrological and oceanic effects and their possible detection using GRACE, J. Geophys. Res., 103(32), 20530.

Wahr, J., S. Swenson, V. Zlotnicki, and I. Velicogna (2004), Time-variable gravity from GRACE: First results, Geophysical Research Letters, 31(11).

Wang, H. J., Y. N. Chen, and Z. S. Chen (2013), Spatial distribution and temporal trends of mean precipitation and extremes in the arid region, northwest of China, during 1960-2010, Hydrological Processes, 27(12), 1807-1818.

Wang, S., Z. Zhang, G. Sun, P. Strauss, J. Guo, Y. Tang, and A. Yao (2012), Multi-site calibration, validation, and sensitivity analysis of the MIKE SHE Model for a large watershed in northern China, Hydrology & Earth System Sciences, 16(12), 4621-4632.

Wang, X., C. de Linage, J. Famiglietti, and C. S. Zender (2011), Gravity Recovery and Climate Experiment (GRACE) detection of water storage changes in the Three Gorges Reservoir of China and comparison with in situ measurements, Water Resour. Res., 47(12), W12502.

Weeks, J. B., E. D. Gutentag, F. J. Heimes, and R. R. Luckey (1988), Summary of the High Plains regional aquifer-system analysis in parts of Colorado, Kansas, Nebraska, New Mexico, Oklahoma, South Dakota, Texas, and Wyoming Rep., 30 pp, U.S. Geological Survey Professional Paper 1400-A.

Werth, S., A. Guntner, R. Schmidt, and J. Kusche (2009), Evaluation of GRACE filter tools from a hydrological perspective, Geophysical Journal International, 179(3), 1499-1515.

Yeh, P. J. F., S. C. Swenson, J. S. Famiglietti, and M. Rodell (2006), Remote sensing of groundwater storage changes in Illinois using the Gravity Recovery and Climate Experiment (GRACE), Water Resour. Res., 42(12), W12203 (12201-12207).

Yirdaw, S. Z., K. R. Snelgrove, and C. O. Agboma (2008), GRACE satellite observations of terrestrial moisture changes for drought characterization in the Canadian Prairie, Journal of Hydrology, 356(1-2), 84-92.

Zaitchik, B. F., M. Rodell, and R. H. Reichle (2008), Assimilation of GRACE Terrestrial Water Storage Data into a Land Surface Model: Results for the Mississippi River Basin, Journal of Hydrometeorology, 9(3), 535-548.

Zhang, Q., C. Liu, C.-y. Xu, Y. Xu, and T. Jiang (2006), Observed trends of annual maximum water level and streamflow during past 130 years in the Yangtze River basin, China, Journal of Hydrology, 324(1–4), 255-265.

Zhiqiang, Z., W. Shengping, S. Ge, S. G. McNulty, Z. Huayong, L. Jianlao, Z. Manliang, E. Klaghofer, and P. Strauss (2008), Evaluation of the MIKE SHE Model for Application in the Loess Plateau, China, Journal of the American Water Resources Association, 44(5), 1108-1120.

Zmijewski, K., and R. Becker (2013), Estimating the Effects of Anthropogenic Modification on Water Balance in the Aral Sea Watershed Using GRACE: 2003–12, Earth Interactions, 18(3), 1-16.

CHAPTER 3

ENHANCING THE SPATIAL RESOLUTION OF TWS ANOMALY FROM GRACE FOR UNDERSTANDING LOCAL TERRESTRIAL WATER CYCLE DYNAMICS

Seyoum, W. M., and A. M. Milewski, Enhancing the Spatial Resolution of TWS Anomaly from GRACE for Understanding Local Terrestrial Water Cycle Dynamics, to be submitted to *Water Resources Research, 04/30/2016*.

Abstract

Investigating the terrestrial water cycle dynamics is vital for understanding the recent climatic variability and human impacts in the hydrologic cycle. In this study, a downscaling approach has been developed and tested, to improve the applicability of terrestrial water storage (TWS) anomaly data from GRACE satellite mission for understanding local terrestrial water cycle dynamics in the Northern High Plains region. A non-parametric, artificial neural network (ANN) – based empirical model was employed to integrate GRACE with other satellite- and model-based datasets. Once the model was tested and validated, it was used to predict higher resolution TWS anomaly for watersheds having a size of 5,000 to 20,000 km^2 in the study area. The downscaled water storage anomaly data was then evaluated using water storage variation calculated from an integrated hydrologic model, land surface models (e.g. Noah), and in-situ groundwater level measurements. The comparison result shows the ANN reproduce the monthly TWS anomaly within the uncertainty for most of the watersheds. Derived groundwater storage anomaly from the ANN correlated well ($r \sim 0.85$) with change in groundwater storage calculated from in-situ groundwater level measurements for a watershed size as small as 6,000 km^2. Moreover, the ANN-downscaled change in TWS simulated replicated the natural water storage variability as a result of the combined effect of climatic variability and human impacts (e.g. abstraction). The implications utilizing finer resolution GRACE data for improving local and regional water resources management decisions and applications are clear. This is especially true with areas lacking in-situ hydrologic monitoring networks.

3.1. Introduction

Beyond the paramount societal importance, water plays a key role in earth system processes such as weather and climate and biogeochemical cycles. Thus, understanding this system not only helps to solve water resources and environmental management issues but also facilitates the understanding of Earth system processes. However, the lack of continuous data availability and adequate monitoring networks has been a challenge to the scientific community. Advancements in remote sensing technology have proven that water resources and hydrologic processes can be examined from space [*Andreadis and Lettenmaier*, 2006; *Birkinshaw et al.*, 2010; *Duan and Bastiaanssen*, 2013; *Milewski et al.*, 2015; *Milewski et al.*, 2009a; *Milewski et al.*, 2009b; *Rodell and Famiglietti*, 2002; *Seyoum et al.*, 2015; *Tadesse et al.*, 2015; *Vinukollu et al.*, 2011], among others. Examples of satellite sensors and the corresponding hydrologic variables used in water studies include GRACE (terrestrial water storage anomaly), AMSR-E (soil moisture), MODIS (vegetation and land surface temperature), Global Precipitation Measurement (GPM) (precipitation), and Jason-1/2 (altimetry), among others. Low spatial resolution is one of the limitations to the existing earth observation satellite missions. For instance, terrestrial water storage (TWS) anomaly from the GRACE mission has the least amount of uncertainty on regions of at least 200,000 km^2 [*Yeh et al.*, 2006]. Though the benefit of obtaining the regional or global context of a given area is not trivial, integrating satellite-based data to investigate local (i.e. small-scale) societal and environmental problems is essential and currently lacking.

This research focused on the Gravity Recovery Climate Experiment Satellite (GRACE) Mission that has provided a continuous measurement of terrestrial water

storage anomaly from space since 2002. The GRACE mission consists of two identical satellites orbiting in tandem at ~500 km altitude with an along-track separation distance of ~220 km and inclination of 89.50 [*Tapley and Bettadpur*, 2004]. The onboard K-band microwave ranging system measures the variation in speed and distance between the twin satellites caused by a change in the orbital motion of the satellites as a result of the gravitational field anomaly related to mass change beneath the satellites. Water being a major contributor to this mass change, the gravity anomaly measurement from GRACE is processed and converted into a terrestrial water storage anomaly product [*Rodell and Famiglietti*, 1999]. GRACE processing for land data involves the removal of atmospheric and oceanic effects, glacial isostatic adjustments, and a series of filtering and smoothing operations to remove systematic and random errors due to GRACE's measurement error and noises [*Landerer and Swenson*, 2012; *S Swenson and Wahr*, 2006]. After these operations, the level-3 product from the GRACE satellite mission consists of aggregate changes in global terrestrial water storage data including change in snow storage, surface water storage, canopy storage, and storage in the unsaturated and saturated zones.

GRACE has been widely used in regional and global hydrological applications. For instance, it has been used to monitor terrestrial water storage [*Ahmed et al.*, 2011; *Long et al.*, 2013], measure groundwater depletion [*Rodell et al.*, 2009], predict surface water [*Swenson and Wahr*, 2009], and monitoring drought [*Thomas et al.*, 2014]. Though many successful applications have been demonstrated, the coarse spatial resolution (~200,000 km^2) of GRACE limits its applicability to only regional and global scale studies and severely limits its use at a local scale. Given the presence of abundant local aquifer systems and vulnerability to human impacts and global change, these systems

require monitoring. Moreover, GRACE data is invaluable, especially in data scarce regions where water cycle monitoring networks are absent or extremely limited. To enhance the applicability of GRACE, however, the spatial resolution of TWS anomaly data from GRACE must be improved, thereby meeting the high-resolution data requirements of local water resources management and hydrology researchers. This necessitates the need to develop methods enabling local scale (small-scale) application of GRACE water storage anomaly data.

Enhancing the spatial resolution of GRACE through GRACE processing is a tradeoff for accuracy [*Landerer and Swenson*, 2012; *Longuevergne et al.*, 2010; *S C Swenson and Wahr*, 2011]. The original GRACE data product consists of spherical harmonic coefficients describing the monthly gravity anomaly. Converting this into TWS anomaly involves a set of processing and filtering techniques to isolate and remove systematic and random errors associated with GRACE observations [*Landerer and Swenson*, 2012]. As a result, the true geophysical signal of interest and spatial resolution suffers from alteration during filtering [*S C Swenson and Wahr*, 2011]. Specifically, in the GRACE data processing for land, a Gaussian filter with a half-width of 300 km was applied to remove random errors of the spherical harmonic coefficient of the higher degree. This filtering involves a smoothing operation where it reduces the spatial resolution of GRACE data by removing the high degree spherical harmonics (corresponding to high-resolution signals); see [*Landerer and Swenson*, 2012] for details. Therefore, obtaining high-resolution GRACE TWS anomaly through GRACE processing comes with a cost of large uncertainty in the data.

Few dynamic (or model-based) [*Houborg et al.*, 2012; *Zaitchik et al.*, 2008] and empirical [*Sun*, 2013] downscaling approaches have been employed on GRACE data to improve the spatial resolution of GRACE observations. *Zaitchik et al.* [2008] used a data assimilation method that integrated coarse GRACE data into a land surface model to improve water storage and hydrologic flux estimates from the land surface model. Though their approach improved the simulation of hydrologic variables (e.g. runoff) at sub-observational (i.e. smaller) scale, no downscaled TWS anomaly product was achieved. On the other hand, *Sun* [2013] used an empirical downscaling model that incorporated GRACE TWS anomaly data, existing groundwater level data, and hydro-meteorological variables to predict changes in groundwater level in wells. This approach can be used to fill data gaps in the absence of continuous ground observations; however its dependency on existing in-situ groundwater level measurements limits its applicability to data sparse regions where there are no existing groundwater measurements.

In this research, we hypothesized that GRACE TWS anomaly integrated with other terrestrial water cycle variables can be used to predict high-resolution TWS anomaly for understanding local (small-scale) terrestrial water cycle dynamics. The objectives of this research were to identify and characterize terrestrial water storage variables (TWSV) controlling the TWS, predict high-resolution TWS anomaly from GRACE and TWSV, and evaluate the predicted high-resolution TWS product using in-situ and model-derived TWS anomaly data. A non-parametric empirical model was developed and tested to calculate high-resolution TWS anomaly data for different size watersheds in the study area. First, TWS variables (e.g. precipitation, discharge) extracted from multi-source datasets were processed and analyzed and integrated with GRACE

TWS anomaly data using an artificial neural network (ANN)-based model to produce a high-resolution TWS anomaly product. The downscaled (high resolution) water storage anomaly product was evaluated using independent, model-derived and insitu-based water storage anomaly data for selected watersheds in the study area. This study improved the high-resolution data requirement of local water resources management and hydrology related science. Further, it enhances the applicability of GRACE in data sparse regions where in-situ monitoring networks are very limited or non-existent and allows for an improved understanding of small-scale hydrologic processes and fluxes.

3.2. Methods and Data

The aforementioned objectives were achieved by first processing and analyzing time-series data of TWS variables (e.g., precipitation, land surface temperature, vegetation coverage) that are governing the water storage characteristics of a given basin for the entire study region. Second, a non-parametric, non-linear empirical relationship was established between these basin TWS variables and TWS anomaly from GRACE using an ANN model. The model was then used to predict high resolution (small-scale) TWS anomaly for selected watersheds in the study area. Lastly, the high-resolution TWS anomaly data from the ANN were evaluated using water storage anomaly data calculated from independent datasets including model-derived and in-situ observational data, and was used to understand local terrestrial water cycle dynamics.

Study Site

A region over the Northern High Plains (Figure 3-1) was selected to test the hypothesis and validate the results. This region was selected due to the availability of

significant in-situ data for validation. Furthermore, an Integrated Hydrologic Model (IHM) was constructed by the authors in a separate study in this region, which allows an independent assessment of the high-resolution TWS anomaly data estimated in the current study. The study area is bounded by $38^{o} – 41^{o}$ N Latitude and $96^{o} – 106^{o}$ W Longitude (Figure 3-1) and covers an area of ~ 500,000 km^2 in the central part of the US. Such a large area is chosen to reduce bias on GRACE TWS anomaly data as a result of smoothing/filtering operation during GRACE processing.

The study area which consists of the Northern High Plains aquifer (NHP), the northern section of the High Plains Aquifer, is an important source of water for drinking, agricultural, and industrial use. From the total groundwater abstraction for irrigation in the US, about 30 % is pumped from the High Plains which constitutes 27 % of the total irrigated land of the country [*Dennehy*, 2000]. The study area lies between the Central Lowlands on the east with an elevation of ~330 m near the Missouri River and the Rocky Mountains on the west with an elevation of ~3000 m. Generally, the NHP region is characterized by high evapotranspiration (average annual AET estimated by National Weather Service ~ 500 mm [*Stanton et al.,* 2011]) with recharge (potential annual recharge estimates in the NHP ranges from 50 – 125 mm [*Stanton et al.*, 2011]) to the aquifer occurring during non-growing seasons when evapotranspiration is low. Precipitation varies from west to east, with mean annual precipitation ranging from 300 mm in the western to 800 mm in the eastern sections of the study area. The average annual minimum and maximum temperatures are ~ 1^{0}C and 18^{0}C, respectively. The landuse is dominated by cropland and rangeland, and the dominant crops growing in the area are corn and soybean.

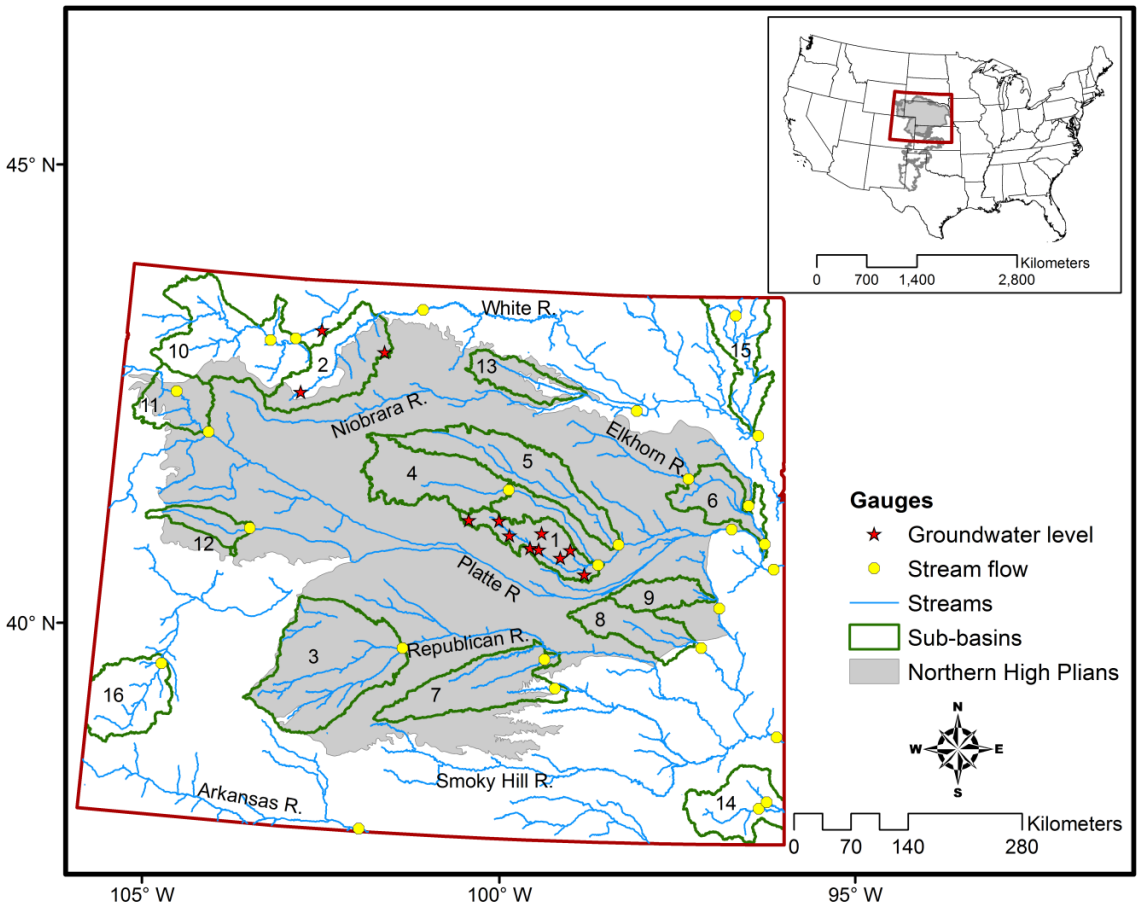

Figure 3-1. The location map of the study area showing the large GRACE scale (red polygon), the downscaled watersheds (green polygons), the NHP aquifer (shaded region), and location of gauges used in the study.

Data Sources and Processing

A suite of multi-source – remote sensing, model-based, and in-situ – datasets were used to downscale GRACE into high-resolution TWS anomaly data. The GRACE data used in this study is based on the latest version (RL-05 gridded (1^{o}x1^{o})) level-3 data from CSR, JPL, and GFZ processing centers [*Landerer and Swenson*, 2012; *S Swenson and Wahr*, 2006]. An ensemble mean of the three GRACE solutions were used to ensure the

highest level of accuracy. GRACE land data are available at http://grace.jpl.nasa.gov, supported by the NASA MEaSUREs Program. The TWS anomaly data obtained ranged from April 2002 to November 2014 and was multiplied by the supplied scale factors to restore the signal reduced during sampling and post-processing of GRACE observations.

Data for terrestrial water storage variables, which includes precipitation, land surface temperature (LST), percent vegetation coverage, soil moisture, water equivalent accumulated snow depth, and stream discharge, obtained from various sources were used in the empirical downscaling model. Finer spatial resolution data is available for some of the TWS variables, though selection of the data sources was based on the availability at a global scale aiming to extend the methodology developed here to other parts of the globe where in-situ hydrological observations are limited. Thus, satellite-derived TWS variables, including precipitation from Tropical Rainfall Measuring Mission (TRMM) (TMPA_3B43 V7) with spatial resolution of 0.25^0 X 0.25^0; LST from Moderate Resolution Imaging Spectroradiometer (MODIS) (MOD11C3) with 0.05^0 X 0.05^0 spatial resolution; and vegetation coverage data extracted from MODIS Normalized Difference Vegetation Index (NDVI) data (MOD13A3) with spatial resolution of 0.011^0 X 0.011^0, were processed and area-average monthly time-series data (2002-2014) were extracted for use in the downscaling model. Variation in percent vegetation coverage from MOD13A3 was calculated using a cutoff greenness index (NDVI) value of 0.7 and applied to the entire temporal dataset in the study area. Appropriate scaling and conversion to standard units were performed to the satellite-based datasets.

Noah Land surface model product [*Ek et al.*, 2003], obtained from National Data Assimilation System (NLDAS) (http://ldas.gsfc.nasa.gov/nldas/, accessed in 09/08/2015),

was used to extract data for water equivalent accumulated snow depth and depth-integrated (0 – 200cm) soil moisture. Both datasets have a spatial resolution of 0.01^0 X 0.01^0. Lastly, net basin surface outflow were approximated using in-situ stream flow data obtained from the USGS water data center. Furthermore, hydrological data from Noah and Variable Infiltration Capacity (VIC) land surface models as well as in-situ groundwater level data obtained from USGS were used to evaluate the downscaled product.

Terrestrial Water Storage Variables

The selection of predictor variables, named terrestrial water storage variables hereafter, is the first step in constructing ANN downscaling model. The terrestrial water storage variables were selected based on the following criteria: (1) they should represent important physical processes in the terrestrial water cycle, (2) they should strongly correlate (have statistically significant correlation) with GRACE TWS anomaly, and (3) they should be readily available time-series data and representing the large-scale variability in GRACE's TWS anomaly. To accomplish this selection process, visual comparison and cross-correlation analysis of the time series data was done. Cross-correlation, specifically lagged correlation, which is the correlation between two time series shifted in time relative to one another, between each terrestrial water storage variable and TWS anomaly from GRACE was computed. Most physical processes especially hydrologic processes exhibit this characteristic where one series (e.g. TWS anomaly) may have a delayed response to the other series (e.g. precipitation). The cross-correlation function of two time series is the product moment correlation (r) as a function

of lag between the time series where mathematically it is the cross-covariance function scaled by the variances of the two time-series, see *Chatfield* [2004] for details.

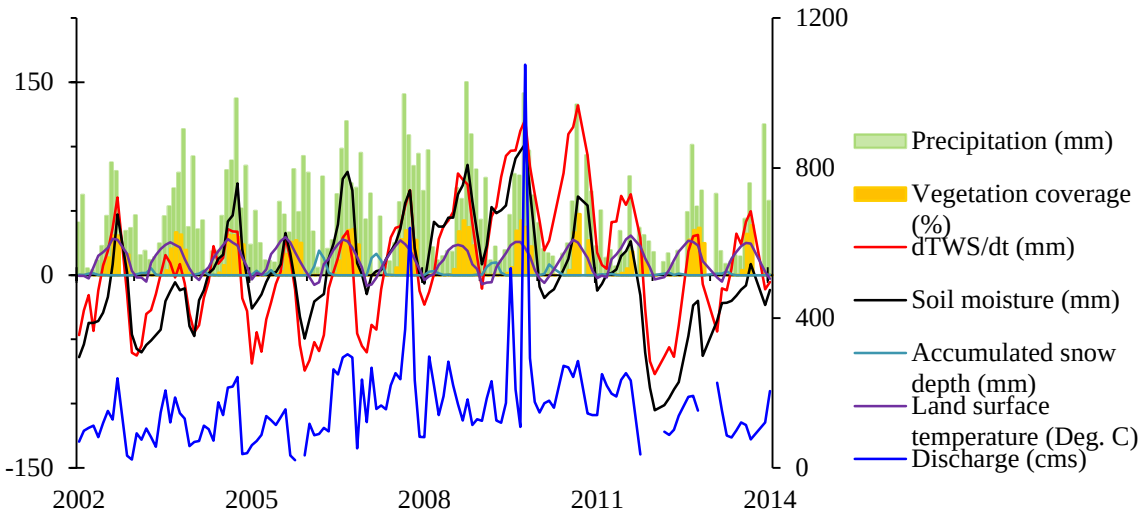

Figure 3-2. Area-averaged time series comparison of each terrestrial water storage variable and TWS anomaly from GRACE (dTWS/dt) in the study area.

As shown in figure 3-2, the area-averaged time series of terrestrial water storage variables shows similar seasonal and long-term patterns of TWS anomaly from GRACE. For instance, from 2006 to 2010 similar increasing long-term trend in the peak TWS anomaly, precipitation, soil moisture, and stream flow data was observed. Likewise, the drought between 2011 and 2013 was indicated by a decrease in TWS anomaly, precipitation, soil moisture, and stream flow. Percent vegetation coverage showed a similar long-term pattern of TWS anomaly whereas the land surface temperature exhibits the opposite long-term trend. The average peak land surface temperature in the study area shows a decreasing pattern during the 2006-2010 wet periods, while the TWS anomaly increased during this period.

Figure 3-3 shows the monthly lagged cross-correlation between each terrestrial water storage variable (predictors) and change in TWS from GRACE (predictand). The predictors are leading and controlling the water storage anomaly, thus only the positive lags where the TWS anomaly (dTWS/dt) is lagging was considered. As shown in figure 3-3, a statistically significant correlation exists between the predictors and dTWS/dt at time zero and different lags. The significant positive correlation at zero lag and inverse relationship in the range of 2 to 4 months lag between precipitation and dTWS/dt (Figure 3-3a) indicates the absence of a direct relationship between precipitation and TWS due to the complexity of hydrologic processes. While the process is complicated, as interpreted with the help of the time-series data, the inverse relationship between precipitation and dTWS/dt occurred during the summer season where the dTWS/dt was decreasing as a result of higher evapotranspiration and increased pumping for irrigation. For the same reason, a similar inverse relation was observed between land surface temperature and vegetation coverage with dTWS/dt (Figure 3-3c and 3-3d respectively) as both are important variables of the evapotranspiration process. Accumulated snow has a positive correlation with dTWS/dt within 3 to 6 months lag; this delayed response of the dTWS/dt to snow implies the snow melting process takes time to impact the TWS. On the other hand, a high correlation was obtained between soil moisture, stream flow and TWS anomaly at zero lag. Both soil moisture and stream flow are characterized by shorter residence times, changing swiftly in response to climatic variation, thus the TWS anomaly. In addition to understanding the link between TWS variables and GRACE's TWS anomaly, adjusting the lags helps to improve the performance of the ANN downscaling model.

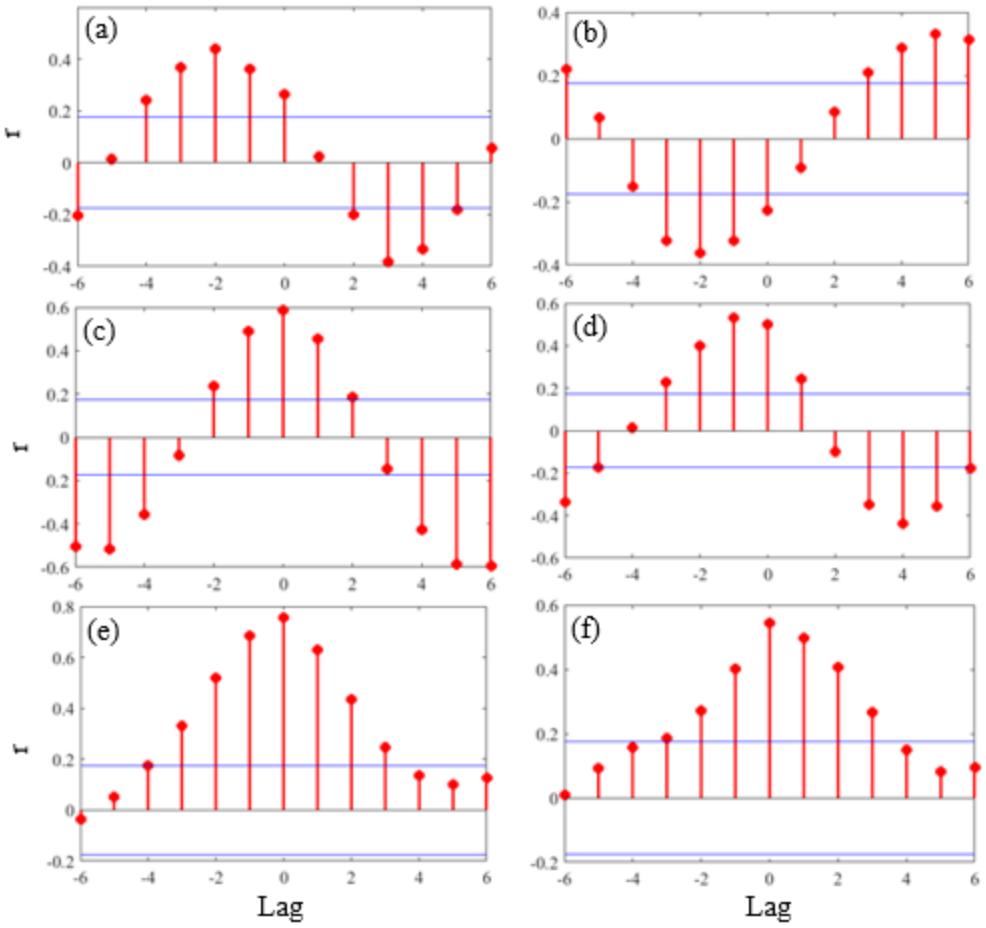

Figure 3-3. Lagged cross-correlation (r) between each TWS variable (a – precipitation, b – accumulated snow water equivalent, c – land surface temperature, d – percent vegetation coverage, e – soil moisture, and f – stream discharge) and GRACE TWS anomaly (Blue line indicates the upper and lower 95% confidence bound).

Empirical Downscaling Model

A non-parametric, Artificial Neural Network (ANN) – based empirical model was developed to downscale GRACE-derived TWS anomaly data. ANN models have been applied in various hydrology (e.g., stream flow, groundwater level prediction) and water resources management applications [*Coppola Jr et al.*, 2003; *Coulibaly et al.*, 2001;

Kasiviswanathan et al., 2013; *Kraller et al.*, 2012; *Nourani et al.*, 2014; *Wang et al.*, 2015]. ANNs have also been widely employed in spatial downscaling of global climate model outputs such as Global Circulation Models (GCMs), temporal downscaling and forecasting of meteorological variables, and spatial disaggregation of satellite-based soil moisture data. For example, *Chadwick et al.* [2011] used an ANN technique to downscale GCMs output parameters – temperature and rainfall – to regional model scale by establishing a relationship between GCMs and corresponding nested Regional Climate Model (RCM) fields. On the other hand, *Tsegaye et al.* [2003] employed a neural-network based disaggregation model to downscale low-resolution microwave satellite observations into high-resolution soil moisture measurements. Of other methods (e.g. multiple regression), ANNs are chosen for their high capacity of establishing complex and non-linear relationship between input-output time series datasets without any functional form and prior assumptions. While other statistical methods such as regression has some functional forms and assumptions. This fact and the flexibility of ANN models make ANNs more powerful and desirable than other methods [*ASCE Task Committee*, 2000]. Furthermore, the distributed processing characteristics of the neural networks allow the error signals in the input and output variables of the ANN to be attenuated, and a result is obtained without any significant loss of accuracy.

ANN design and training

ANNs are capable of establishing complex, empirical, non-linear relationships between a set of input variables and corresponding output (target) variable(s) using historical data. In this case, the input variables (the predictors) are the terrestrial water storage variables (TWSVs) (e.g., precipitation, accumulated snow depth) whereas the

target is GRACE-derived TWS anomaly. Once the relationship was established the ANN model was used to predict high-resolution GRACE equivalent TWS anomaly data (Figure 4a) using high-resolution TWSV inputs. This approach assumes that the relationship established for the entire study area is consistent with the smaller scale or downscaled watersheds within the study area while the predictor variables are changing spatially in the study area.

A feed-forward, multi-layer perceptron (MLP) neural network method was applied to establish the relationship between the input terrestrial water storage variables and the target GRACE TWS anomaly. The MLP, which is the most widely used ANN, consists of a system of simple interconnected neurons, or nodes organized in a series of two or more layers (Figure 3-4b). The information flow in the network is in one direction, layer by layer, from the input to the output layer, which is called a feed-forward network (see *Gardner and Dorling* [1998] for details about MLP). There are no set of rules for developing ANN models except following the existing procedures. However, a trial and error approach can be implemented to decide the optimal and best performance design of the ANN model on the generalization of the dataset [*ASCE Task Committee*, 2000]. A simple two-layered neural network with 6 input, 10 hidden and 2 output nodes connected by 70 neurons (weights) (Figure 3-4b) was developed through an iterative process and used for downscaling.

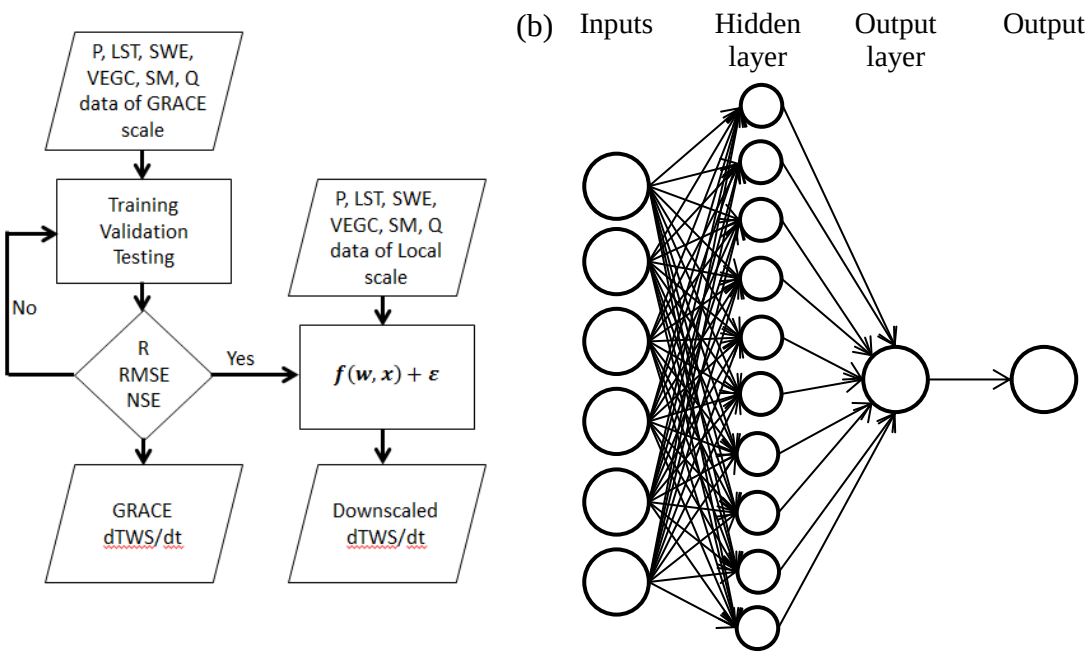

Figure 3-4. (a) The conceptual model for the ANN downscaling method and (b) The network design used for the downscaling.

In order to be used for the intended purpose, a neural network is prepared through training, validation, and testing processes. The training is performed through an iterative process during which ANNs modify their weights while minimizing the error between the predicted output (ANN) and the target (GRACE). The network was trained using the Levenberg-Marquardt back propagation algorithm in MATLAB [*Hagan and Menhaj*, 1994; *Marquardt*, 1963]. To prevent overfitting, a cross-validation was performed where the network halted training whenever the generalization stops improving. Finally, in order to provide an independent measure of the network performance during and after training, the model was tested using a dataset independent of the training and validation data. Therefore, the total sample size (140), which is limited by GRACE's sample size, was randomly divided into training (70%), validation (15%), and testing (15%). Statistical measures such as coefficient of determination (R^2), root-mean-square error

(RMSE), and Nash-Sutcliffe efficiency (NSE) were used to evaluate the performance of the neural network.

Additional Sources of Water Storage Anomaly Estimates

We evaluated the performance of the calibrated and evaluated predicted high resolution TWS anomaly data from the ANN model versus change in water storage from an Integrated Hydrologic Model (IHM) and land surface models (Noah), and in-situ groundwater level data at a similar scale. Moreover, derivative groundwater storage anomaly product from the high-resolution ANN TWS anomaly data, which was calculated by removing the remaining terrestrial water storage compartments (e.g. soil moisture storage) from the ANN TWS anomaly data, was assessed by comparing it with change in groundwater storage estimated from in-situ groundwater level measurements for selected watersheds.

Integrated Hydrologic Model

An Integrated Hydrologic Model (IHM), capable of simulating the entire terrestrial water cycle including overland flow, channel flow, evapotranspiration, flow in the unsaturated and saturated zone, was constructed for the Norther High Plains (shaded region in Figure 3-1) by *Seyoum and Milewski* [2016]. A fully-distributed physically based model – MIKE SHE, coupled with a channel flow model – MIKE11, was used to simulate the terrestrial water cycle and estimate the TWS anomaly. MIKE SHE combines different process-based modules each representing the water movement in the hydrologic cycle, and has a range of numerical methods for each hydrologic process. For example, the saturate zone was simulated by a finite-difference method while a two-layer root zone

water balance model was used to simulate the unsaturated zone, see *Seyoum and Milewski* [2016] for details.

The IHM, constructed mainly using in-situ data, was calibrated and validated using field measured groundwater level, stream flow, and soil moisture data. Thus, this calibrated model was used to estimate TWS anomaly for each downscaled watershed for the purpose of evaluating the downscaled TWS anomaly estimated from the ANN model developed in the current study.

Land Surface Models (LSM)

Similarly, a comparable replication of GRACE TWS anomaly for each local-scale watershed was calculated from land surface model products, the community Noah LSM (Noah) [*Ek et al.*, 2003] and the Variable Infiltration Capacity (VIC) [*Liang et al.*, 1994] models, using a monthly basin-scale terrestrial water balance equation (Equation 3-1) suggested by *Syed et al.* [2008].

$$\left[\frac{dTWS}{dt}\right]_N = \sum_{N-1}^{N} P - \sum_{N-1}^{N} E - \sum_{N-1}^{N} R \text{..... Equation 3-1}$$

Where *N* is a month, *P* is precipitation, *E* is evapotranspiration, and *R* is runoff.

In-situ Groundwater Level Data

The TWS variation represents water storage changes in the terrestrial water cycle including surface storage, canopy storage, snow storage, storage in the unsaturated zone, and storage in the saturated zone. A previous study by *Seyoum and Milewski* [2016] in the study area proved snow storage, storage in the unsaturated zone, and storage in the saturated zone are the significant components of the terrestrial water storage where

storage in the saturated zone is the most dominant in the terrestrial water balance. Thus, a derivative groundwater storage anomaly was calculated from the downscaled ANN-based TWS anomaly data. Given the ANN-based terrestrial water storage variations (dTWS/dt), groundwater storage anomaly was computed by subtracting model-based (Noah model) changes in soil moisture and snow water equivalent from the total dTWS/dt. The result was compared with groundwater storage anomaly (dGWS/dt) computed using data from groundwater monitoring wells obtained from the USGS. Groundwater storage anomaly from in-situ observations were approximated using the following equation (Equation 3-2):

$$\frac{dGWS}{dt} = S_y \frac{dh}{dt} \quad \text{..... Equation 3-2}$$

Where S_y is the specific yield of an unconfined aquifer in the watershed and *dh/dt* is the change in groundwater level in monitoring wells in the respective watershed.

3.3. Results and Discussion

The ANN was trained using a randomly selected subset from the data (70% of the total sample) for the period ranging from 2002 – 2014, and the remaining 30% of the dataset was used for cross-validation and testing purposes. Multiple network designs were iteratively tested and the sensitivity was determined by changing the number of nodes in the hidden layer. The network was insensitive with nodes higher than ten in the hidden layer. Using this network, the ANN was run multiple times until satisfactory performance measures were achieved. The statistical measure (R^2) for the best simulated network for model training, validation, and testing was 0.96, 0.82, and 0.87, respectively, with an overall network generalization of 0.92, 16 mm, and 0.82 for R^2, RMSE, and NSE,

respectively. Figure 3-5 shows the time series values for ANN simulated and target (GRACE-derived) dTWS/dt for the study area. The ANN successfully reproduced the TWS anomaly using the predictor variables (TWSV) compared to the GRACE measured TWS anomaly. The timing and the amplitude matched well except in some instances where the ANN very slightly over – and under – predicted the amplitudes of TWS anomaly (e.g. 2008 and 2010, respectively).

The total error in the GRACE data, which includes leakage error due to post-processing and measurement error by the satellite, was calculated to be ~ 18 mm [*Seyoum and Milewski*, 2016]. Due to the characteristics of the ANNs, the error due to input (predictor) variables was assumed to be distributed in the networks with minimal effect. However, the total error from GRACE dTWS/dt – where the GRACE dTWS/dt was used as a target in the ANN simulation – can propagate into the ANN model, and then to the downscaled TWS anomaly data. This error was approximated by adding the GRACE total error (18 mm) and ANN model error (16 mm). The resulting maximum propagated error to the downscaled TWS anomaly product would be ~ 34 mm (shown by the shaded region in Figure 3-6).

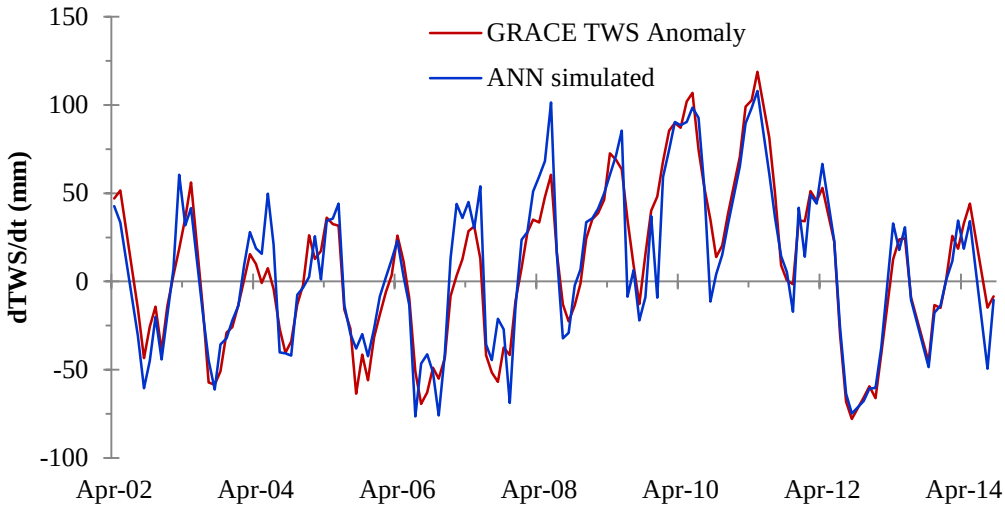

Figure 3-5. ANN simulated (blue line) and GRACE-derived (red line) monthly time series TWS anomaly data for the entire study site.

Evaluation of the ANN Downscaled TWS Anomaly Data

Following the calibration and validation of the ANN downscaling model, the model was used to calculate TWS anomaly for higher resolution (small-scale) watersheds in the study area. The watersheds range in size from 5,000 to 20,000 km^2 (green polygons in Figure 3-1). For each high-resolution watershed, time series and statistical comparison was made between TWS anomaly data calculated from the ANN and derived from other models (IHM, Noah, and VIC). In addition, to interpret the long-term pattern of water storage variations, periodic groundwater level measurement data from the respective watersheds were superimposed over the TWS anomaly products.

The ANN downscaling model was able to successfully reproduce the TWS anomaly in the representative watersheds within the uncertainty of the data. Figure 3-6 displays the monthly time series TWS anomaly data from ANN, IHM, VIC, and Noah models (left axis) and periodic in-situ groundwater level data (right axis) for the

investigated watersheds in the study area. The ANN is reasonably simulating the monthly TWS variation in the watersheds (e.g., Figure 3-6a, 3-6b, 3-6c, 3-6g, 3-6h, and 3-6i). The ANN simulated the timing, the seasonal variation as well as the amplitude, except in some instances where the ANN over- and under-predicted. For example, in almost all of the cases (Figure 3-6), the ANN was overestimating the TWS anomaly during the time period between 2009 and 2011. On the other hand, the discrepancy in timing and seasonal variability was observed in a number of watersheds (Figure 3-6d, 3-6e, and 3-6f). Nevertheless, there was consistency in amplitude between the ANN and other TWS anomaly products. The discrepancy was observed in watersheds located in the western part of the NHP aquifer where the region is characterized by a relatively dryer climate, less recharge, and aquifers with low specific yield. Moreover, relatively higher groundwater depletion rates are present in this part of the region compared to other parts of the study area [*McGuire*, 2014]. Accurately incorporating groundwater abstraction from the aquifers and water use in general is one of the challenges in the modeling process given the lack of the availability of temporal water use data [*Pokhrel et al.*, 2015; *Seyoum and Milewski*, 2016]. Inconsequently, an inadequate representation of water storage variations by the models thereby increases the inconsistency between the model estimated TWS anomalies and the ANN downscaled for the watersheds in the western part of the study area.

For most of the watersheds, a distinct long-term pattern (shown by the dashed line in Figure 3-6 which is the annual moving average over the ANN) was observed in the TWS anomaly data simulated by the ANN. This long-term pattern in TWS anomaly from ANN mimic the long-term trend in groundwater level change observed in monitoring

wells in the respective watersheds (indicated by the purple line in Figure 3-6). It was assumed that these wells represent the regional groundwater level variation in the watersheds. As determined in the previous study [*Seyoum and Milewski*, 2016], the groundwater storage is the dominant component of the terrestrial water balance in the study area and has a significant influence on the total TWS anomaly. Thus, the long-term ANN-simulated TWS was largely showing the groundwater signal. Oppositely, this long-term pattern was not depicted in the model-derived (e.g., IHM, VIC) TWS anomaly data which makes the ANN more desirable for simulating the long-term pattern in water storage variation.

Larger changes in the amplitude of the TWS was rendered by the ANN downscaling model between 2008 and 2011 followed by a decreasing TWS anomaly between 2012 and 2013. As stated previously, this pattern was also depicted by the in-situ groundwater level data. The increasing trend in TWS anomaly matches well with the increasing trend in wetness in the study area which occurred between 2006 and 2010 and the decline in precipitation thereafter (area-averaged precipitation in the study area is shown in Figure 3-2). The lowest TWS anomaly (2012-2013) corresponds to the Midwest drought that occurred in the region during this period. Even though seasonal anomalies were detected by the models (IHM, Noah, and VIC), no such pattern in TWS variation was observed in the TWS anomaly estimated by the models as a result of climatic influences. This indicates that people tend to pump less from the aquifer during a wet period, as conditions are wet enough to rely on rainfall alone or sustain with less supplement from the aquifer. This promotes an increase in terrestrial water storage, mainly the groundwater storage, which is the case for the increase between 2008 and

2011. Not surprisingly, pumping or abstraction occurred more than usual during the dry period. Furthermore, the aquifer is getting less replenishment from rainfall during this time causing faster water storage declines. This can be seen in 2012 and 2013 due to the drought afflicting the Midwest [*Mallya et al.*, 2013]. Therefore, this variation in TWS anomaly, as a result of the combined effect of climate variability and human impact, was clearly simulated by the ANN (shown by the dashed line in Figure 3-6). However, neither the IHM nor the LSMs replicated these long-term patterns in water storage variations. This is because the variability in pumping during the above scenarios was not included in the IHM due to the lack of availability of pumping rate data (e.g. IHM) [*Seyoum and Milewski*, 2016]. Excluding simulation of storage in the saturated zone is an additional cause for the case of the land surface models (e.g. Noah LSM).

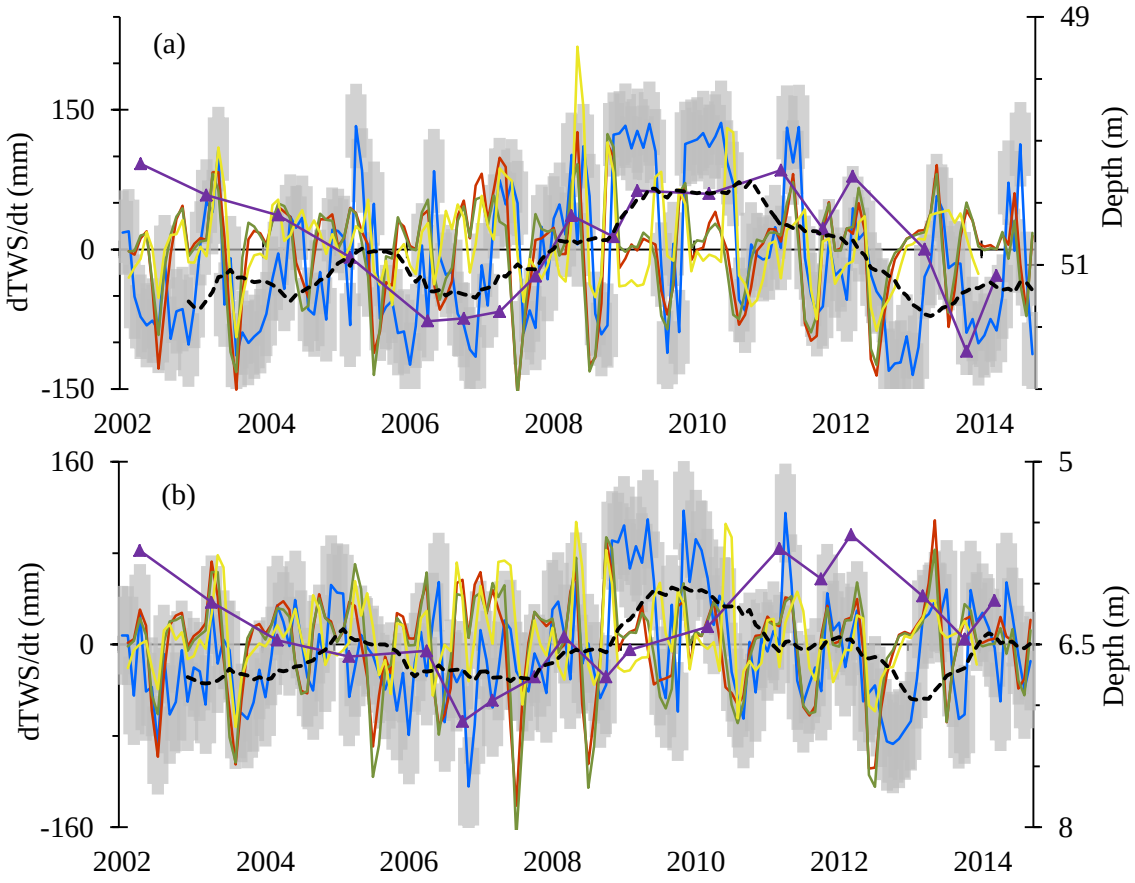

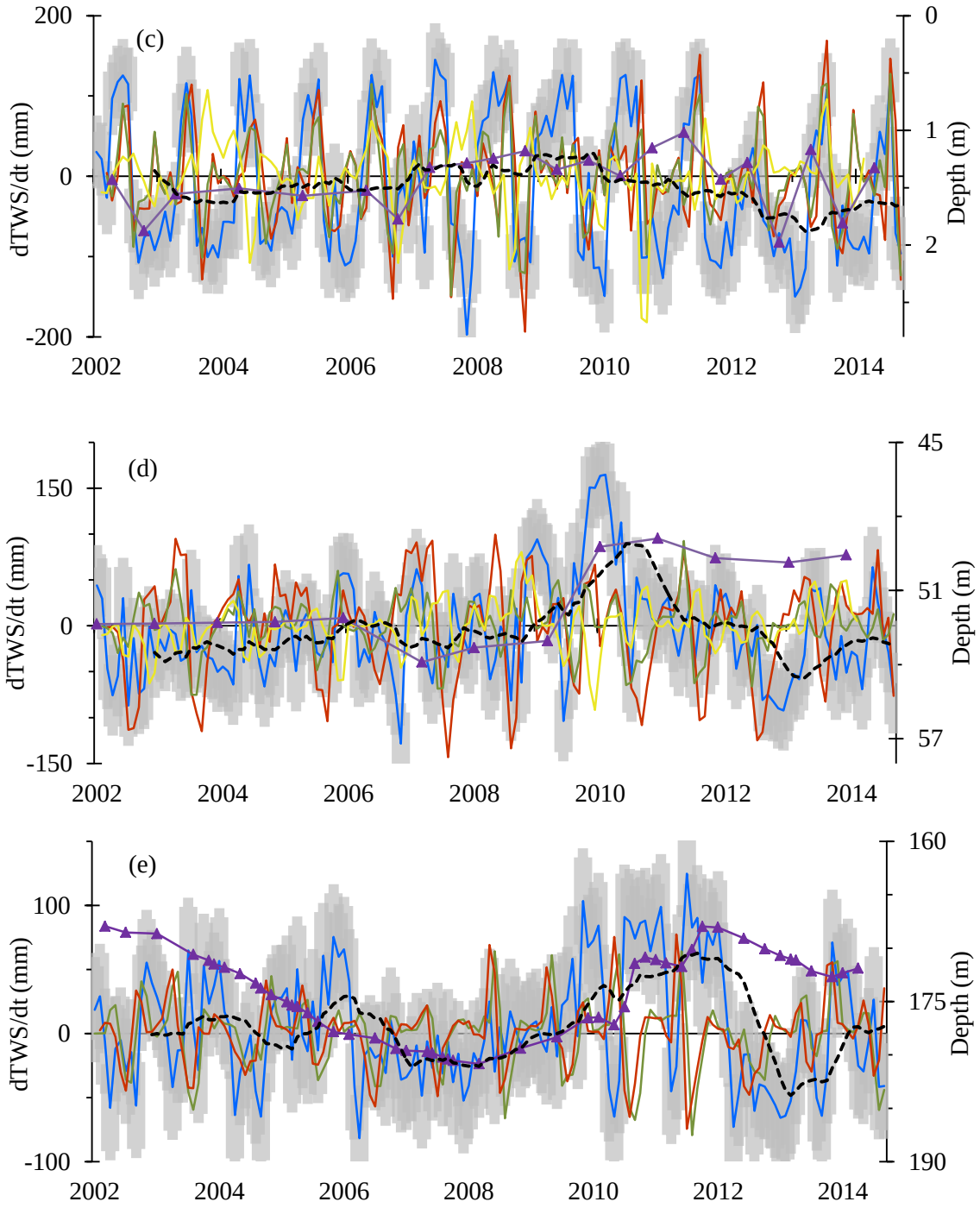
(c)
dTWS/dt (mm)
200
0
-200
Depth (m)
0
1
2
2002
2004
2006
2008
2010
2012
2014
(d)
dTWS/dt (mm)
150
0
-150
Depth (m)
45
51
57
(e)
dTWS/dt (mm)
100
0
-100
Depth (m)
160
175
190

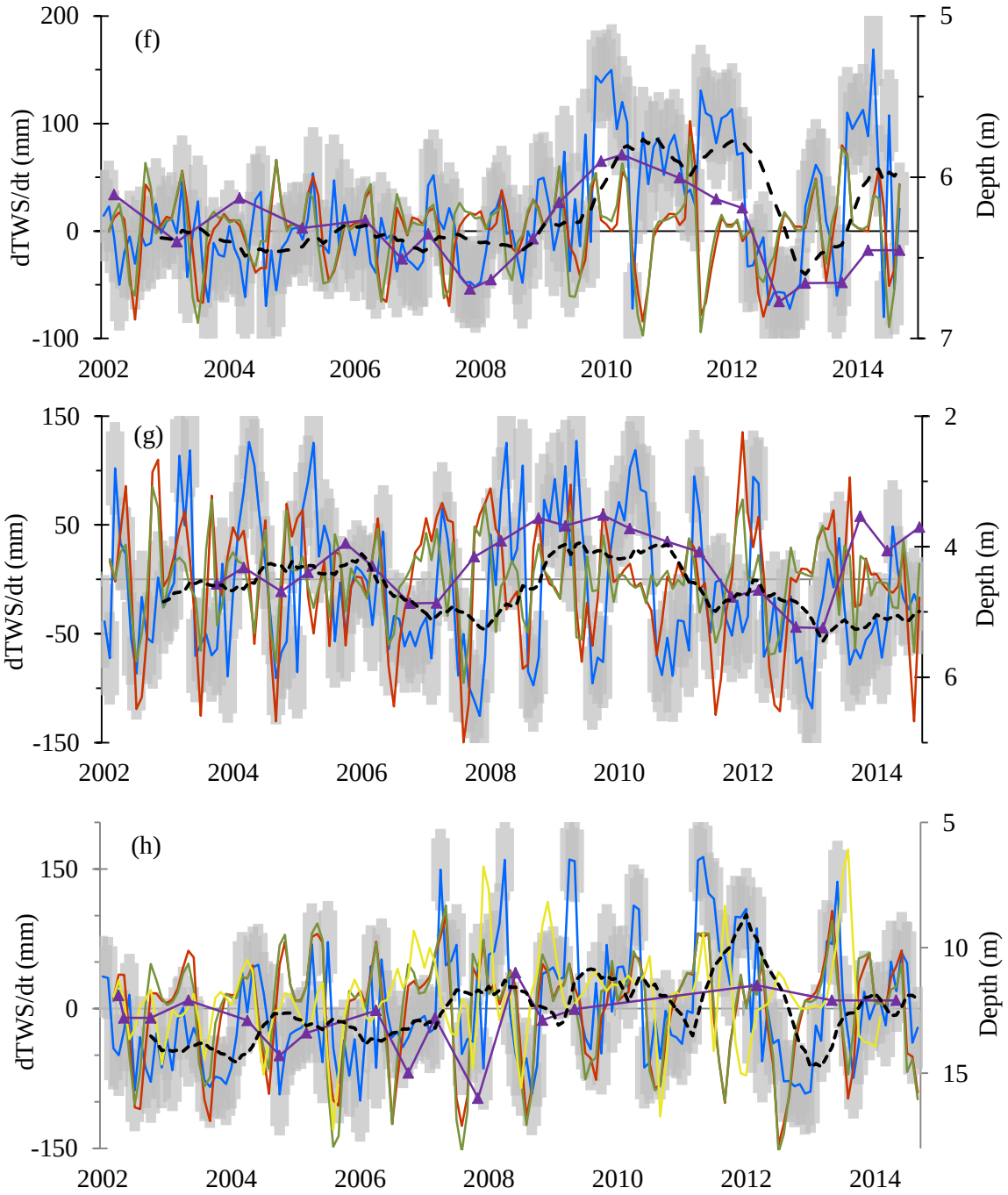
(f)
dTWS/dt (mm)
Depth (m)
200
100
0
-100
5
6
7
2002
2004
2006
2008
2010
2012
2014
(g)
dTWS/dt (mm)
Depth (m)
150
50
-50
-150
2
4
6
2002
2004
2006
2008
2010
2012
2014
(h)
dTWS/dt (mm)
Depth (m)
150
0
-150
5
10
15
2002
2004
2006
2008
2010
2012
2014

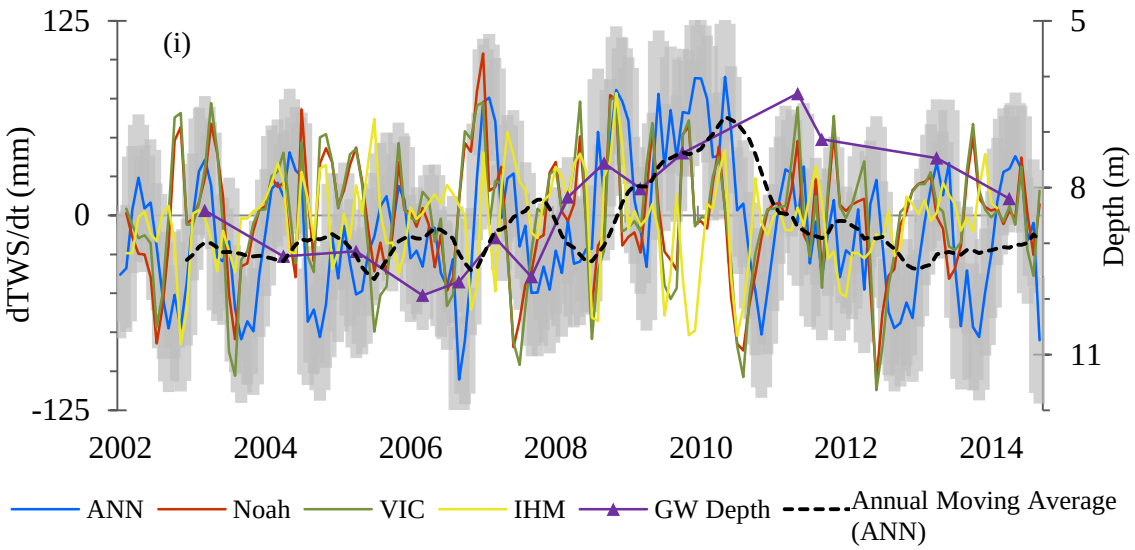

Figure 3-6. Time-series comparison of terrestrial water storage anomaly from different products (yellow line – IHM, blue line – ANN, red line – Noah, green line – VIC, purple line – depth to the groundwater level, the gray shaded region is the uncertainty over the ANN, and the dashed line represents the annual moving average over the ANN) for watersheds in the study area (a) South Loup River (1) (b) North Loup River (5) (c) Elkhorn River (3) (d) Republican River (e) Cheyenne River (10) (f) White River (2) (g) Neosho River (14) (h) Keya Paha River (13) and (i) Sappa – Prairie Dog Creek (7) (Note: the number in parentheses indicate the location of the watersheds in Figure 3-1).

Pearson correlation coefficient was calculated to evaluate the performance of the ANN-downscaled TWS anomaly data. Since there was a shift in timing among the various TWS anomaly products, the correlation was calculated with an adjustment of 0 to 2 months lags. Table 3-1 shows the statistical comparison between the ANN (downscaled) versus model-based (IHM, Noah, and VIC) TWS anomaly data for the watersheds in the study site. On a monthly time scale, the correlations between the ANN and model-based TWS anomaly products were satisfactory with an average value of ~0.4.

Generally, the watersheds in the central and eastern part of the study area have a relatively higher correlation between the ANN and model-based TWS anomaly products. Among the different TWS anomaly products, the ANN-downscaled TWS anomaly performed relatively well with the land surface models (e.g. Noah) compared to the regional integrated hydrologic model – IHM.

Table 3-1. Monthly statistical (correlation) comparison between different TWS anomaly products (ND: No data, NSS: Not statistically significant, the statistical bound is ± 0.167)

Watersheds	Area (km^2)	ANN vs. IHM	ANN vs. Noah	ANN vs. VIC
South Loup River	6,000	0.30	0.47	0.46
North Loup River	11,200	0.25	0.43	0.44
Elkhorn River	5,700	0.35	0.47	0.55
Sappa – Prairie Dog Cr.	10,900	0.30	0.50	0.43
Republican River	19,400	NSS	0.25	NSS
Cheyenne River	15,000	ND	0.33	0.33
White River	9,800	ND	0.24	NSS
Neosho River	7,300	ND	0.45	0.35
Keya Paha River	4,500	0.38	0.53	0.52
Sioux River	7,300	ND	0.40	0.42
Little Blue River	5,800	0.35	0.46	0.45
Middle Loup River	10,100	0.22	0.27	0.23
Big Blue River	3,500	0.25	0.46	0.45

Since, the ANN-downscaled change in TWS – which is a product of large scale GRACE and other terrestrial water storage variables (e.g. stream flow) – simulated the natural water storage response of the watersheds, it can be used to improve the performance of hydrologic models and land surface models. Multiple previous GRACE studies [*S Swenson and Wahr*, 2006; *Syed et al.*, 2008; *Wahr et al.*, 2004] indicated that missing or poor model representations of the components of the terrestrial water cycle as

the main reason why models cannot reproduce GRACE-observed storage anomalies, as is the case here in the derived TWS product from the ANN. Thus, having a high-resolution TWS anomaly from the ANN could further enhance the performance of the global land surface models and regional models at a local scale (small-scale).

Groundwater storage anomaly estimated from the ANN vs. in-situ groundwater observations

Groundwater storage anomaly was calculated as a residual from the total TWS anomaly calculated from the ANN downscaling model for each watershed after subtracting snow and soil moisture storage anomalies. Likewise, groundwater storage from in-situ groundwater observational data was calculated using equation 3-2. Figure 3-7 shows monthly groundwater storage anomaly calculated from the ANN and groundwater storage estimated from periodic (semi-annual to annual) in-situ groundwater level measurements for sample watersheds – South Loup River (area = 6,000 km^2) and White River (area = 10,000 km^2). As seen in the figures, the long-term groundwater storage anomaly (GWSA) derived from the ANN downscaling model (dashed line) simulated the GWSA calculated from in-situ groundwater level data (the average estimate indicated by a purple line). The ANN-derived GWSA simulated the natural response of the aquifer extremely well. Also seen in Figure 3-7, the ANN-derived GWSA depicted the rise in storage from 2006 to 2010 which was as a result of the wet condition during this period. Furthermore, it depicts the decline in aquifer storage that occurred between 2011 and 2013, which was the result of the drought combined with heightened groundwater abstraction from the aquifer in the area. The Pearson correlation coefficient (r) and percent bias (PBIAS) calculated between the ANN and in-situ based long-term

GWSA estimates were r=0.85, PBIAS=0.12 and r=0.84, PBIAS=0.04 for South Loup and White River Watersheds, respectively. This demonstrates the potential of GRACE merged with other publically available global datasets to measure long-term groundwater storage variation for a watershed as small as 6,000 km^2.

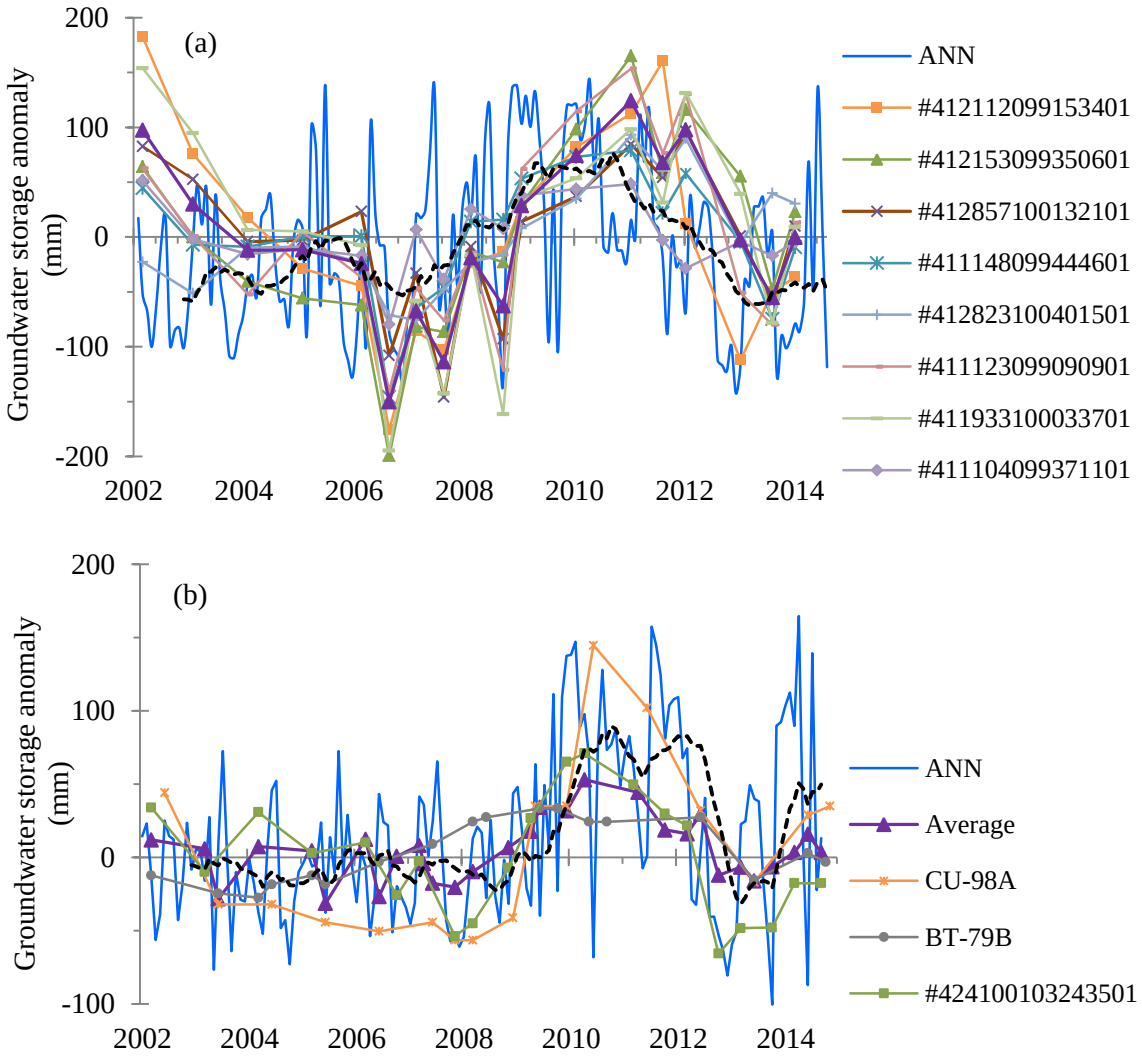

Figure 3-7. Groundwater storage anomaly calculated using the ANN downscaled TWS and in-situ groundwater level data for (a) South Loup River watershed and (b) White River watershed (blue line is the ANN-derived GWSA anomaly, the black dashed line is the annual moving average over the ANN, and the purple line is the average groundwater

storage anomaly estimated from periodic groundwater level measurements in the watersheds).

3.4. Conclusions

This research presents a methodology for integrating GRACE TWS anomaly data with additional publically available satellite data representing the terrestrial water cycle to improve the spatial resolution of GRACE and better understand local terrestrial water dynamics. A calibrated and validated ANN-based downscaling model was developed and used to calculate local TWS anomaly for watersheds ranging in size from 5,000 to 20,000 km^2 in the Northern High Plains region. The performance of the ANN downscaling model was evaluated by comparing the result with TWS anomaly estimates from land surface models (e.g. Noah), an integrated hydrologic model, and in-situ observational data. The following conclusions were drawn from this research:

(1) Generally, the ANN downscaling method was able to successfully reproduce the monthly TWS variations in the representative watersheds within the uncertainty of the data.

(2) Unlike the TWS anomaly data derived from the IHM and LSM, the downscaled ANN TWS product displayed a distinct long-term pattern in TWS variation that mimics the long-term trend in groundwater level variation from monitoring wells in the watersheds.

(3) The ANN-based downscaled TWS anomaly simulated the natural water storage variation as a result of the combined effect of climatic variability and human abstraction. It also performed well during climatic stress periods (e.g., wet years [2006-2010] and drought periods [2012-2013]).

(4) The long-term pattern in TWS anomaly resulting from the combined climatic and human was not replicated by the IHM and LSMs. This is attributed to the lack of pumping rate variability as a result of climatic variations (e.g. IHM), and the lack of consideration of water use and excluding the saturated zone in the simulation for the case of the land surface models (e.g. Noah).

(5) Derived groundwater storage anomaly data from the ANN correlated very well (r=0.85) with groundwater storage anomaly data calculated from in-situ groundwater level measurements for sample watersheds.

Most importantly, this study demonstrated the potential of GRACE satellite mission data merged with other satellite datasets to quantify groundwater storage anomaly for watersheds as small as 6000 km^2 as well as to predict long-term patterns in TWS variation. The implications utilizing finer resolution GRACE data for improving local and regional water resources management decisions and applications are clear. This is especially true with areas lacking hydrologic monitoring networks. Moreover, the ability of the ANN to predict the natural storage variability shows the potential of using it to further enhance the performance of global land surface models and regional hydrologic models. Lastly, such an approach could be used for filling the data gap between the current GRACE and future GRACE-FO missions given predictions or availability of future data for the TWS variables (e.g. precipitation).

References

Ahmed, M., M. Sultan, J. Wahr, E. Yan, A. Milewski, W. Sauck, R. Becker, and B. Welton (2011), Integration of GRACE (Gravity Recovery and Climate Experiment) data with traditional data sets for a better understanding of the time-dependent water partitioning in African watersheds, Geology, 39(5), 479-482.

Andreadis, K. M., and D. P. Lettenmaier (2006), Assimilating remotely sensed snow observations into a macroscale hydrology model, Advances in Water Resources, 29(6), 872-886.

ASCE Task Committee, o. A. o. A. N. N. i. H. (2000), Artificial Neural Networks in Hydrology. I: Preliminary Concepts, Journal of Hydrologic Engineering, 5(2), 115-123.

Birkinshaw, S. J., G. M. O'Donnell, P. Moore, C. G. Kilsby, H. J. Fowler, and P. A. M. Berry (2010), Using satellite altimetry data to augment flow estimation techniques on the Mekong River, Hydrological Processes, 24(26), 3811-3825.

Chadwick, R., E. Coppola, and F. Giorgi (2011), An artificial neural network technique for downscaling GCM outputs to RCM spatial scale, Nonlinear Processes in Geophysics, 18(6), 1013-1028.

Chatfield, C. (2004), The analysis of time series : an introduction, Boca Raton : Chapman & Hall/CRC, c2004. 6th ed.

Coppola Jr, E., F. Szidarovszky, M. Poulton, and E. Charles (2003), Artificial Neural Network Approach for Predicting Transient Water Levels in a Multilayered Groundwater System under Variable State, Pumping, and Climate Conditions, JOURNAL OF HYDROLOGIC ENGINEERING, 8(6), 348 - 360.

Coulibaly, P., F. Anctil, R. Aravena, and B. Bobee (2001), Artificial neural network modeling of water table depth fluctuations, Water Resour. Res., 37(4), 885–896.

Dennehy, K. F. (2000), High Plains regional ground-water studyRep. U.S. Geological Survey Fact Sheet FS–091–00, 6 pp.

Duan, Z., and W. G. M. Bastiaanssen (2013), Estimating water volume variations in lakes and reservoirs from four operational satellite altimetry databases and satellite imagery data, Remote Sensing of Environment, 134, 403-416.

Ek, M. B., K. E. Mitchell, Y. Lin, E. Rogers, P. Grunmann, V. Koren, G. Gayno, and J. D. Tarpley (2003), Implementation of Noah land surface model advances in the National Centers for Environmental Prediction operational mesoscale Eta model, Journal of Geophysical Research: Atmospheres, 108(D22), n/a-n/a.

Gardner, M. W., and S. R. Dorling (1998), Artificial neural networks (the multilayer perceptron)—a review of applications in the atmospheric sciences, Atmos. Environ., 32(14–15), 2627-2636.

Hagan, M. T., and M. B. Menhaj (1994), Training feedforward networks with the Marquardt algorithm, IEEE Transactions on Neural Networks, 5(6), 989-993.

Houborg, R., M. Rodell, B. Li, R. Reichle, and B. F. Zaitchik (2012), Drought indicators based on model-assimilated Gravity Recovery and Climate Experiment (GRACE) terrestrial water storage observations, Water Resour. Res., 48(7), W07525.

Kasiviswanathan, K. S., R. Cibin, K. P. Sudheer, and I. Chaubey (2013), Constructing prediction interval for artificial neural network rainfall runoff models based on ensemble simulations, Journal of Hydrology, 499, 275-288.

Kraller, G., M. Warscher, H. Kunstmann, S. Vogl, and T. Marke (2012), Water balance estimation in high Alpine terrain by combining distributed modeling and a neural network approach (Berchtesgaden Alps, Germany), Hydrology and earth system sciences, 16(7), 1969-1990.

Landerer, F. W., and S. C. Swenson (2012), Accuracy of scaled GRACE terrestrial water storage estimates, Water Resour. Res., 48(4), W04531.

Liang, X., D. P. Lettenmaier, E. F. Wood, and S. J. Burges (1994), A simple hydrologically based model of land surface water and energy fluxes for general circulation models, Journal of Geophysical Research: Atmospheres, 99(D7), 14415-14428.

Long, D., B. R. Scanlon, L. Longuevergne, A. Y. Sun, D. N. Fernando, and H. Save (2013), GRACE satellite monitoring of large depletion in water storage in response to the 2011 drought in Texas, Geophysical Research Letters, 40(13), 3395-3401.

Longuevergne, L., B. R. Scanlon, and C. R. Wilson (2010), GRACE Hydrological estimates for small basins: Evaluating processing approaches on the High Plains Aquifer, USA, Water Resour. Res., 46(11), n/a-n/a.

Mallya, G., L. Zhao, X. Song, D. Niyogi, and R. Govindaraju (2013), 2012 Midwest Drought in the United States, Journal of Hydrologic Engineering, 18(7), 737-745.

Marquardt, D. W. (1963), An Algorithm for Least-Squares Estimation of Nonlinear Parameters, Journal of the Society for Industrial and Applied Mathematics, 11(2), 431-441.

McGuire, V. L. (2014), Water-Level Changes and Change in Water in Storage in the High Plains Aquifer, Predevelopment to 2013 and 2011–13. U.S. Geological Survey Scientific Investigations Report 2014–5218 Rep., 14 pp.

Milewski, A., R. Elkadiri, and M. Durham (2015), Assessment and Comparison of TMPA Satellite Precipitation Products in Varying Climatic and Topographic Regimes in Morocco, Remote Sensing, 7(5), 5697.

Milewski, A., M. Sultan, S. M. Jayaprakash, R. Balekai, and R. Becker (2009a), RESDEM, a tool for integrating temporal remote sensing data for use in hydrogeologic investigations, Computers & Geosciences, 35(10), 2001-2010.

Milewski, A., M. Sultan, E. Yan, R. Becker, A. Abdeldayem, F. Soliman, and K. A. Gelil (2009b), A remote sensing solution for estimating runoff and recharge in arid environments, Journal of Hydrology, 373(1–2), 1-14.

Nourani, V., A. Hosseini Baghanam, J. Adamowski, and O. Kisi (2014), Applications of hybrid wavelet–Artificial Intelligence models in hydrology: A review, Journal of Hydrology, 514, 358-377.

Pokhrel, Y. N., S. Koirala, P. J. F. Yeh, N. Hanasaki, L. Longuevergne, S. Kanae, and T. Oki (2015), Incorporation of groundwater pumping in a global Land Surface Model with the representation of human impacts, Water Resour. Res., n/a-n/a.

Rodell, M., and J. S. Famiglietti (1999), Detectability of variations in continental water storage from satellite observations of the time dependent gravity field, Water Resour. Res., 35(9), 2705-2723.

Rodell, M., and J. S. Famiglietti (2002), The potential for stellite-based monitoring of groundwater storage changes using GRACE: the High Plains aquifer, Central US, Journal of Hydrology, 263, 245 - 256.

Rodell, M., I. Velicogna, and J. S. Famiglietti (2009), Satellite-based estimates of groundwater depletion in India, Nature, 460(7258), 999-1002.

Seyoum, W. M., and A. M. Milewski (2016), Monitoring and comparison of terrestrial water storage changes in the Northern High Plains using GRACE and in-situ based integrated hydrologic model estimates Advances in Water Resources.

Seyoum, W. M., A. M. Milewski, and M. C. Durham (2015), Understanding the relative impacts of natural processes and human activities on the hydrology of the Central Rift Valley lakes, East Africa, Hydrological Processes, 29(19), 4312-4324.

Stanton, J. S., S. L. Qi, D. W. Ryter, S. E. Falk, N. A. Houston, S. M. Peterson, S. M. Westenbroek, and S. C. Christenson (2011), Selected approaches to estimate water-budget components of the High Plains, 1940 through 1949 and 2000 through 2009: U.S. Geological Survey Scientific Investigations Report 2011–5183, pp. 79.

Sun, A. Y. (2013), Predicting groundwater level changes using GRACE data, Water Resour. Res., 49(9), 5900-5912.

Swenson, S., and J. Wahr (2006), Post-processing removal of correlated errors in GRACE data, GEOPHYSICAL RESEARCH LETTERS, 33(L08402:), 1-4.

Swenson, S., and J. Wahr (2009), Monitoring the water balance of Lake Victoria, East Africa, from space, Journal of Hydrology, 370(1-4), 163-176.

Swenson, S. C., and J. M. Wahr (2011), Estimating signal loss in regularized GRACE gravity field solutions, Geophysical Journal International, 185(2), 693-702.

Syed, T. H., J. S. Famiglietti, M. Rodell, J. Chen, and C. R. Wilson (2008), Analysis of terrestrial water storage changes from GRACE and GLDAS, Water Resour. Res., 44(2), W02433.

Tadesse, T., G. B. Senay, G. Berhan, T. Regassa, and S. Beyene (2015), Evaluating a satellite-based seasonal evapotranspiration product and identifying its relationship with other satellite-derived products and crop yield: A case study for Ethiopia, Int J Appl Earth Obs, 40, 39-54.

Tapley, B. D., and S. Bettadpur (2004), The gravity recovery and climate experiment: Mission overview and early results, Geophysical Research Letters, 31(9), L09607.

Thomas, A. C., J. T. Reager, J. S. Famiglietti, and M. Rodell (2014), A GRACE-based water storage deficit approach for hydrological drought characterization, Geophysical Research Letters, 41(5), 1537-1545.

Tsegaye, T. D., W. L. Crosson, C. A. Laymon, M. P. Schamschula, and A. B. Johnson (2003), Application of a neural network-based spatial disaggregation scheme for addressing scaling of soil moisture, In Scaling Methods in Soil Physics, Y. Pachepsky, D.E. Radcliffe and H.M. Selim, Eds., CRC Press, Boca Raton, FL, 261-277.

Vinukollu, R. K., E. F. Wood, C. R. Ferguson, and J. B. Fisher (2011), Global estimates of evapotranspiration for climate studies using multi-sensor remote sensing data: Evaluation of three process-based approaches, Remote Sensing of Environment, 115(3), 801-823.

Wahr, J., S. Swenson, V. Zlotnicki, and I. Velicogna (2004), Time-variable gravity from GRACE: First results, Geophysical Research Letters, 31(11).

Wang, W.-c., K.-w. Chau, L. Qiu, and Y.-b. Chen (2015), Improving forecasting accuracy of medium and long-term runoff using artificial neural network based on EEMD decomposition, Environ. Res., 139, 46-54.

Yeh, P. J. F., S. C. Swenson, J. S. Famiglietti, and M. Rodell (2006), Remote sensing of groundwater storage changes in Illinois using the Gravity Recovery and Climate Experiment (GRACE), Water Resour. Res., 42(12), W12203 (12201-12207).

Zaitchik, B. F., M. Rodell, and R. H. Reichle (2008), Assimilation of GRACE Terrestrial Water Storage Data into a Land Surface Model: Results for the Mississippi River Basin, Journal of Hydrometeorology, 9(3), 535-548.

CHAPTER 4

UNDERSTANDING THE RELATIVE IMPACTS OF NATURAL PROCESSES AND HUMAN ACTIVITIES ON THE HYDROLOGY OF THE CENTRAL RIFT VALLEY LAKES, EAST AFRICA

Seyoum, W. M., A. M. Milewski, and M. C. Durham, Understanding the relative impacts of natural processes and human activities on the hydrology of the Central Rift Valley lakes, East Africa, 2015, *Hydrological Processes*, *29*(19), 4312-4324, Reprinted here with permission of the publisher.

Abstract

Significant changes have been observed in the hydrology of Central Rift Valley (CRV) lakes in Ethiopia, East Africa as a result of both natural processes and human activities during the past three decades. This study applied an integrated approach (remote sensing, hydrologic modeling, and statistical analysis) to understand the relative effects of natural processes and human activities over a sparsely gauged Central Rift Valley basin. Lake storage estimates were calculated from a hydrologic model constructed without inputs from human impacts such as water abstraction, and compared with satellite-based (observed) lake storage measurements to characterize the magnitude of human-induced impacts. A non-parametric Mann-Kendall test was used to detect the presence of climatic trends (e.g. a decreasing or increasing trends in precipitation), while the Standard Precipitation Index (SPI) analysis was used to assess the long-term, inter-annual climate variability within the basin. Results indicate human activities (e.g. abstraction) significantly contributed to the changes in the hydrology of the lakes, while no statistically significant climatic trend was seen in the basin, however inter-annual natural climate variability, extreme dryness and prolonged drought has negatively affected the lakes. The relative contributions of natural and human-induced impacts on the lakes were quantified and evaluated by comparing hydrographs of the CRV lakes. Lake Abiyata has lost ~ 6.5m in total lake height between 1985 and 2006, 70% (~ 4.5 m) of the loss has been attributed to human-induced causes, whereas the remaining 30% is related to natural climate variability. The relative impact analysis utilized in this study could potentially be used better plan and create effective water management practices in

the basin and demonstrates the utility of this integrated methodology for similar studies assessing the relative natural and human-induced impacts on lakes in data sparse areas.

4.1. Introduction

The effect of climate change (e.g. changes in precipitation and temperature) and human activities (e.g. water abstraction, and landuse change) on the water cycle is a major concern in water resources management [*St. Jacques et al.*, 2010; *Ferguson and Maxwell*, 2012]. Humans impact the hydrologic cycle at various scales. At a global scale, human-driven climate change is observed through alternating patterns and intensity of precipitation and temperature [*Bates et al.*, 2008] which in turn affects surface and groundwater storages. At local scales, water abstraction and consumption by humans directly alters surface water (e.g. lakes, rivers) and groundwater storages. On the other hand, natural climate variability, variation in intensity and duration of wet and dry condition, is as significant as human-driven processes that affect the water cycle [*Hulme et al.*, 1999; *Chen et al.*, 2012]. Understanding the relative impact of both natural and human-induced processes on the water cycle is crucial for considering appropriate water policy measures and thus the purpose of this research.

Significant changes have been observed in the hydrology of the Rift Valley lakes in Ethiopia over the past four decades. A number of lakes (e.g. Lake Beseka and Lake Awassa) expanded while others (e.g. Lake Abiyata) have declined in size or storage [*Tenalem Ayenew*, 2007]. Human interventions such as abstraction from lakes or tributaries, climate change, irrigation, deforestation, and urbanization have all been known to disrupt the natural flow regime of the lakes and overall hydrologic system with

potentially irreversible damages. For example, Lake Haromaya, East Africa dried out in 2005 as a result of excessive surface and groundwater withdrawal [*Alemayehu et al.,* 2006a]. Development of large-scale irrigation and industrial abstraction from the Central Rift Valley (CRV) lakes and their tributaries dates back to the early 1980s. As a result, poor water management practices have altered the hydrology of most lakes in the region [*Legesse et al.*, 2004; *Tenalem Ayenew*, 2007].

Lakes naturally fluctuate in response to natural climate variability. For instance, *Makin et al.* [1976] observed a significant lake level fluctuation in the CRV lakes in the 1940s and 1960s, a period of limited or no human activities in the area. During this time the highest recorded change in Lake Abiyata's lake level, which is equivalent to the recent change estimated in this study, was seven meters. *Street* [1979], through the use of aerial photographs, estimated the Lake Abiyata surface area to be 143, 182, and 168 km^2 in 1956, 1972, and 1974, respectively. During this period, the lakes are assumed to be responding to the natural condition with little human influence. Similar magnitudes of variations in lake size were also determined in this study during the period of 1985-2010 when human influences were significant. Therefore, the hypothesis of this study is that both natural climate variability and human activities affected the hydrology of the lakes in the Central Rift Valley (CRV) basin, East Africa.

The hydrology of the Rift Valley has been a subject of investigations in the past [*Makin et al.*, 1976; *Cherenet*, 1993; *Darling et al.*, 1996; *Hailemarian*, 1999; *Tenalem Ayenew*, 2007] with several specifically focused on the CRV basin lakes [*Kebede et al.*, 1994; *Legesse et al.*, 2004; *T. Ayenew and Gebreegziabher*, 2006]. Most of the studies used traditional methods such as lake water balance calculations and hydrogeochemical

approaches [*Tenalem Ayenew*, 2002; *Alemayehu et al.*, 2006b]. Unfortunately, quantitative analysis to understand the relative impact of natural processes and human activities on the lakes or the CRV basin is not available. Some of the cited research followed localized approaches focusing only on lakes [*Legesse et al.*, 2004]. Though, the ultimate effect is on the lakes, the impacts could be basin-wide affecting the rivers and tributaries that feed the lakes. Therefore, the objective of this study was to conduct a thorough investigation of the relative impact of both natural processes and human activities on the hydrology of the CRV lakes using an integrated approach (remote sensing, hydrologic modeling, and statistical analysis).

4.2. Study Area

The Main Ethiopian Rift (MER), part of the Great East African Rift Valley system, is subdivided into three sections: the Northeastern, Central, and Southwestern. Clusters of lakes are found occupying the floor of the Central and Southwestern sections. The Central Rift Valley (CRV) basin, a part of the Central Section of MER, is an endorheic basin with an area of 10,185 km^2 and has three major surficially interconnected lakes: Lake Abiyata, Lake Langano and Lake Ziway (Figure 4-1). Lake Ziway, located within the upstream section of the CRV is fed by two major perennial rivers: Meki River and Katar River. Lake Ziway overflows by way of the Bulbula River to Lake Abiyata. Similarly, Lake Langano receives surface inflow from the eastern escarpment of the rift valley and overflows intermittently to Lake Abiyata. Human-induced abstractions from the lakes and their tributaries are primarily used for agricultural and industrial production in the area. Large-scale agricultural abstraction (irrigation) from Lake Ziway, its tributaries, and the Bulbula River is used in the production of horticulture, vegetables,

and flowers. Industrial abstraction from Lake Abiyata is primarily used for soda ash production. In the early to mid-2000s, the total annual water use in the basin was estimated to be approximately160 MCM [*Jansen et al.*, 2007].

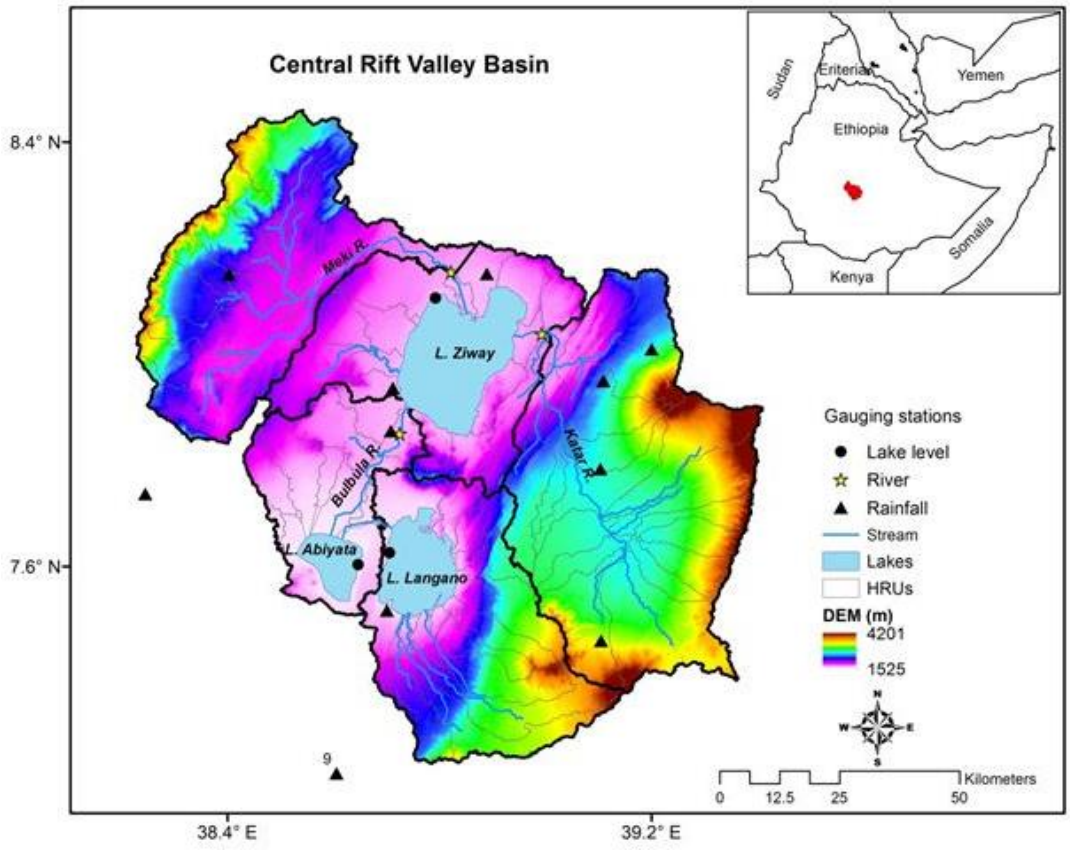

Figure 4-1. Location map of the study area showing the DEM, gauging stations, surface waters, and sub-basins (outlined in black). Inset map shows location of the CRV lakes basin in East Africa.

The CRV basin is bounded to the east and west by the escarpment of the Rift Valley and the highlands. Topographically, this region is characterized by mountainous terrain on the eastern and western escarpments (elevation ~ 4200m) and flat to gentle slopes of the rift valley floor (elevation ~ 1600m) (Figure 4-1). The CRV lakes receive

runoff from the eastern and western escarpment of the Rift Valley. Lake Ziway (~ 450 km^2) is a fresh water lake with an average surface elevation of ~1636 m and an average depth of ~5 m. Lake Langano (~ 250 km^2), a slightly saline (brackish) lake, has an average surface elevation of ~ 1585 m and average depth of ~55 m. The saline Lake Abiyata (~ 115 km^2) has an average surface elevation of ~ 1575 m and an average depth ~14 m.

Generally, the CRV basin has two climatic zones: (1) sub-humid to humid climate of the escarpment and highland regions (eastern and western sections), receiving relatively high annual precipitation (~1050 mm) and low temperatures (15 ^oC) and (2) semi-arid climate of the Rift Valley floor (central section) receiving relatively low annual precipitation (~700 mm) and average high temperatures (20 ^oC). June, July, and August are typically the wettest months of the year producing relatively high rainfall, while December, January, and February are typically the driest months. The Meki River and Katar River catchments, total catchment area of 5200 km^2 (~ 50% of the total basin area), replenish Lake Ziway throughout the year with average annual flows of 410 and 265 MCM, respectively.

4.3. Method

The focus of this study was to integrate different techniques (remote sensing, hydrologic modeling, and statistical analysis) with the best available data (in-situ and satellite-based) to understand the effect of human activities and natural processes over the sparsely gauged CRV basin. First, satellite data were analyzed to map the temporal variations of lake size and storage. Hydrologic modeling, which doesn't take into account

the human impacts (e.g. water abstraction), was applied to simulate lake level and storage variation. Thus, comparison between model simulated and satellite-based (observed) lake storage was used to understand and quantify the magnitude of the human impact on the lakes. In addition, available temporal gauge data (e.g. precipitation and lake level) were analyzed using statistical methods (e.g. Mann-Kendall) to understand the effect of climate variability on the lakes in the CRV basin.

Satellite-based Lake Surface Area

The ability to monitor water resources using satellite remote sensing has emerged as a viable alternative or supplement to in-situ data in ungauged or sparsely gauged basins. One of the applications of satellite-based data is monitoring surface water bodies through the use of VIS/NIR sensors. There are several methods for delineating lake/water inundation areas using remote sensing imagery [*Smith*, 1997; *Alsdorf et al.*, 2007; *Prigent et al.*, 2007; *Ward et al.*, 2014]. The Normalized Difference Water Index (NDWI), a commonly used optical remote sensing method, involves spectral index calculation of two or more spectral bands. Several NDWI equations were previously developed for different satellite products [*Gao*, 1996; *McFeeters*, 1996; *Rogers and Kearney*, 2004; *Xu*, 2006]. *Ji et al.* [2009] analyzed different MNDWI (Modified Normalized Difference Water Index) equations to determine the best performing index and establish appropriate thresholds for identifying water features from imageries such as LANDSAT, ASTER, and MODIS satellites. They suggested the MNDWI equation of (green - SWIR) / (green + SWIR), where the SWIR band in the region of shorter wavelength (1.2 - 1.8 mm), has the most stable threshold to map water bodies. The calculated MNDWI values range from -1 to 1with water pixels identified by MNDWI values within a range of 0 to 1. However,

adjustment of a threshold value is necessary based on actual site conditions [*Ji et al.*, 2009].

In this study, temporal variation of lake surface area was mapped using cloud free LANDSAT TM/ETM+ imagery obtained from the USGS (http://glovis.usgs.gov/, date accessed: 2/3/2013). Standard processing techniques such as radiometric calibration and atmospheric correction were applied to the satellite images. Using processed satellite images, NDWI was calculated from the green and SWIR bands of LANDSAT TM/ETM+. In the CRV study site, the water surfaces have distinct MNDWI values (MNDWI > 0.5). Using this threshold, the images were classified to keep consistency while delineating lake inundation areas. Finally, the images were processed in ArcGIS and used to calculate the surface area of the lakes. In addition to the temporal analysis of surface area measured from satellite imagery, it was also used to calculate changes in lake storage using bathymetric data for the lake.

Hydrologic Modeling

Hydrological modeling was used to understand and estimate the magnitude of the human-induced impact (e.g. water abstraction) on the lakes. Analogous to the work of *Van Loon and Van Lanen* [2013], the basic assumption is that the hydrologic models simulate a condition that would have occurred without human influence (e.g. abstraction from the lakes and tributaries), the "natural" condition which would be solely a result of climate forcing. Based on this assumption, if there is a major shift of the hydrograph between model simulated and observed satellite-based lake storage, the shift is most likely a result of human-induced impacts. The human impact considered in this study is

only due to abstraction of water from the lakes and tributaries; landuse is assumed constant throughout the model simulation period. To minimize the inclusion of human impacts in the model simulation, the model was calibrated using gauging stations upstream of the Lakes (Figure 4-1), where there is no major abstraction during the calibration period. Major water abstraction occurred from the lakes and the Bulbula River, tributary river that connects Lake Ziway and Lake Abiyata. The modeling involved: (1) the development of a hydrologic model, the Soil Water Assessment Tool (SWAT) to simulate the total surface runoff to the lakes, and (2) the calculation of lake water budgets and lake storage simulation.

SWAT Model

SWAT is a continuous, semi-distributed, physically based model developed by the US Department of Agriculture - Agriculture Research Service (USDA-ARS). It predicts the impact of land management practices on water, sediment and agricultural chemicals within a watershed [*Neitsch et al.*, 2005]. SWAT has been found to replicate hydrologic and pollutant loads at a variety of spatial scales and at sufficient accuracy that makes it a useful tool for watershed simulation throughout the world [*Gassman et al.*, 2007]. Model calculations are performed on Hydrologic Response Units (HRU) which are sub-units of sub-basins with unique combinations of soil and land use characteristics that are considered to be hydrologically homogeneous. The flow variables are routed from HRU to sub-basin and subsequently to the watershed outlet. For a more detailed description of SWAT, see *Neitsch et al.* [2005]. The soil water balance is the primary process in each HRU and is represented below after *Arnold et al.* [1998]:

$$\Delta SW = SW_t - SW = \sum_{i=1}^{t}(R_i - Q_i - ET_i - P_i - QR_i) \quad (4\text{-}1)$$

Where: *SW* is the soil water content, *i* is the time in days from the simulation period *t*, and *R, Q, ET, P* and *QR* respectively are the daily precipitation, runoff, evapotranspiration, percolation, and return flow in mm.

SWAT Model Input

SWAT spatial data inputs include topography, climate, landuse, and soil. These model inputs include: (1) 30 m resolution Digital Elevation Model (ASTER GDEM V2) obtained from https://lpdaac.usgs.gov/data_access, date accessed: 4/8/2013 (Figure 4-1); (2) landuse map [*FAO-UN*, 2009] and soil map from Harmonized World Soil Database [*FAO et al.*, 2012] used to delineate the watershed, sub-basins, and HRUs; and (3) weather data which includes daily precipitation data from 11 gauging stations (Figure 4-1) obtained from the Ethiopian Meteorological Service Agency, and daily temperature, wind speed, solar radiation and humidity data from the National Centers for Environmental Prediction (NCEP) Climate Forecast System Reanalysis (CFSR) accessed from http://globalweather.tamu.edu/, date accessed: 3/14/2013.

Model Evaluation

Evaluation of a model's ability to simulate watershed response accurately is vital before further application of the model. Model evaluation is a three step process including sensitivity analysis, calibration, and validation. Parameter sensitivity provides insight into the model response to changes in model parameters which helps to identify sensitive calibration parameters as well as adjust initial range of values for further model

calibration. Model calibration involves establishing a statistical relationship between model parameters and the characteristics of the watershed whereas validation is a technique for testing the performance of a calibrated model. Due to variability of input data, conceptual model design, model parameters, and output uncertainties, hydrologic model calibration requires uncertainty analysis. To account for these uncertainties, various statistical approaches were developed and previously used for SWAT models [*Yang et al.*, 2008; *Abbaspour*, 2013; *Zhou et al.*, 2014]. The degree of uncertainties is quantified by the P-factor (percentage of the simulated values bracketed by the 95% probability band) and r-factor (the width of the 95% probability band).) The theoretical value of the P-factor ranges between 0 and 1, while that of the r-factor ranges between 0 and infinity. A P-factor of 1 and r-factor of zero indicates that a simulation corresponds exactly to the measured data [*Abbaspour*, 2013].

Model evaluation was conducted on a monthly time scale for the period of 1980-2000 using a combination of manual and automatic calibration methods. A period of 11 years (1985-1995) was selected for calibration and five years (1995-2000) designated for validation, the initial five years reserved as the models warm-up period. The ParaSol procedure in SWAT-CUP (SWAT Calibration and Uncertainty Procedures) was used for automatic calibration, sensitivity, and uncertainty analysis, see *Abbaspour* [2013] for details about SWAT-CUP. Table 4-1 shows model calibration parameters, sensitivity analysis results, and simulated values. The t-stat in Table 4-1 provides a measure of the sensitivity of the parameters where the larger absolute value is more sensitive. Likewise, the p-value determines the significance of the sensitivity results. Values closer to zero are considered more statistically significance.

Table 4-1. SWAT model parameters used for calibration, sensitivity analysis results indicated by t-Stat and p-value, model initial, and final simulated values; the ranges indicate the lower and upper bounds.

Parameter Name	t-Stat	P-Value	Initial values	Simulated values
Saturated hydraulic conductivity (SOL_K)	15.697	0	0 - 2000	0.1 – 300
Baseflow alpha factor, in days (ALPHA_BF)	7.303	0	0 - 1	0.05 – 0.5
Baseflow alpha factor for bank storage (ALPHA_BNK)	7.862	0	0 - 1	0.1
Soil evaporation compensation factor (ESCO)	3.083	0.002	0 - 1	0.4 – 0.75
Deep aquifer percolation fraction (RCHRG_DP)	2.125	0.034	0 - 1	0.05
Effective hydraulic conductivity in main channel (CH_K2)	-2.029	0.043	0.01 - 500	0.01
Groundwater "revap" coefficient (GW_REVAP)	-1.97	0.049	0.02 - 0.2	0.15
Mannings ‘n’ value for the main channel (CH_N2)	-1.31	0.19	0.01 - 0.3	0.014
Available water capacity (SOL_AWC)	1.25	0.211	0 - 1	0.1 - 0.7
Threshold depth of water in the shallow aquifer, mm (GWQMN)	1.147	0.252	0 - 5000	60 - 75
Mannings ‘n’ value for overland flow (OV_N)	0.566	0.571	0.01 - 30	0.01 - 0.15
Threshold depth of water in the shallow aquifer for "revap" to occur, in mm (REVAPMN)	0.468	0.64	0 - 500	50 - 120
SCS runoff Curve No (CN2)	-0.382	0.703	35 - 98	38 - 78
Plant uptake compensation factor (EPCO)	0.312	0.755	0 - 1	0.5
Groundwater delay, days (GW_DELAY)	-0.127	0.899	0 - 500	31 - 38

The model was calibrated and validated with two gauging stations (obtained from Ethiopian Ministry of Water Resources) located on the Meki River and Katar River (Figure 4-1). Objective functions, such as coefficient of determination (R^2) and Nash-Sutcliffe model efficiency (NSE) were used for optimization of the parameters. According to *Liew et al.* [2007], the simulation result considered good if NSE value > 0.75 whereas for values of NSE between 0.75 and 0.36, the simulation results are considered to be satisfactory. Mean and total flow values between simulated and observed were also compared as an independent evaluation of model performance. After model calibration and validation, the model run was extended up to 2010 which allowed

the inclusion of human-induced impacts as a result of recent increases in water consumption due to expansion of human activities in the basin.

Lake water-budget and storage simulation

The calibrated SWAT model provides continuous runoff data from gauged and ungauged sub-basins of the lakes. Total runoff along with precipitation and evaporation data was analyzed to calculate a lake water budget (Equation 4-2).

$$\frac{\Delta S}{\Delta t} = P + R - S_o - E - A \quad (4\text{-}2)$$

Where: ΔS is the change in lake storage, P is the precipitation directly to the lake, R is the surface runoff to the lake, S_o is the surface outflow from the lake, E is the evaporation from the lake surface, and A is water abstraction, all units are in mm.

Using digital bathymetry data and the lake water budget, a relationship between lake height, surface area and volume was established (e.g. Equations 4-3 and 4-4) for Lake Abiyata. Model simulated lake storage (or height), which does not take into account water use (excluding water abstraction - variable "A" from the Equation 4-2), was then compared to storage estimated from satellite-based data (Landsat) and bathymetry data (Sources: *Legesse et al.* [2004] for Lake Abiyata and *Makin et al.* [1976] for Lake Ziway).

$$V = 122.97 \times h - 1092.3 \quad (4\text{-}3)$$

$$A = 15.23 \times h - 186.4 \quad (4\text{-}4)$$

Where: *V* is the lake volume, *A* is the lake surface area, and *h* is the lake surface elevation.

Groundwater flow into and out of the lake was assumed to be at a steady state, which means that the change in lake storage with time due to groundwater is zero. Precipitation over the lake was estimated by the Theissen Polygon method using rain gauge data around the lake and evaporation data was obtained from existing studies [*Vallet-Coulomb et al.*, 2001; *Tenalem Ayenew*, 2003].

Statistical analysis

Statistical methods, the Mann-Kendall (MK) test and Standard Precipitation Index (SPI), were applied to understand the effect of climate in the CRV basin. The Mann-Kendall test was used to detect the presence of a climatic trend (e.g. a decreasing or increasing trend in precipitation), while the SPI analysis was used to assess the long-term, inter-annual climate variability in the CRV basin.

Trend analysis determines whether a measured variable increases or decreases during a specified time period. The MK test was used to detect the existence of increasing or decreasing trends [*Mann*, 1945; *Kendall*, 1975] in both the lake and precipitation time series data. The MK trend, a non-parametric test, is suitable for non-normally distributed (skewed) data which is the case for most hydro-meteorological data [*Ehsanzadeh et al.*, 2012] and is effectively used to detect trends in hydrological applications [*Liu et al.*, 2009; *Wang et al.*, 2013; *Pingale et al.*, 2014; *Y F Zhang et al.*, 2014]. Available data for the test consisted of monthly precipitation data from 11 precipitation stations distributed over the CRV basin and lake height data for the three lakes (L. Abiyata, Langano and

Ziway) for the period of 1980-2010. The null hypothesis for the MK test is that there is no trend in the data which was tested using a significance level, alpha = 0.05. At a significance level of 0.05, if p-value ≤ 0.05, then the existing trend is considered to be statistically significant, for details about MK tests see [*Q Zhang et al.*, 2006; *Pingale et al.*, 2014].

The Standard Precipitation Index (SPI) was used to assess the existence of long-term climate variability in relation to the fluctuation of lake storage. SPI provides a normalized measure of length and intensity of dry or wet periods at a given location which is based on historical precipitation observations and cumulative probability distributions, more details of SPI can be found in *McKee et al.* [1993], *Guttman* [1999b], *Hayes et al.* [1999], and *Blain* [2014]. SPI is calculated from a continuous monthly precipitation data of at least 30 years using defined time scales (1, 3, 6, 12, and 24 months). The short time scale (weeks to months) provides short-term climate information (e.g. agricultural applications), whereas calculations based on longer time scales (12 to 24 months) are suitable for monitoring hydrological conditions (e.g. stream flows and reservoir levels) and the impact of drought on the water resources [*Gocic and Trajkovic*, 2014].

The SPI was calculated using 51 years of precipitation data (1960-2010) collected from precipitation stations covering the three physiographic regions (central, eastern and western sections) of the CRV basin. Precipitation data was obtained from the Global Precipitation Climatology Centre [*Schneider et al.*, 2011]. A time scale of 12 months was selected to assess the effect of precipitation variation over the lakes. Generally, SPI values range between -3 and 3 where positive values indicate wet conditions and negative

values indicate dry conditions. SPI values within the range of ±1 represent normal conditions where values greater than 1 and less than -1 indicate moderate to extreme wet and dry conditions, respectively [*Guttman*, 1999a].

4.4. Results and Discussion

In this study, the impact of both natural climate variability and human impacts on the hydrology of the CRV, specifically Lake Abiyata, was assessed using an integrated approach. The human impacts were evaluated using analysis of Landsat imagery, gauge data, and a hydrologic model along with ancillary information (e.g. bathymetry). Statistical tests (MK and SPI) were used to detect trend and long-term climate variability to understand the climate induced effects. Finally, all the information was combined and analyzed to evaluate the relative impacts of both the natural processes and human activities on Lake Abiyata.

Human-induced impact analysis

Satellite-based temporal mapping of lake surface area was computed using Landsat imagery from 1984 to 2013 for the CRV lakes. The surface area of Lakes Ziway, Langano and Shala remained relatively constant during this period, however the surface area of Lake Abiyata changed drastically during this same period (Table 4-2: Lake Abiyata surface area: High in 1985: ~ 180 km^2, and Low in 2005: ~ 95 km^2). Figure 4-2 shows the temporal variation in surface area of Lake Abiyata and the surrounding CRV lakes. Lake Abiyata has lost approximately 65 km^2 (35%) of inundated area since 1985. The estimated volume of water lost from Lake Abiyata is approximately 830 MCM (1130 MCM in 1985 to 300 MCM in 2006) which is nearly 70% of the original 1985 lake

volume. The recent (May 2013) volume estimation for Lake Abiyata (~ 530 MCM) represents ~50% of the 1985 high volume stage.

Table 4-2. Model simulated and satellite-based lake size and storage comparison for Lake Abiyata.

	Satellite-based		Model simulated elevation (m)	Satellite-based Lake volume (MCM)	Model simulated Lake volume (MCM)	Volume difference (MCM)	% lost from 1985 volume
	Area (km^2)	Equivalent elevation (m)					
Jan-85	183	1578.82	1578.79	1130	1064	66	6
Jan-87	159	1577.24	1578.78	874	1063	-189	-17
Jan-95	154	1576.92	1578.75	833	1059	-226	-20
Jan-99	164	1577.57	1578.79	914	1064	-150	-13
Nov-00	164	1577.57	1579.3	914	1127	-212	-19
Dec-00	135	1575.67	1578.85	680	1071	-391	-35
Dec-05	95	1572.91	1578.74	341	1058	-717	-63
Oct-07	120	1574.68	1579.81	559	1189	-630	-56
Nov-09	125	1575.01	1578.85	599	1071	-472	-42

Figure 4-3 shows a time series comparison of model simulated and observed monthly stream flow data (Katar and Meki Rivers) for both the calibration period (1985-1995) and validation period (1996-2000). The SWAT model consistently predicts stream flow well for the simulation period, although some peaks indicate over or under prediction. Monthly flow statistics computed for the calibration and validation periods have shown a good correlation between the simulated and measured flows. The performance and uncertainty measures, R^2, NSE, r- and p-factor, values are in the range of 0.62 to 0.83, 0.57 to 0.75, 1.04 to 1.59, and 0.44 to 0.90, respectfully (Table 4-3). Based on the calibration statistical values, the simulation result is considered satisfactory [*Liew et al.*, 2007].

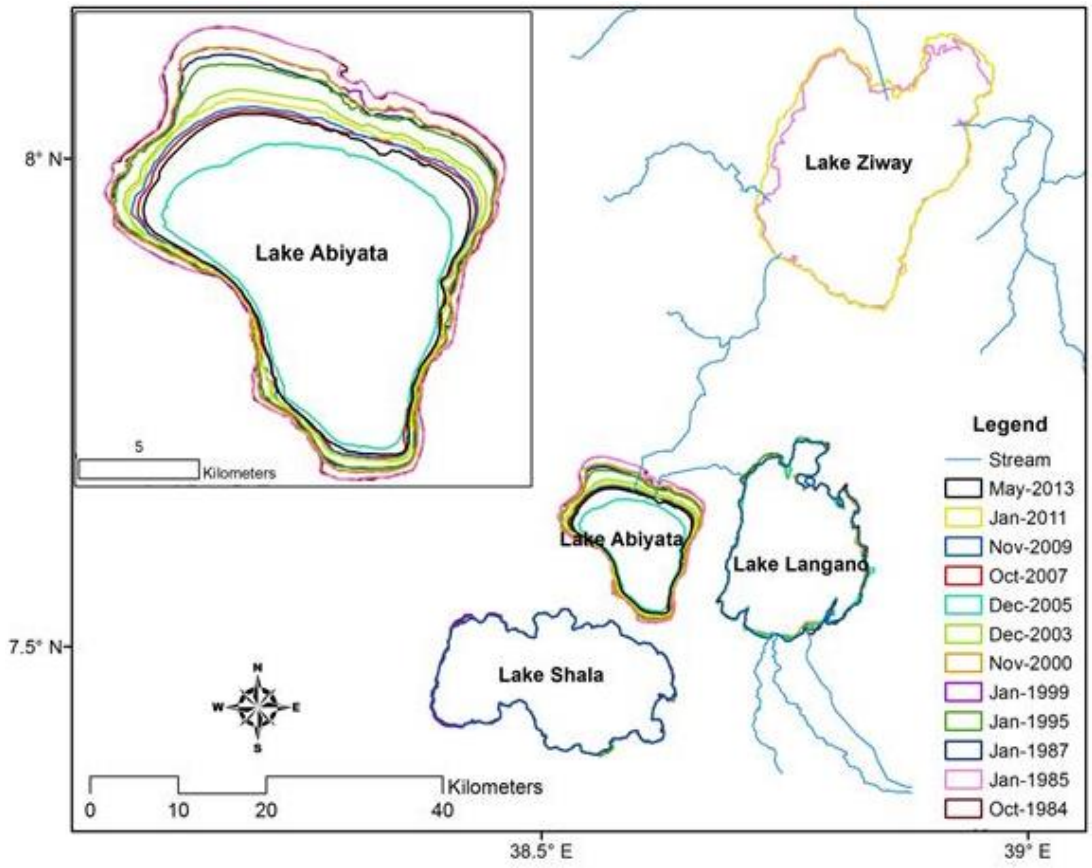

Figure 4-2. Changes in surface areas of CRV lakes (Ziway, Abiyata, Langano, and Shala) derived from Landsat NDWI (1984-2013). Inset map shows enlarged surface area variation of Lake Abiyata.

Comparison between model simulated and satellite-based lake storage variation (Table 4-2) for Lake Abiyata indicates a close comparison in 1985, however the differences in lake volume increased with time. The highest estimated lake volume difference is ~700 MCM in 2005, which is nearly 50% of the total volume of the lake in 1985 (~ 1130 MCM). This difference is attributed to human-induced impacts such as water abstraction from the lakes and tributaries. Human abstraction (industrial and

agricultural) from the lakes and tributaries in the region started in the early 1980s and has increased with time.

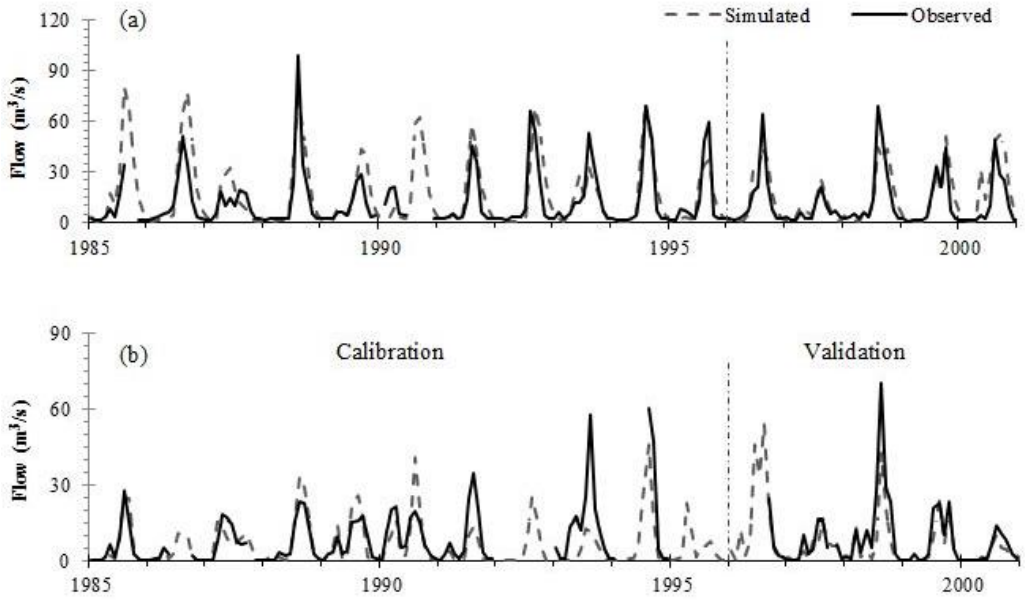

Figure 4-3. Observed (solid line) and model simulated (dashed line) hydrographs of (a) Katar River and (b) Meki River.

Table 4-3. SWAT calibration and validation objective functions.

	Katar River	**Meki River**	
R^2	0.69	0.62	Calibration
NSE	0.57	0.58	
p-factor	0.90	0.44	
r-factor	1.04	1.59	
R^2	0.71	0.83	Validation
NSE	0.66	0.75	

Similarly, model simulated lake height data were compared to observed lake height data for Lake Ziway (Figure 4-4a). Results show a general agreement between the two data sets with the exception of 1985-1994 and 2008-2010. Based on the assumption

of the model, the offsets in these periods are related to human impacts (agricultural abstraction) from Lake Ziway and its tributaries. There is a large difference between model simulated and observed lake height of Lake Abiyata (Figure 4-4b). Likewise the offset between simulated and observed lake height is attributed to human impacts (industrial abstraction) from Lake Abiyata and the effect from upstream Lake Ziway and tributaries.

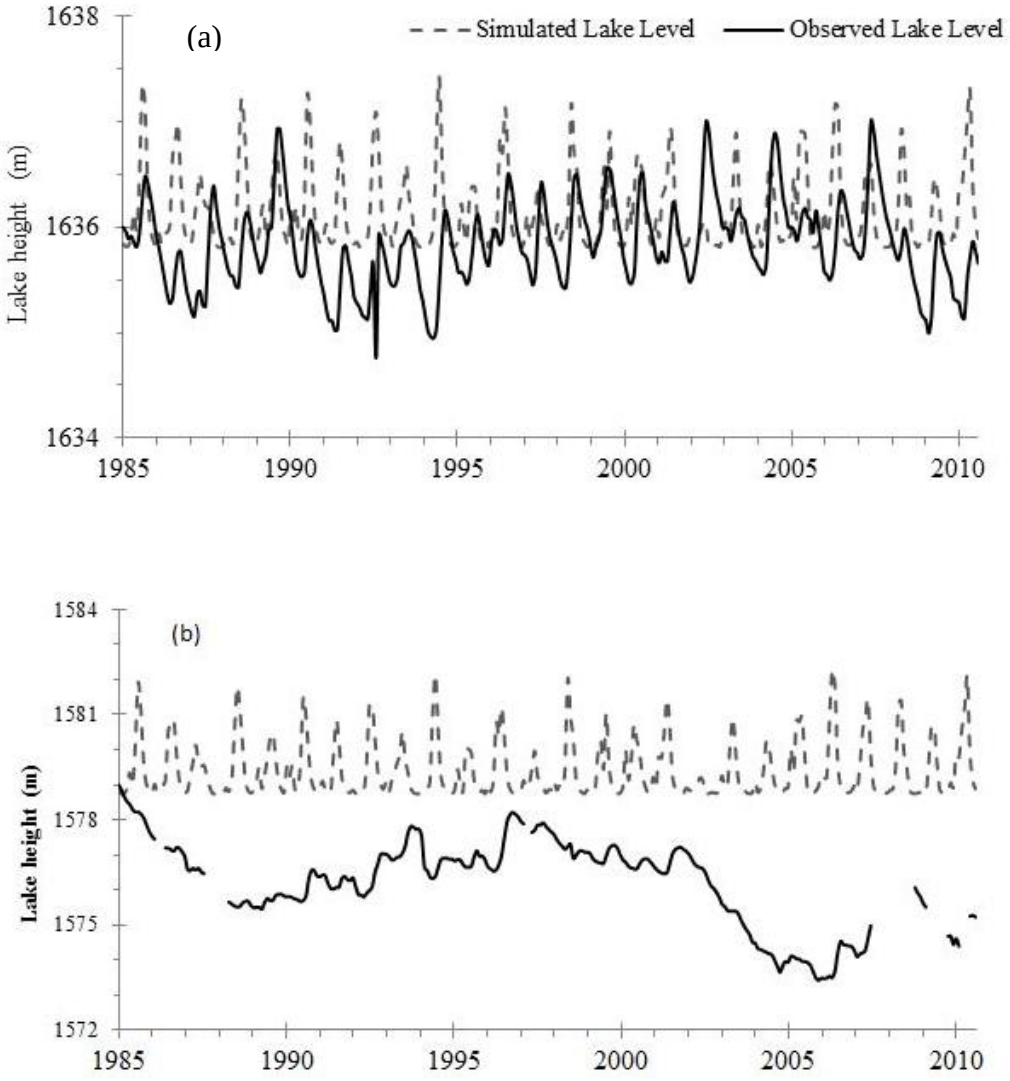

Figure 4-4. Observed (solid line) and simulated lake height (dashed line) for (a) Lake Ziway and (b) Lake Abiyata from 1985-2010.

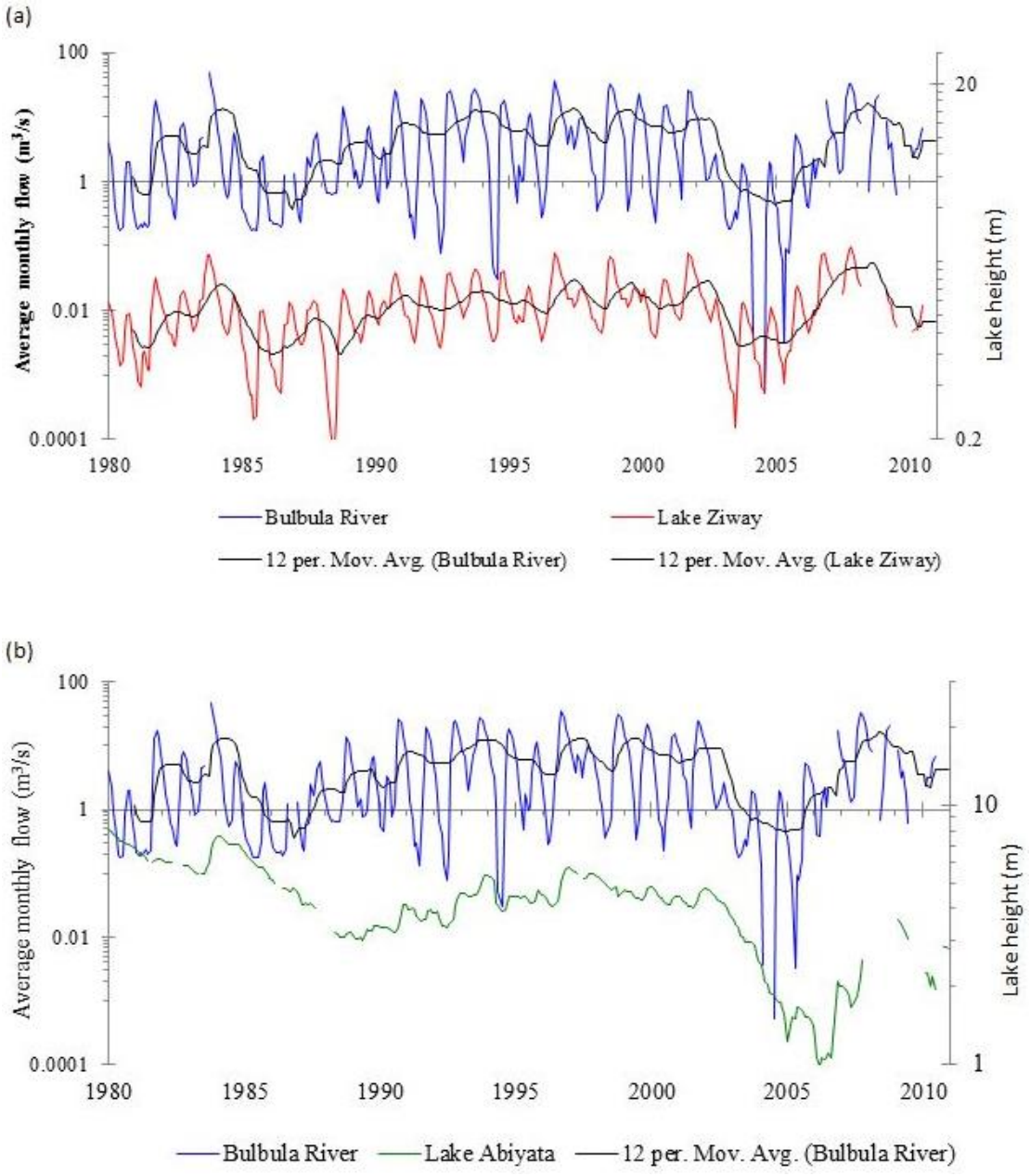

Figure 4-5. Semi-log plot showing the relationship between (a) Lake Ziway (solid red line) and Bulbula River (solid blue line), and (b) Bulbula River (solid blue line) and Lake Abiyata (Solid green line), and 12 months moving average (solid black line).

Due to the hydrologic characteristics of the CRV lakes, the impact on the upstream lakes and rivers is observed on the downstream rivers and Lake Abiyata. The

outflow from Lake Ziway (Bulbula River) clearly follows the lake height pattern of Lake Ziway (Figure 4-5a). The trend of lake height in Lake Abiyata also follows the same pattern as the flow of its tributary, Bulbula River (Figure 4-5b).

Climate variability

A Mann-Kendall trend test on precipitation data from gauging stations in the CRV basin have shown no statistically significant trends (increasing or decreasing) in precipitation except in station 9 (Figure 4-1), which is located outside the basin (Table 4-4). However, SPI results on the four regions, showed an anomalous variation in magnitude and duration of wet and dry conditions in the basin (Figure 4-6). Relatively abnormal magnitudes in dryness (SPI value < -1.0) and longer dry periods are observed in the central section of the CRV basin from the mid-1990s to 2005. Severe droughts and longer dry periods are observed in the northeastern section of CRV basin from 1990 to 2005 (Figure 4-6a). This indicates that the region, especially the central and eastern sections, was relatively dry during this period. The long-term drought from 1990 to mid-2000s in the northeastern section (Figure 4-6a) is not observed in the simulated Katar flow (Figure 4-3a). This could be due to the poor spatial resolution of the precipitation data used to calculate the SPI as well as the dissimilarity of the time span used for both analysis (SPI: 1960 to 2010; Flow simulation: 1985 to 2000) limits to see the long-term pattern. However, in Figure 4-3a, the model simulated a relatively higher flow (peak) between 1985 and 1990 compared to later time.

Similarly the SPI depicted anomalously wet periods between 1980 and 1990 and dry period afterwards. More precipitation and subsequent runoff from the eastern

escarpment affects the CRV lakes more than the western escarpment given the climatic and hydrologic differences. This is consistent with the size (height) variation of Lake Abiyata which shows a considerable decreasing trend during this period. Alternating dry-wet conditions are observed in the western section of the CRV basin with no significant abnormal patterns.

Table 4-4. Mann-Kendall trend test on precipitation data (H_o: the null hypothesis).

Station	Lat	Long	tau	p-value	Decision
1	8.15	38.82	-0.157	0.221	Accept the H_o
2	7.96	39.14	-0.183	0.153	Accept the H_o
3	7.46	39.09	-0.093	0.475	Accept the H_o
4	7.73	38.23	0.174	0.174	Accept the H_o
5	7.83	39.10	-0.239	0.062	Accept the H_o
6	7.93	38.70	0.153	0.234	Accept the H_o
7	8.15	38.37	-0.002	0.98	Accept the H_o
8	7.54	38.68	0.093	0.475	Accept the H_o
9	7.20	38.60	-0.406	0.001	Reject the H_o
10	8.01	39.16	-0.062	0.634	Accept the H_o
11	7.78	39.10	-0.120	0.371	Accept the H_o

Relative (natural vs. human) impact analysis

The relative impact and the effect of climate variability as compared to anthropogenic contributions are demonstrated from hydrologic modeling, satellite-based and observed data analysis, and statistics. Instances where the observed flow and simulated flow differ suggest that anthropogenic impacts are the primary contributor to the changes in lake levels from 1985-1994 (Figure 4-4a). Similar trends occurred again from 2008-2010; however the lack of observed data prohibits confirmation. Whereas, the change in lake levels from 1994-2008 is related to natural climate variability.

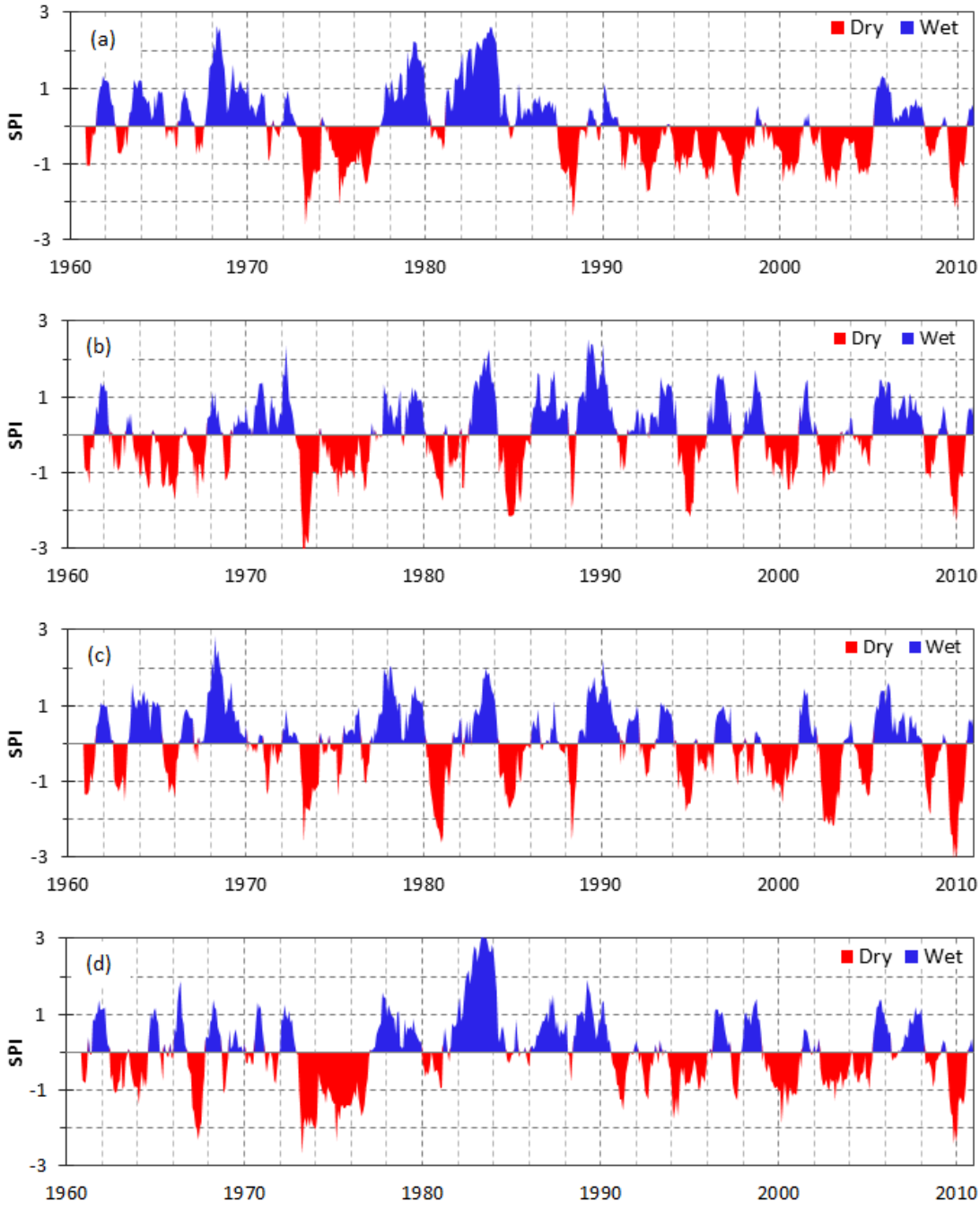

Figure 4-6. SPI results from 1960-2010 illustrating dry vs wet conditions in the (a) northeastern, (b) western, (c) central, and (d) southeastern sections of the CRV basin.

Lake Langano, which is located ~5km due east of Lake Abiyata (Figure 4-1), is used as a climate index to examine the effect of climate variability. Both lakes are located within the same climatic zone and are fed by runoff from the CRV basin sub-catchments. Lake Langano, a brackish lake, hasn't experienced human-induced impacts (abstraction from the lake or tributaries) which alter the hydrology of the lake making it a suitable indicator of climate variability. Therefore, graphical comparisons in lake height data of two adjacent lakes, Lake Langano and Lake Abiyata, provide the effect of climate variability.

The deviation in the lake level patterns of Lake Abiyata and Lake Langano prior to 1990; suggest anthropogenic impacts are responsible for the decline in the lake level of Lake Abiyata. The lake height hydrographs (Figure 4-7) generally follow a similar pattern after 1998 suggesting climate variability is the main contributor.

From 1989 to 1996, both Lake Abiyata and Lake Langano exhibit similar (increasing) trends in lake height. During this period Lake Abiyata stabilized and re-gained part of the losses attributed to human impact. This is possibly because there was less need for irrigation, especially in the central section where irrigation is extensive, as conditions were wet enough to rely on rainfall alone. This is consistent with the SPI analysis result where the central and western sections were relatively wetter during this period (Figure 4-6b and 4-6c). During this period the eastern section was relatively dry, however the dryness in the southeastern section (Figure 4-6d) was not as extreme as the northeastern section (Figure 4-6a).

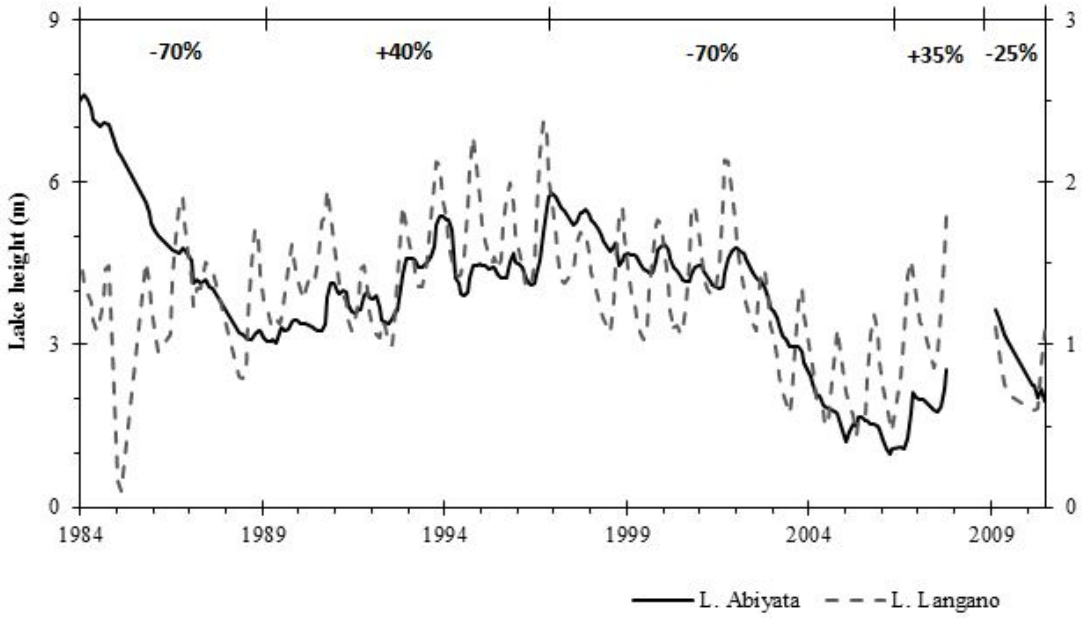

Figure 4-7. Comparison of lake heights (Lake Abiyata: solid line; Lake Langano: dashed line) from 1984-2010 and break down of percentage change of lake level of Lake Abiyata.

After 1997, both Lake Abiyata and Lake Langano show a decreasing trend with the lowest lake heights recorded in 2006. From 1997 to 2006, Lake Abiyata lost ~ 4.5 m in lake height (~ 450 MCM in lake volume) while the larger Lake Langano lost an average lake height of 2 m during this period. Using an average surface area (250 km^2) of Lake Langano, the equivalent lake volume lost is approximately 500 MCM, indicating that the volume lost from the two lakes during this period was nearly the same. The observed decline in lake height in both lakes during this period is probably associated with natural climate variability (e.g. drought) that affected the region. This agrees with the result from SPI analysis where a severe and prolonged drought occurred during this period in the central and eastern sections (Figure 4-6) of the CRV basin. Considering the

period from 1985 to 2006, Lake Abiyata shows a decreasing trend with a total loss of approximately 6.5 m in lake height which is due to combined effect of natural climate variability and human activities. However, the lake level variation of Lake Langano is primarily due to natural climate variability.

Quantitative Analysis of Relative Impacts

Using the relative impact analysis, the magnitude of the relative impact by human and natural processes was quantified for Lake Abiyata. The pre-1989 decrease in lake height of Lake Abiyata is considered human-induced abstraction whereas the post-1989 change is caused by natural climate variability (Figure 4-7). The total loss in lake height of Lake Abiyata from early 1980's to 2006 is approximately 6.5 m. Human-induced abstraction (pre-1989) accounts for nearly 70% (4.5 m) of the total lake height loss. Lake Abiyata re-gained nearly 40% of its lake height during the period 1990 to 1997. From 1997 to 2006, Lake Abiyata lost the same magnitude of lake height (70% of the total loss) as the pre-1989 drop through a combination of human impact and natural climate variability. The net effect due to climate variability is 30% (2m) of the total loss in lake height. Therefore, from the total loss in lake volume from 1985 to 2005, ~ 78% (650 MCM) of the volume loss is due to anthropogenic impacts, whereas nearly 22% (180 MCM) of the volume loss was a result of natural climate variability. After 2006, the lake gained 35% and lost 25% of its lake height, with a net gain of 10% of its total lake height change. Though, the impact has occurred basin-wide, due to its hydrological characteristics the effect was seen mostly on Lake Abiyata.

The limitation of this study is uncertainties associated with the various estimates from satellite-based approach and modeling. For instance errors might be introduced from the satellite data or bathymetry data where the accuracy of area or volume estimation from these data depends on their spatial resolution. In addition, the magnitude of errors in the modeling result depends on the performance or accuracy of the hydrologic model. As the study area is a data-sparse region, integrating remote sensing data is the best available option as this study demonstrated.

4.5. Conclusions

In summary, this study combined the use of satellite and in-situ datasets, hydrologic modeling, and statistical techniques to evaluate the impacts of human activities and natural processes in the Central Rift Valley lakes of Ethiopia, East Africa. The following conclusions are made based on the results: (1) the comparison of observed and model simulated results of Lake Abiyata and Lake Ziway indicate that human impacts contributed to the changes in the hydrology of the lakes and Lake Abiyata is the most affected by human impacts; (2) trend test results reveal no statistically significant trend (increases or decreases) in precipitation within the basin; (3) SPI analysis has shown an inter-annual climate variability (severe drought and prolonged dry periods) in the central and eastern sections of the basin which is consistent with the fluctuation in lake height data; (4) quantitative analysis revealed human impacts were mostly responsible for the change in Lake Abiyata; (5) the climatic and anthropogenic impacts affected Lake Abiyata more than the other CRV lakes because it is the terminal lake and hydrologic characteristics (relatively high ET and low rainfall conditions).

In the basin, human activities, such as agricultural abstraction from Lake Ziway and the main upstream tributaries and industrial abstraction from Lake Abiyata, are the major anthropogenic stresses affecting the hydrologic cycle and causing a decrease in lake storage. The relative impact analysis developed in this study can be applied in an effort to plan effective water management practices for the lakes and the greater CRV basin. Similar integrated approaches could be applied in understanding relative impacts on lakes in other data sparse regions. Modeling and prediction of the lakes' response with respect to future climate change scenarios due to global warming is suggested for further studies.

References

Abbaspour, K. C. (2013), SWAT-CUP 2012: SWAT Calibration and Uncertainty Programs - A User Manual *Rep.*, Eawag.

Alemayehu, T., W. Furi, and D. Legesse (2006a), Impact of water overexploitation on highland lakes of eastern Ethiopia, *Environ. Geol.*, *52*(1), 147-154.

Alemayehu, T., T. Ayenew, and S. Kebede (2006b), Hydrogeochemical and lake level changes in the Ethiopian Rift, *Journal of Hydrology*, *316*(1-4), 290-300.

Alsdorf, D. E., E. Rodríguez, and D. P. Lettenmaier (2007), Measuring surface water from space, *Reviews of Geophysics*, *45*(2).

Arnold, J. G., R. Srinivasan, R. S. Muttiah, and J. R. Williams (1998), Large area hydrologic modeling and assessment Part 1: model development, *Journal of American Water Resources Assocaition*, *34*(1), 73 - 89.

Ayenew, T. (2002), Recent changes in the level of Lake Abiyata, central main Ethiopian Rift, *Hydrological Sciences-Journal'des Sciences Hydrologiques 47*(3), 493 - 503.

Ayenew, T. (2003), Evapotranspiration estimation using thematic mapper spectral satellite data in the Ethiopian rift and adjacent highlands, *Journal of Hydrology*, *279*(1-4), 83-93.

Ayenew, T. (2007), Water management problems in the Ethiopian rift: Challenges for development, *Journal of African Earth Sciences*, *48*(2-3), 222-236.

Ayenew, T., and Y. Gebreegziabher (2006), Application of a spreadsheet hydrological model for computing the long-term water balance of Lake Awassa, Ethiopia, *Hydrol. Sci. J.-J. Sci. Hydrol.*, *51*(3), 418-431.

Bates, B., Z. W. Kundzewicz, S. Wu, and J. Palutikof (2008), Climate change and water, *Technical Paper of the Intergovernmental Panel on Climate Change (Geneva: IPCC Secretariat)*, pp 210–214.

Blain, G. C. (2014), Extreme value theory applied to the standardized precipitation index, *Acta Sci.-Technol.*, *36*(1), 147-155.

Chen, Z., Y. Chen, and B. Li (2012), Quantifying the effects of climate variability and human activities on runoff for Kaidu River Basin in arid region of northwest China, *Theoretical and Applied Climatology*, *111*(3-4), 537-545.

Cherenet, T. (1993), Hydrogeology of Ethiopia and Water Resources Development *Rep.*, Ethiopian Institute of Geological Survey, Addis Ababa.

Darling, W. G., B. Gizaw, and M. K. Arusei (1996), Lake-groundwater relationships and fluid-rock interaction in the east African rift valley: Isotopic evidence, *Journal of African Earth Sciences*, *22*(4), 423-431.

Ehsanzadeh, E., G. van der Kamp, and C. Spence (2012), The impact of climatic variability and change in the hydroclimatology of Lake Winnipeg watershed, *Hydrological Processes*, *26*(18), 2802-2813.

FAO-UN (2009), Land cover of Ethiopia - Globcover Regional, FAO, Rome, Italy.

FAO, IIASA, ISRIC, ISSCAS, and JRC (2012), Harmonized World Soil Database (version 1.2), FAO, Rome, Italy and IIASA, Laxenburg, Austria.

Ferguson, I. M., and R. M. Maxwell (2012), Human impacts on terrestrial hydrology: climate change versus pumping and irrigation, *Environmental Research Letters*, *7*(4), 044022.

Gao, B.-C. (1996), NDWI A Normalized Difference Water Index for Remote Sensing of Vegetation Liquid Water From Space *REMOTE SENS. ENVIRON*, *58*, 257 - 266.

Gassman, P. W., M. R. Reyes, C. H. Green, and J. G. Arnold (2007), The Soil and Water Assessment Tool: Historical Development, Applications, and Future Reseach Directions, *American Society of Agricultural and Biological Engineers*, *50*(4), 1211 - 1250.

Gocic, M., and S. Trajkovic (2014), Spatiotemporal characteristics of drought in Serbia, *Journal of Hydrology*, *510*, 110-123.

Guttman, N. B. (1999a), ACCEPTING THE STANDARDIZED PRECIPITATION INDEX: A CALCULATION ALGORITHMAccepting the Standardized Precipitation Index: a calculation algorithm, *JOURNAL OF THE AMERICAN*

WATER RESOURCES ASSOCIATIONJournal of the American Water Resources Association, *35*(2), 311-322.

Guttman, N. B. (1999b), Accepting the Standardized Precipitation Index: A calculation algorithm, *Journal of American Water Resources Assocaition*, *35*(2), 311-322.

Hailemarian, K. (1999), Impact of climate change on the water resources of Awash River Basin, Ethiopia, *Climate Res*, *12*(2-3), 91-96.

Hayes, M. J., M. D. Svoboda, D. A. Wilhite, and O. V. Vanyarkho (1999), Monitoring the 1996 drought using the standardized precipitation index, *Bull. Amer. Meteorol. Soc.*, *80*(3), 429-438.

Hulme, M., Elaine M. Barrow, Nigel W. Arnell, Paula A. Harrison, Timothy C. Johns, and T. E. Downing (1999), Relative impacts of human-induced climate change and natural climate variability, *Nature*, *397*, 688-691.

Jansen, H., H. Hengsdijk, D. Legesse, T. Ayenew, P. Hellegers, and P. Spliethoff (2007), Land and Water Resources Assessment in the Ethiopian Central Rift Valley *Rep.*, Wageningen, NL.

Ji, L., L. Zhang, and B. Wylie (2009), Analysis of Dynamic Thresholds for the Normalized Difference Water Index, *Photogrammetric Engineering & Remote Sensing*, *75*(11), 1307 - 1317.

Kebede, E., Z. Gebremariam, and A. Ahlgren (1994), The Ethiopian Rift valley lakes. Chemical characteristics along a salinity–alkalinity series, *Hydrobiologia*, *288*, 1 - 12.

Kendall, M. (1975), Rank correlation measures, *Charles Griffin, London*, *202*.

Legesse, D., C. Vallet-Coulomb, and F. Gasse (2004), Analysis of the hydrological response of a tropical terminal lake, Lake Abiyata(Main Ethiopian Rift Valley) to changes in climate and human activities, *Hydrological Processes*, *18*(3), 487-504.

Liew, M. W. V., T. L. Veith, D. D. Bosch, and J. G. Arnold (2007), Suitability of SWAT for the Conservation Effects Assessment Project: Comparison on USDA Agricultural Research Service Watersheds, *J. Hydrol. Eng.*, *12*(2), 173-189.

Liu, Q., Z. Yang, B. Cui, and T. Sun (2009), Temporal trends of hydro-climatic variables and runoff response to climatic variability and vegetation changes in the Yiluo River basin, China, *Hydrological Processes*, *23*(21), 3030-3039.

Makin, M. J., T. J. Kingham, A. E. Waddams, C. J. Birchall, and B. W. Eavis (1976), Prospects for irrigation development around lake Ziway, Ethiopia *Rep.*, 270 pp, 26, Tolworth, UK.

Mann, H. B. (1945), Non-parametric test against trend, *Econometrica*, *13*, 245-259.

McFeeters, S. K. (1996), The use of the Normalized Difference Water Index (NDWI) in the delineation of open water features, *International Journal of Remote Sensing*, *17*(7), 1425-1432.

McKee, T. B., N. J. Doesken, and J. Kleist (1993), The relationship of drought frequency and duration to time scales, *Eighth Conference on Applied Climatology, Anaheim, California*.

Neitsch, S. L., J. G. Arnold, J. R. Kiniry, J. R. Williams, and K. W. King (2005), Soil and Water Assessment Tool Theoretical Documentation: Version 2009, *Texas Water Resources Institute Technical Report No. 406, Texas A&M University System, College Station, Tx.*

Pingale, S. M., D. Khare, M. K. Jat, and J. Adamowski (2014), Spatial and temporal trends of mean and extreme rainfall and temperature for the 33 urban centers of the arid and semi-arid state of Rajasthan, India, *Atmos. Res.*, *138*, 73-90.

Prigent, C., F. Papa, F. Aires, W. B. Rossow, and E. Matthews (2007), Global inundation dynamics inferred from multiple satellite observations, 1993–2000, *Journal of Geophysical Research*, *112*(D12).

Rogers, A. S., and M. S. Kearney (2004), Reducing signature variability in unmixing coastal marsh Thematic Mapper scenes using spectral indices, *International Journal of Remote Sensing*, *25*(12), 2317-2335.

Schneider, U., A. Becker, P. Finger, A. Meyer-Christoffer, B. Rudolf, and M. Ziese (2011), GPCC Full Data Reanalysis Version 6.0 at 0.5 Deg: Monthly Land-Surface Precipitation from Rain-Gauges built on GTS-based and Historic Data.

Smith, L. C. (1997), Satellite remote sensing of river inundation area, stage, and discharge: a reveiw, *Hydrological Processes*, *11*, 12.

St. Jacques, J.-M., D. J. Sauchyn, and Y. Zhao (2010), Northern Rocky Mountain streamflow records: Global warming trends, human impacts or natural variability?, *Geophysical Research Letters*, *37*(6), n/a-n/a.

Street, F. A. (1979), Late Quaternary Lakes in the Ziway-Shala Basin, Southern Ethiopia (UK), *PhD Thesis [Quaternaire: STR-80.094]*.

Vallet-Coulomb, C., D. Legesse, F. Gasse, Y. Travi, and T. Cherenet (2001), Lake Evaporation Estimates in Tropical Africa (Lake Ziway, Ethiopia), *Journal of Hydrology*, *245*, 1-18.

Van Loon, A. F., and H. A. J. Van Lanen (2013), Making the distinction between water scarcity and drought using an observation-modeling framework, *Water Resour. Res.*, *49*(3), 1483-1502.

Wang, H. J., Y. N. Chen, and Z. S. Chen (2013), Spatial distribution and temporal trends of mean precipitation and extremes in the arid region, northwest of China, during 1960-2010, *Hydrological Processes*, *27*(12), 1807-1818.

Ward, D. P., A. Petty, S. A. Setterfield, M. M. Douglas, K. Ferdinands, S. K. Hamilton, and S. Phinn (2014), Floodplain inundation and vegetation dynamics in the Alligator Rivers region (Kakadu) of northern Australia assessed using optical and radar remote sensing, *Remote Sensing of Environment, 147*, 43-55.

Xu, H. (2006), Modification of normalised difference water index (NDWI) to enhance open water features in remotely sensed imagery, *International Journal of Remote Sensing*, *27*(14), 3025-3033.

Yang, J., P. Reichert, K. C. Abbaspour, J. Xia, and H. Yang (2008), Comparing uncertainty analysis techniques for a SWAT application to the Chaohe Basin in China, *Journal of Hydrology*, *358*(1-2), 1-23.

Zhang, Q., C. Liu, C.-y. Xu, Y. Xu, and T. Jiang (2006), Observed trends of annual maximum water level and streamflow during past 130 years in the Yangtze River basin, China, *Journal of Hydrology*, *324*(1–4), 255-265.

Zhang, Y. F., D. X. Guan, C. J. Jin, A. Z. Wang, J. B. Wu, and F. H. Yuan (2014), Impacts of climate change and land use change on runoff of forest catchment in northeast China, *Hydrological Processes*, *28*(2), 186-196.

Zhou, J., Y. Liu, H. Guo, and D. He (2014), Combining the SWAT model with sequential uncertainty fitting algorithm for streamflow prediction and uncertainty analysis for the Lake Dianchi Basin, China, *Hydrological Processes, 28*(3), 521-533.

CHAPTER 5

SUMMARY AND CONCLUSIONS

In this research, the application of various satellite products (i.e. GRACE, TRMM, and Landsat) integrated with in-situ datasets and modeling for understanding terrestrial water dynamics in relation to climate variability and human impacts at different scales has been demonstrated. Firstly, storage in the various terrestrial water compartments was quantified using an integrated hydrologic model (IHM) – MIKE SHE that simulates the entire terrestrial water cycle and GRACE satellite data to compare the change in total water storage estimates in the intensively irrigated Northern High Plains (area ~ 250,000 km^2). Secondly, a downscaling approach has been developed and tested, to improve the applicability of terrestrial water storage (TWS) anomaly data from GRACE satellite mission for understanding local (i.e. small-scale) terrestrial water cycle dynamics in the same region. Lastly, an integrated approach (remote sensing, hydrologic modeling, and statistical analysis) was applied to assess the relative effects of natural processes and human activities on the water resources over a sparsely gauged Central Rift Valley basin. The following major conclusions were drawn from this research:

1) At a regional scale, the TWS anomaly from IHM reproduced the monthly TWS anomaly from GRACE with few discrepancies, both exhibit similar long-term trends.
2) Agreement between GRACE-derived TWS and IHM-derived TWS anomalies on monthly and seasonal time scales confirms the potential for

using GRACE gravity measurements to infer trends in TWS changes in an area of 250,000 km^2 and in a region with intense irrigation.

3) The pattern of the TWS anomaly from both GRACE and the model depicted the natural TWS variation as a result of climatic variability and human impact (e.g. the 2012 drought).
4) Moreover, in the irrigation season where in-situ TWS monitoring is difficult, GRACE provides suitable firsthand information to monitor terrestrial water anomalies.
5) At local scale application of GRACE, the neural network downscaling approach was able to successfully reproduce the monthly TWS variations in the watersheds with size ranges from 5,000 to 20,000 km^2.
6) Alike the regional scale GRACE, the downscaled TWS anomaly simulated the natural water storage variation as a result of the combined effect of climatic variability and human abstraction. It has simulated the TWS variability as a result of the wet years (groundwater pumping decreases) and drought periods (where pumping heightened) occurred in the study area.
7) Neither the regional hydrologic model nor the land surface models replicated the long-term pattern in TWS anomaly resulting from the combined climatic and human impact. This is attributed to the lack of pumping rate variability as a result of climatic variations (e.g. IHM), and the lack of consideration of water use and excluding the saturated zone in the simulation for the case of the land surface models (e.g. Noah). This

makes the GRACE-based downscaled product preferable in reproducing the natural water storage variability.

8) Derived groundwater storage anomaly data from the downscaled TWS anomaly data correlated very well with groundwater storage anomaly calculated from in-situ groundwater level measurements for sample watersheds with size as small as 6,000 km^2.
9) The relative impact analysis between human vs. climate variability on lakes developed in this study can be applied in an effort to plan effective water management practices for the lakes and the greater CRV basin. Similar integrated approaches could be applied in understanding relative impacts on lakes in other data sparse regions.

Most importantly, this study demonstrated the potential of satellite mission products (e.g. GRACE) merged with other datasets and models to estimate the terrestrial water cycle components such as groundwater storage anomaly at local (small-scales) scales. This enables scientists to integrate satellite products in local and regional water resources management applications, especially in areas where there are no or limited ground observational data. Moreover, the ability of the developed and tested method in this study and the product to predict the natural storage variability shows the potential of using it to further enhance the performance of the global land surface models and regional hydrologic models. The ANN approach developed in this study could be used toward filling the data gap which will be created between the current GRACE and future GRACE-FO follow-up missions given future data availability of the terrestrial water

variables. Moreover, the relative impact analysis developed in this study can be applied in understanding relative impacts on lakes in other data sparse regions.

The techniques developed here allow for a better assessment and understanding of the variability of hydrologic fluxes and storage in relation to climatic and human impact at different spatial and temporal scales. This enables integration of publically available satellite remote sensing data in local water resources management decisions. Furthermore, the spatiotemporal coverage of satellite products allows inexpensive and holistic assessment of local water resources compared to insitu-based monitoring networks which depend on indispensable local resources. Locally, in the intensively irrigated NHP region, the ANN method developed here can be used to predict water storage variables in advance, thus, it can be used as an early indicator of changes in the water resources, especially the groundwater and help understand how to mitigate the change and unwanted impacts. Therefore, insights gained from this integrated approach using global publically available data will be of broad interest to water managers, policy makers, and local communities.